

**Biochemical Characterization of *Toxoplasma gondii*
Type II NADH Dehydrogenases - Physiological
Impact on Mitochondrial Functions
and Energy Metabolism**

vorgelegt von

San San Lin

aus

Hong Kong

zur Erlangung des Doktorgrades
der Biologischen Fakultät
der Georg-August-Universität Göttingen

2009

**Biochemical Characterization of *Toxoplasma gondii*
Type II NADH Dehydrogenases - Physiological
Impact on Mitochondrial Functions
and Energy Metabolism**

submitted by

San San Lin

from

Hong Kong

for the Degree of Doctor of Philosophy
through the Faculty of Biology
at The Georg-August-Universität Göttingen

2009

D7

Referent: Prof. Dr. Uwe Groß

Korreferent: Prof. Dr. Gerhard Braus

Tag der mündlichen Prüfung:

That is the essence of science: ask an impertinent question, and you are on the way to a pertinent answer.

– Jacob Bronowski

Declaration

I declare that this thesis represents my own work, except where due acknowledgement is made, and that it has not been previously included in a thesis, dissertation or report submitted to this University or to any other institution for a degree, diploma or other qualification.

San San Lin

9th December, 2009, Göttingen

Acknowledgements

I would like to thank all of those who have contributed to this study.

Especially I would like to express my deepest gratitude to my direct supervisor, Dr. Wolfgang Bohne, for his supervision, support and encouragement throughout the years. His invaluable guidance, advice and ideas make my thesis possible here. Thank you very much for sharing ideas and all the inspiring discussions.

I would like to thank Prof. Uwe Groß for accepting me as a PhD candidate and his support during my study. Thank you for giving me the opportunity to attend a variety of conferences. Also thank you for being the first referee of my thesis.

I would also like to thank Prof. Gerhard Braus for being the second referee of my thesis. Many thanks to Prof. Botho Bowien, Prof. Ivo Feussner, Prof. Wilfried Kramer and Prof. Jörg Stülke for being my examination committee members.

I specially thank Croucher Foundation for the financial support that enables me to pursue my PhD study abroad.

I thank Dr. Stefan Kerscher for his teaching and advice for the enzymatic analyses. Many thanks to Karen, Marialice, Diana, Nicole, Andrea, Malik, Albert, Javid, Britta, Anna, Kristin, Oliver and Friedrich for their support, helps and all the good times over the past years. I also want to thank Prof. Carsten Lüder, Dr. Lugert Raimond for their support, and all the members of the Institute of Medical Microbiology for making such a nice working atmosphere.

I thank Karen and Rebecca for our friendship, and for being honest and real. Many thanks to my incredible family members for their love, support, trust and understanding. You are always on my side.

Table of Contents

Declaration	i
Acknowledgements	ii
Tables of Contents	iii
List of Figures	vii
List of Tables	viii
List of Abbreviations	ix

CHAPTER I Introduction

1.1 <i>Toxoplasma gondii</i> as a Genetic Model System	1
1.1.1 The Establishment of Transgenic Parasites	1
1.1.2 The Establishment of <i>Toxoplasma</i> Mutants	4
1.2 <i>T. gondii</i> as a Model System for Apicomplexan Drug Discovery	6
1.2.1 The Identification of Drug Targets	7
1.2.2 The Validation of Drug Targets	9
1.3 Apicomplexan Organelles	10
1.3.1 Apicoplast and Mitochondrion as promising Drug Targets	10
1.3.2 The Apicomplexan Mitochondrial Respiratory Chain	11
1.3.2.1 Oxidative Phosphorylation	14
1.3.3 Type II NADH Dehydrogenases	15
1.3.3.1 Structural Characteristics of NDH2s	16
1.3.3.2 Membrane Interaction of NDH2s	20
1.3.4 Electrophysiology of Mitochondrial Membrane Potential	23
1.4 Objectives of the Study	24

CHAPTER II Materials and Methods

2.1 Materials	25
2.1.1 Cell Cultures	25
2.1.1.1 <i>T. gondii</i> Strains	25
2.1.1.2 Mammalian Cell Lines	26
2.1.1.3 <i>Escherichia coli</i> Strains	26
2.1.1.4 <i>Yarrowia lipolytica</i> Strains	26
2.1.2 Plasmids	27
2.1.3 Cosmids	28
2.1.4 Oligonucleotides	28
2.1.5 Antibodies	31

2.1.6	Enzymes	31
2.1.7	Kits	32
2.1.8	Molecular Weight Markers	32
2.1.9	Antibiotics	32
2.1.10	Fluorescent Probes	33
2.1.11	Chemicals for Substrates Complementation	33
2.1.12	Standard Media and Buffers	34
2.1.12.1	Mammalian Culture Media and Reagents	34
2.1.12.2	Bacterial Culture Media and Reagents	35
2.1.12.3	Standard Buffers	35
2.1.13	Chemicals	37
2.1.14	Apparatus	38
2.2	Methods	39
2.2.1	Bioinformatics	39
2.2.2	Plasmid Construction	39
2.2.2.1	Plasmid Construction for <i>Y. lipolytica</i> Transformation	39
2.2.2.2	Plasmid Construction for Split GFP Complementation	39
2.2.2.3	Gel Purification	40
2.2.2.4	PCR Cloning	40
2.2.2.5	Restriction Endonuclease Digestion of DNA	40
2.2.2.6	Alkaline Phosphatase Reaction	41
2.2.2.7	Ligation of DNA	41
2.2.2.8	Preparation of chemically Competent <i>E. coli</i> Cells	41
2.2.2.9	Cell Transformation	41
2.2.2.10	Plasmid Preparation	42
2.2.2.10.1	Screening Clones	42
2.2.2.10.2	Determination of DNA Concentration	42
2.2.2.10.3	DNA Precipitation	42
2.2.3	Cosmid Recombineering	42
2.2.3.1	Preparation of Electrocompetent cells	42
2.2.3.2	Electroporation of Cosmid DNA	43
2.2.3.3	Preparation of SW103 containing Cosmid	43
2.2.3.4	Cosmid Modification	43
2.2.3.5	Cosmid DNA Precipitation	44
2.2.4	Analysis of Gene Expression	44
2.2.4.1	Isolation of Genomic DNA	44
2.2.4.2	Total RNA Isolation	44
2.2.4.3	Reverse Transcription-Polymerase Chain Reaction (RT-PCR)	45
2.2.4.3.1	Synthesis of cDNA	45
2.2.4.3.2	Polymerase Chain Reaction (PCR)	45
2.2.4.3.3	Real-time PCR	45

2.2.4.3.4 Fusion-PCR	46
2.2.5 Cell Cultures	46
2.2.5.1 Cultivation of Human Foreskin Fibroblasts	46
2.2.5.2 <i>In vitro</i> Cultivation of <i>T. gondii</i>	46
2.2.5.3 <i>In vitro</i> Differentiation of Tachyzoites to Bradyzoites	47
2.2.5.4 Transfection of <i>T. gondii</i>	47
2.2.5.5 Generation of Conditional Knock-out Mutants	47
2.2.5.6 Cloning of Transgenic Lines	48
2.2.5.7 Cryopreservation of <i>T. gondii</i>	48
2.2.5.8 Immunofluorescence Assay	49
2.2.5.9 Detection of $\Delta\Psi_m$ in <i>T. gondii</i>	49
2.2.5.10 Determination of Intracellular ATP level	49
2.2.5.11 Time-lapse Microscopy	49
2.2.5.12 Drug Treatment	49
2.2.5.13 Cell Count	50
2.2.5.14 Statistical Method	50
2.2.6 Analysis of Protein Expression	50
2.2.6.1 Growth of <i>E. coli</i> Expression Cultures	50
2.2.6.2 Growth of <i>Y. lipolytica</i> Cultures	50
2.2.6.3 Protein Extraction	50
2.2.6.4 Western Blot Analysis	51
2.2.6.4.1 Quantification of Protein Concentration	51
2.2.6.4.2 Sodium Dodecyl Sulphate-Polyacrylamide Gel Electrophoresis (SDS-PAGE)	51
2.2.6.4.3 Electroblotting of SDS-PAGE	51
2.2.6.4.4 Blocking, Washing and Antibody Incubation	51
2.2.6.4.5 Affinity Purification of Polyclonal Antibodies	52
2.2.6.4.6 Protein Detection	52
2.2.6.5 Kinetic Measurements	52
CHAPTER III	Results
3.1 Biochemical Characterization of TgNDH2s as Drug Targets for HDQ	53
3.2 Physiological Consequences of TgNDH2s Inhibition in <i>T. gondii</i>	54
3.3 Functional Analysis of TgNDH2s	55
3.3.1 Elucidating the Orientations of Inner Mitochondrial Membrane-associated TgNDH2s	55
3.3.1.1 TgNDH2-II is an Internal Enzyme	55
3.3.1.2 TgNDH2-I is also an Internal Enzyme	56
3.3.2 Phenotypic Analysis of TgNDH2s Depletion Mutants	61

3.3.2.1 Conditional TgNDH2-I and TgNDH2-II Knock-out Mutants achieved by a cosmid-based Approach	61
3.3.2.2 TgNDH2-I and TgNDH2-II are non-essential for <i>T. gondii</i> Replication	64
3.3.2.3 TgNDH2-I or TgNDH2-II Depletion does not affect mRNA of the intact Isoform	64
3.3.2.4 TgNDH2-I or TgNDH2-II Depletion does not affect Extra-cellular Viability	67
3.3.2.5 TgNDH2-I Depletion Mutant is less sensitive to HDQ Treatment	67
3.3.2.6 TgNDH2-I or TgNDH2-II Depletion does not affect $\Delta\psi_m$	70
3.3.2.7 Bradyzoite Differentiation is not influenced in Δ TgNDH2-I and Δ TgNDH2-II Parasites	70

CHAPTER IV Discussion

4.1 Both Isoforms of TgNDH2s are Internal Enzymes	73
4.2 TgNDH2-I is a Drug Target for HDQ	75
4.3 TgNDH2-I and TgNDH2-II are non-essential for Replication Growth	79
4.4 A proposed Model explaining the Importance of TgNDH2s in <i>T. gondii</i>	81
Summary	84
References	86
Appendix I	98
Appendix II	106
Publications	116
Curriculum Vitae	118

List of Figures

CHAPTER I	Introduction	
Figure 1.1	Genetic manipulation in <i>T. gondii</i>	5
Figure 1.2	Organelles and subcellular structures of <i>T. gondii</i>	13
Figure 1.3	Model of the apicomplexan mitochondrial respiratory chain	18
Figure 1.4	Eukaryotic type II NADH dehydrogenases	22
CHAPTER III	Results	
Figure 3.1	TgNDH2-II is oriented internally at inner mitochondrial membrane	58
Figure 3.2	TgNDH2-I is oriented internally at inner mitochondrial membrane	59
Figure 3.3	TgNDH2-I is not an external enzyme	60
Figure 3.4	Cosmid modification by recombineering	62
Figure 3.5	Generation of conditional knock-out mutants for TgNDH2s	63
Figure 3.6	TgNDH2-I and TgNDH2-II depletion mutants display unaltered growth rates	65
Figure 3.7	Quantitative RT-PCR for assaying mRNA transcripts of knock-out mutants	66
Figure 3.8	TgNDH2-I and TgNDH2-II depletion mutants show unaltered extracellular viability	68
Figure 3.9	TgNDH2-I depletion is less sensitive to HDQ	69
Figure 3.10	TgNDH2-I and TgNDH2-II depletion mutants show normal $\Delta\psi_m$	71
Figure 3.11	Depletion of either TgNDH2-I or TgNDH2-II does not affect bradyzoite differentiation	72
CHAPTER IV	Discussion	
Figure 4.1	A proposed model depicting the importance of type II NADH dehydrogenases in the energy metabolism of <i>T. gondii</i>	83

List of Tables

CHAPTER I

Introduction

Table 1.1	Applications of the reporter genes in <i>T. gondii</i>	3
Table 1.2	Novel drug targets in <i>Plasmodium</i> and <i>Toxoplasma</i>	8
Table 1.3	Functions of the unique organelles in <i>T. gondii</i>	13
Table 1.4	Properties of the dehydrogenases in <i>T. gondii</i>	17
Table 1.5	Structural and functional properties of the apicomplexan respiratory complexes	19

CHAPTER II

Materials and Methods

Table 2.1	Oligonucleotides used for cosmid recombineering	28
Table 2.2	Oligonucleotides used for real-time PCR	29
Table 2.3	Oligonucleotides used for split GFP complementation	29
Table 2.4	Antibodies used for Western blots (WB) and immunofluorescence assays (IFA)	31
Table 2.5	Working concentration used for selection	32
Table 2.6	Working concentration used for staining $\Delta\psi_m$ in <i>T. gondii</i>	33
Table 2.7	Working concentration used for substrate complementation	33

List of Abbreviations

ADP	Adenosine
AMP	Ampicillin selection cassette
AP	Alkaline phosphatase
APS	Ammonium peroxodisulfate
ATc	Anhydrotetracycline
ATP	Adenosine 5' triphosphate
ATPase	ATP synthase
BAG1	Bradyzoite antigen 1
BCIP	5-Bromo-4-chloro-3-indolylphosphate
BLAST	Basic Local Alignment Search Tool
BLE	Phleomycin resistance gene
BSA	Bovine serum albumin
CAT	Chloramphenicol acetyl transferase
cDNA	Complementary DNA
CoA	Coenzyme A
CoQ	Ubiquinone
CoQH ₂	Ubiquinol (reduced CoQ)
Cox	Cytochrome c oxidase
Cyt <i>c</i>	Cytochrome <i>c</i>
CytoC	Putative cytochrome <i>c</i>
Cy2	Carbocyanin
Cy3	Incocarbocyanin
DBQ	<i>n</i> -Decylubiquinone
ddFKBP	Ligand-regulatable FKBP destabilization domain
ddH ₂ O	Double distilled water
DHAP	Dihydroxyacetone phosphate
DHFR-TS	Dihydrofolate reductase-thymidylate synthase
DHOD	Cihydroorotate dehydrogenase
DMSO	Dimethyl sulfoxide
DNA	Deoxyribonucleic acid
dNTP	Dinucleotide phosphate
DPI	Diphenylene iodonium chloride
DTT	1,4-Dithiothreitol
DV	Aspartic acid and serine
EA	Glutamic acid and Alanine
ECL	Enhanced chemiluminescent detection
ENO	Enolase
ETC	Electron transport chain
FAD	Flavin adenine dinucleotide

FADH ₂	Reduced FAD
FAS	fatty acid synthesis
FCS	Fetal calf serum
Fe-S	Iron-sulfur
Fig	Figure
FITC	Fluorescein isothiocyanate
FL	Full-length
FMN	Flavin mononucleotide
FNR	Ferredoxin-NADP ⁺ reductase
g	Force of gravity
GENT	Gentamycin selection cassette
GFP	Green fluorescence protein
GRA	Dense-granule proteins
GSH	Glutathione
G3P	Glycerol-3-phosphate
G3PDH	Glycerol-3-phosphate dehydrogenase
h	Hour/Hours
HA	Hemagglutinin
HDQ	1-Hydroxy-2-dodecyl-4(1H)quinolone
HFF	Human foreskin fibroblast
HRP	Horseradish peroxidase
HSP	Heat shock protein
HXGPRT	Hypoxanthine- xanthine-guanine phosphoribosyl transferase
IC ₅₀	Inhibitory concentration 50%
IFA	Immunofluorescence assay
IgG	Immunoglobulin G
IMPDH	Inosine 5-monophosphate-dehydrogenase
IPTG	Isopropyl beta-D-thiogalactopyrano-side
kb	Kilo base pair
kDa	Kilo dalton
LacZ	B-galactosidase
LB	Luria Broth
M	Molar
MIC	Microneme protein
ml	Milliliter
MDH	Malate:ubiquinone oxidoreductase
min	Minute
mg	Milligram
μF	Micro Faraday
μg	Microgram
μl	Microliter

µm	Micrometer
mRNA	Messenger RNA
MT	Microtubules
mtDNA	Mitochondrial DNA
MyoA	Myosin A
NAD ⁺	Nicotinamide adenine dinucleotide
NADH	Reduced NAD
NADPH	Reduced nicotinamide adenine dinucleotide and phosphate
NAD(P)H	Both NADH and NADPH
NBT	Nitrotetrazolium blue chloride
NDH2	Type II NADH dehydrogenase
NDH2-I	NDH2 isoform I
NDH2-II	NDH2 isoform II
NUAM	<i>Yarrowia</i> mitochondrial complex I targeting sequence
OAA	Oxaloacetate
OD	Optical density
ORFs	Open reading frames
<i>p</i>	<i>P</i> value
PAGE	Polyacrylamide gel electrophoresis
PBS	Phosphate buffered saline
PCR	Polymerase chain reaction
Pf	<i>P. falciparum</i>
PFA	Paraformaldehyde
PKG	Cyclic GMP-dependent protein kinase
Q	Quinone
QS	Glutamine and Serine
RFP	Red fluorescence protein
RNA	Ribonucleic acid
RNAi	RNA interference
ROP	Rhoptry protein
rpm	Revolutions per minute
RT	Room temperature
RT-PCR	Reverse transcription-polymerase chain reaction
s	Second
SCSβ	Succinyl-CoA synthetase beta subunit
SDS	Sodium dodecyl sulphate
Shld1	Shield-1
TATi	Transactivator
TC	Tissue Culture
TCA	Tricarboxylic acid cycle
tet	Tetracycline

TetO	Tet operator
TetTA	Tet-transactivator protein
Tg	<i>T. gondii</i>
TIM	Translocase of the inner membrane complexes
Tm	Annealing temperature
TMPD	Tetramethyl-phenylene-diamine
TOM	Translocase of the outer membrane complexes
TUB1	α -tubulin
U	Unit
UMP	5'-Monophosphate
UPRT	Uracil phosphoribosyltransferase
UV	Ultraviolet
V	Voltage
v	Volume
w	Weight
WB	Western blot
X-Gal	5-Bromo-4-Chloro-3-Indolyl- β -D-Galactopyranoside
YFP	Yellow fluorescence protein
$\Delta\Psi_m$	Mitochondrial membrane potential

CHAPTER I

Introduction

1.1 *Toxoplasma gondii* as a Genetic Model System

Toxoplasma gondii is a very successful protozoan parasite, infecting more than one third of the world's population. Since its discovery in 1908 (Nicolle and Manceaux, 1908; Splendore, 1908), it has been highly implicated in the pathogenesis of congenital neurological defects in developing fetuses and encephalitis among the immunocompromised individuals (Luft and Remington, 1992; Montoya and Rosso, 2005). *Toxoplasma* belongs to the phylum Apicomplexa including other important human and veterinary pathogens: *Plasmodium*, the causative agent of malaria; *Babesia*, *Eimeria* and *Cryptosporidium*, the enteric pathogens; and *Neospora* and *Theileria*, the systemic veterinary pathogens (Kim and Weiss, 2004).

Among these apicomplexan parasites, *Toxoplasma* is much easier to handle for genetic manipulation. Experimental techniques for both classical forward and reverse genetics have been well established over the past decades (Kim and Weiss, 2004). Moreover, *Toxoplasma* can be cultivated both *in vitro* and in mouse animal models without great difficulty. Thereby, it stands out as a very useful tool for studying the cell biology of the apicomplexan parasites. Herein, the detailed genetic manipulation approaches involved in the establishment of transgenic parasites and mutants will be delineated.

1.1.1 The Establishment of Transgenic Parasites

In order to successfully manipulate the *Toxoplasma* genome, several criteria need to take into consideration, including the efficiency of DNA transfection, the suitability of the selectable markers, and the relevance of the promoters used for the constructs.

T. gondii was the first apicomplexan parasite to be successfully transfected (Donald and Roos, 1993; Kim *et al.*, 1993; Soldati and Boothroyd, 1993). The remarkably high transfection efficiency allows *T. gondii* to be developed as an attractive tool for gene expression. Since then, an increasing number of heterologous reporter transgenes has

been generated. These reporters include green fluorescent protein (GFP), epitope tagging, and enzymes such as chloramphenicol acetyl transferase (CAT) and β -galactosidase (LacZ) (Table 1.1; Gubbels *et al.*, 2007). The expansion of this application on *T. gondii* has advanced our knowledge in understanding the parasite's intracellular development, protein trafficking and organellar targeting.

Beyond the transfection efficiency, the suitability of the selectable markers is another key consideration. Typically a plasmid DNA harbors two expression cassettes. The first one encodes the target gene and the second one is with the selectable marker (Striepen and Soldati, 2007). After electroporation, the plasmid DNA is introduced into the parasites, mainly tachyzoites, and the expression of the selectable marker subsequently enables the transformants to be selected. A wide variety of selection markers is available to *T. gondii*, such as CAT, dihydrofolate reductase-thymidylate synthase (DHFR-TS), and hypoxanthine- xanthine-guanine phosphoribosyl transferase (HXGPRT). The drug selection is very specific for the parasites, normally without causing substantial toxicity to the host cells. Hence, the establishment of a stable transgenic line is reasonably successful and efficient in *Toxoplasma*.

Transcription in *Toxoplasma* is monocistronic in nature and the transcription efficiency depends on the promoter elements that are closely in the proximity to the transcription start site (Striepen and Soldati, 2007). The choice of a suitable promoter for the expression vector is very critical since it affects the timing and the expression of the transgenes (Gubbels *et al.*, 2007). Despite these concerns, it is generally not an obstacle to transgenes establishment. Both constitutive and regulatable promoters were designed for *Toxoplasma* expression vector, which may be different in transcription strength and can be stage-specific. The commonly used constitutive promoters are derived from α -tubulin (TUB1), DHFR, several dense-granule proteins (GRAs), rhoptry protein 1 (ROP1), and microneme protein 2 (MIC2). The GRAs and MIC2 promoters are the strongest promoters and the DHFR promoter is the weakest one. All these promoters are specific for the tachyzoite stage while the bradyzoite antigen 1 (BAG1), heat shock protein 70 (HSP70) and enolase 2 (ENO2) promoters are for the bradyzoites. For the regulatable promoter, the tetracycline (tet) repressor system is the most effective system, also known as 'tet off' model (Meissner *et al.*, 2001). In this system, the promoter is activated once the Tet operator (TetO) is occupied by the

Tet-transactivator protein (TetTA). When anhydrotetracycline (ATc) is present, TetTA is displaced from the TetO region. Consequently, the promoter is inactivated and in turn leads to the gene suppression (Fig. 1.1A; Meissner *et al.*, 2007).

Table 1.1 Applications of the reporter genes in *T. gondii*
(summarized from Gubbels *et al.*, 2007)

Reporter gene	Examples	Applications
Enzyme	CAT	Enzymatic assay, colorimetric assay or bioluminescent assay for drug screening and growth comparison
	Luciferase LacZ	Bioluminescent imaging
Epitope tagging	HA	Subcellular localisation
	Myc	Protein processing
	FLAG	Immunoprecipitation
Fluorescence	GFP	Microscopic analysis
	YFP	Organelle biogenesis
	RFP	Parasite trafficking
		Growth assay Counter-selection by flow cytometry
Reporters for animal models	YFP-YFP	Infection process
	luciferase	Real-time imaging Toxoplasmosis and immunological studies
		Bioluminescent imaging and two-photon microscopy

1.1.2 The Establishment of *Toxoplasma* Mutants

To evaluate the importance of a target gene, a detailed phenotypic analysis on its knock-out or knock-down depletion mutant can provide informative data regarding its specific functional roles. This section will briefly describe the approaches for the establishment of mutants in *T. gondii*.

Gene knock-out approach in *T. gondii* is based on homologous recombination between the target locus in the genome and the modified locus presented in the transfected plasmid. Homologous recombination can be either single or double (Fig 1.1B; Striepen and Soldati, 2007). Although *T. gondii* is haploid organism, the generation of knock-out mutants is still not an easy task due to the high frequency of non-homologous recombination. One improved strategy is to increase the homologous regions (Donald and Roos, 1994) in order to increase the frequency of homologous recombination. An alternative approach is to introduce a negative selection marker that can be used to counter-select against the non-homologous integration (Mazumder *et al.*, 2006). The latest approach is to use a mutant parasite strain deficient in end-joining repair mechanisms for the non-homologous recombination, which can efficiently achieve gene replacement (Fox *et al.*, 2009; Huynh and Carruthers, 2009).

In case of studying an essential gene in *T. gondii*, a ‘tet-off’ based conditional knock-out approach is commonly used. First, a parental parasite line is stably transfected with an additional copy of the target gene, which can be suppressed by a tetracycline repressor system (Meissner *et al.*, 2002; see **Section 1.1.1**). Secondly, the endogenous target gene is knocked out in these parasites. As a result, the exogenous copy of the target gene in knock-out mutant can be suppressed in the presence of ATc. Another approach is using site-specific recombination to temporally knock out the target gene by using inducible recombinase such as Cre or Flp, which was reported in *Plasmodium* (Carvalho *et al.*, 2004). Although the site-specific system was successfully established in *T. gondii* (Brecht *et al.*, 1999), a ‘tet-off’ based recombination system has not yet established (Meissner *et al.*, 2007).

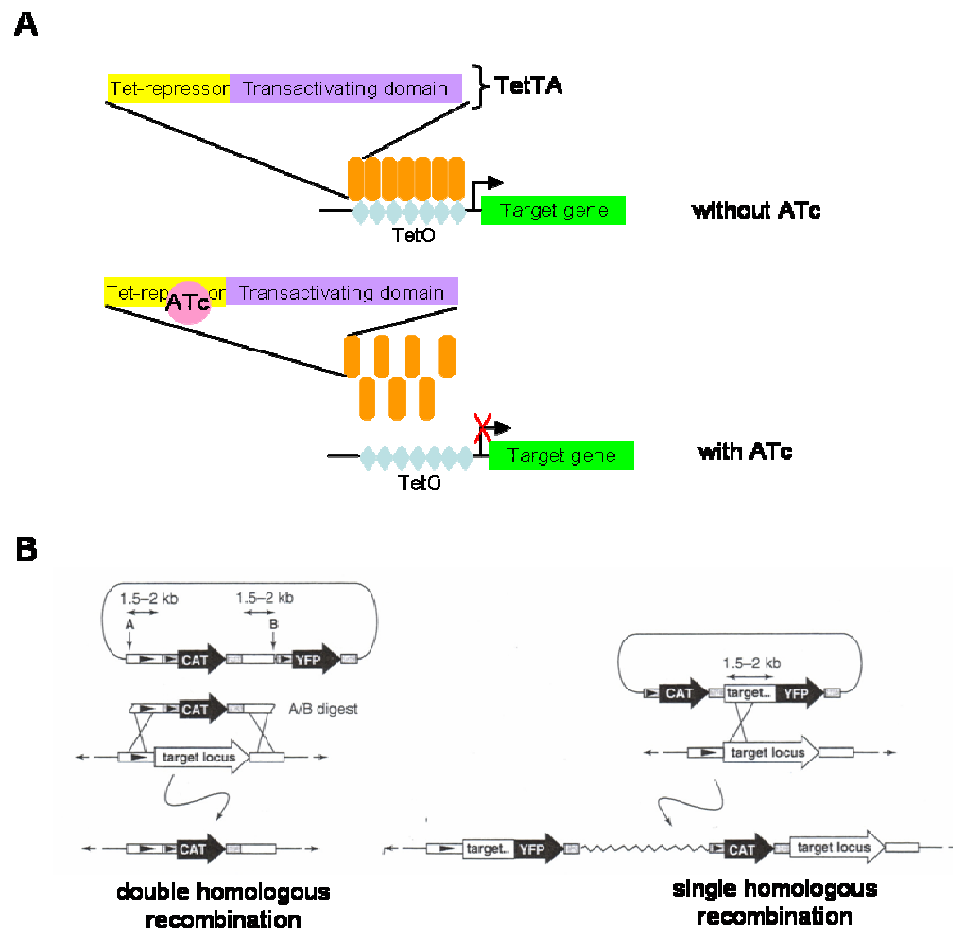


Figure 1.1 Genetic manipulation in *T. gondii*. (A) The ‘tet off’ system. It consists of a cascade of Tet-Operator (TetO) DNA repeats and Tet-transactivator protein (TetTA), a fusion of *E. coli* Tet-repressor and *T. gondii* transactivating domain. In the absence of anhydrotetracycline (ATc), the TetTA is bound to the TetO repeat that activates the promoter and in turn leads to the gene expression. In the presence of ATc, the promoter is inactivated due to the displacement of TetTA from the TetO repeats (modified from Meissner *et al.*, 2007). (B) Schematic diagram describing gene knock-out approach through double (left panel) or single homologous recombination (right panel). The transfected plasmid (linear plasmid on left panel; circular plasmid on right panel) contains a selection cassette CAT and the homologous regions (white boxes) or even a negative selection marker such as YFP. A crossover event leads to the disruption of the endogenous gene locus (adapted from Striepen and Soldati, 2007).

For gene knock-down, recent studies have adapted a ligand-regulatable FKBP destabilization domain (ddFKBP) to control the protein expression both in *Plasmodium* and *Toxoplasma* (Armstrong and Goldberg, 2007; Herm-Gotz *et al.*, 2007). This system is modified from the original finding (Banaszynski *et al.*, 2006) that an engineered human FKBP12 was able to be stabilized by the binding of a synthetic ligand, called Shield-1 (Shld1). When ddFKBP is fused a target protein, the destabilization domain causes the degradation of the fusion protein. But in the presence of Shld-1, this domain is stabilized so that the fusion protein is able to be expressed. Accordingly, the parasites expressing ddFKBP-MyoA fusion were successfully and reversibly regulated in Shld1-dependent manner within few hours (Herm-Gotz *et al.*, 2007). Such a rapid protein regulation will be an impressive tool in studying the protein functions in apicomplexan parasites.

Another feasible method for gene knock-down is the application of RNA interference (RNAi). It has been predicted that the *Toxoplasma* but not *Plasmodium* genome encodes the necessary proteins for the RNAi pathway (Ullu *et al.*, 2004). Previous works also have demonstrated that by using hammerhead ribozymes and dsRNA could significantly suppress the target mRNA (Al-Anouti and Ananvoranich, 2002; Al-Anouti *et al.*, 2003). However, the application of RNAi in *T. gondii* is still uncertain since several groups failed to knock down their target genes by using this approach (Gubbels *et al.*, 2007). Since RNAi technique is around the corner and has been successfully applied to different organisms, it remains a considerable alternative for gene knock-down in *T. gondii* in the future.

1.2 *T. gondii* as a Model System for Apicomplexan Drug Discovery

In the past decades, the widespread of drug resistance has emerged as a major impediment to the treatment of parasitic diseases. In particular, malaria resistance to chloroquine has been increasingly reported throughout many endemic regions (Carlton *et al.*, 2008; Fidock *et al.*, 2008). Therefore, the development of a novel and potent antiparasitic drug is essential. Several emerging novel drug targets, including the apicoplast metabolic pathways, the mitochondrial enzymes, and the histones involved in epigenetic regulation, sound promising and attractive (Table 1.2; Donald, 2007; Fidock *et al.*, 2008). However, it should be noted that the members in Apicomplexa

have their diversity of metabolism. These drug targets may not be applicable to all the members. Therefore, the validation of drug target is another important topic of drug discovery. Moreover, it should be emphasized that drug resistance can only partly explain the chemotherapeutic failure. Under this circumstance, drug validation will provide critical information for improving the drug efficacy. Although drug resistance currently seems not a major clinical issue for the treatment of *T. gondii* (McFadden *et al.*, 2001), *T. gondii* has been implicated in the discovery of antiparasitic drugs as well as used for the validation of drug targets (Donald, 2007). Some examples of using *Toxoplasma* as a model for drug identification and target validation will be delineated in the following section.

1.2.1 The Identification of Drug Targets

Previous studies have observed that the antibiotics such as tetracycline, macrolides and clindamycin could efficiently protect against several parasitic infections (Luft and Remington, 1988; Roos *et al.*, 1999; McFadden *et al.*, 2001). These antibiotics are known to inhibit bacterial translation, suggesting that the protozoan parasites may possess similar prokaryotic translation machinery. Specifically, one typical example is the large subunit antibiotics including macrolides and lincosamides, which targets the large subunit of the ribosome in prokaryotes. When *Toxoplasma* and *Plasmodium* both were treated with these antibiotics, a delayed replication was consistently observed (Divo *et al.*, 1985; Fichera *et al.*, 1995). Initially, it was thought that the antibiotics targeted at mitochondrial translation. Until the identification of the non-photosynthetic plastid-like sequence from *Plasmodium* in late 1990s, it partly explains the inhibitory effects of these prokaryotic antibiotics. However, the clear evidence provided actually was obtained in *Toxoplasma* indicating that the apicoplast is indeed the target of these antibiotics. First, DNA hybridization analysis provides direct evidence that the plastid genome was selectively lost in response to clindamycin treatment (Fichera and Roos, 1997). Secondly, experiment results showed that the cytosolic and mitochondrial protein syntheses were not affected by these antibiotics (Beckers *et al.*, 1995). Moreover, the plastid DNA gyrases were identified as the targets for ciprofloxacin, a fluoroquinolone compound (Fichera *et al.*, 1995). Taken together, *T. gondii* has been used as an important model to identify that the apicoplast is the target organelle (Beckers *et al.*, 1995; Fichera and Roos, 1997).

Table 1.2 Novel drug targets in *Plasmodium* and *Toxoplasma*
(summarized from Donald, 2007; Fidock *et al.*, 2008)

Targets	Specific pathways involved
Apicoplastic metabolism	1-deoxy-D-xylulose 5-phosphate reductase Lipid metabolism Protein synthesis and transcription
Cytoskeletal proteins	Tubulin polymerization
Cytosolic pathways	Choline synthesis Shikimate pathway Thioredoxin reductase Vitamine B6 synthesis
Epigenetic regulation	Histone deacetylase and acetyltransferase
Mitochondrial enzymes	Dihydroorotate dehydrogenase Electron transport enzyme complexes
Proteases	Subtilisin-like proteases Cysteine/aspartic proteases
Protein kinases (Doerig <i>et al.</i> , 2008)	Cyclin-dependent kinases Caesein kinase 1
Transporters	V-type H ⁺ - ATPase Folate-biopterin transporters

Since *T. gondii* is amenable to genetic manipulation, using complementation strategy is another method for target validation. An earlier work has shown that a *Cryptosporidium* library could complement *T. gondii* HXGPRT-deficient mutant in the presence of mycophenolic acid, an inosine 5-monophosphate-dehydrogenase (IMPDH) inhibitor that prevents purine salvage pathway. This finding identified that the IMPDH (Striepen *et al.*, 2002) is as a promising target against *Cryptosporidium parvum*. Due to the difficulty of *in vitro* propagation of *Cryptosporidium*, *T. gondii* is a useful tool for studying the nucleotide metabolism of *C. parvum* (Striepen *et al.*, 2004). Moreover, *Toxoplasma* has been used as a model for understanding apicomplexan lipid metabolism and cytoskeletal architecture. Chemotherapeutic targets of the fatty acid synthesis (FAS) II pathway and tubulin polymerization have been validated in *T. gondii* (Donald, 2007).

1.2.2. The Validation of Drug Targets

The mitochondrial complex III inhibitor atovaquone is one of the effective antimalaria drugs. However, the target of atovaquone was identified with the help of *Toxoplasma*. Atovaquone belongs to the hydroxynaphthoquinone compound, which is structurally similar to ubiquinone (CoQ), the electron carrier in the respiratory chain. CoQ can occupy cytochrome bc_1 complex at Q_1 site to accept electrons and at Q_o site to donate electrons. Although biochemical analysis in *Plasmodium* suggests that atovaquone interferes with ubiquinone by targeting at the cytochrome bc_1 complex (Fry and Pudney, 1992), the identification of the atovaquone binding site was eventually validated in *Toxoplasma* (McFadden *et al.*, 2000). Two mutation sites were identified in the Q_o domain of the cytochrome b gene from the atovaquone-resistant mutant (Pfefferkorn *et al.*, 1993), suggesting that either of these two mutations within the Q_o domain is the key for the drug resistance. Additionally, parasites resistant to another mitochondrial inhibitor decoquinate were observed with a similar mutation within the Q_o domain (McFadden and Boothroyd, 1999), indicating that atovaquone and decoquinate both inhibit the activity of Q_o domain. Later on, the atovaquone-resistant *Plasmodium* was analysed revealing that the mutated residues consistently were restricted to the Q_o domain. *In vitro* drug resistant parasites have become an important tool to identify and validate drug targets.

Besides, *T. gondii* was used as a model to validate the drug target of compound 1 in *Eimeria* (Donald *et al.*, 2002; Donald and Lieberator, 2002) regarding its biological similarity. However, the life cycle of *Eimeria* cannot be completed *in vitro*, direct drug validation in *Eimeria* is very limited. *T. gondii* was firstly used for heterologous expression of the *Eimeria* cGMP-dependent protein kinase (PKG) that was failed to be expressed in other systems including *E. coli* and yeast (Gurnett *et al.*, 2002). When *Eimeria* PKG was transfected into PKG-resistance mutants, parasites were resistant to compound 1, suggesting that PKG is the major target for compound 1. More drug validation on the other PKG inhibitors and the identification of the second targets of PKG inhibitors were performed in *Toxoplasma* (Donald, 2007).

1.3 Apicomplexan Organelles

The phylum Apicomplexa is characterized by an apical complex of cytoskeletal structures and secretory organelles (Nishi *et al.*, 2008). These organelles including the micronemes, the rhoptries and the dense granules all are engaged in invasion process (Carruthers and Sibley, 1997; Black and Boothroyd, 2000). Most of the apicomplexan parasites also contain the eukaryotic organelles such as endoplasmic reticulum, mitochondrion and nucleus. Additionally, a plastid-like organelle, called apicoplast, is identified in most of the apicomplexa parasites including *Toxoplasma* and *Plasmodium*. The subcellular organelles in *Toxoplasma* are illustrated in Fig 1.2 and Table 1.3.

1.3.1 Apicoplast and Mitochondrion as promising Drug Targets

Among these organelles in apicomplexan parasites, apicoplast and mitochondrion are considered as the intriguing targets for drug development. The apicoplast, a non-photosynthetic plastid-like organelle, is believed to be the product of a secondary endosymbiotic event. Genomic analysis indicates that the apicoplast in *Toxoplasma* and *Plasmodium* is responsible for many essential pathways such as fatty acids, isoprenoid and heme syntheses (Roos *et al.*, 1999; Ralph *et al.*, 2004). Because of its uniqueness in apicomplexan parasites, it has been regarded as a promising organelle for drug development. More importantly, previous works have clearly demonstrated that the apicoplast was essential for parasitic replication and survival (Fichera and

Roos, 1997; Mazumdar *et al.*, 2006). Moreover, the metabolism taking place in the apicoplast is more related to the prokaryotic pathways (Kim and Weiss, 2004), implying that the drugs target very specifically to the parasites rather than the mammalian cells. Collectively, these intriguing observations have ushered the apicomplexan apicoplast as a potential candidate for the strategic drug discovery.

The apicomplexan mitochondrion is considered another important antiparasitic target owing to the significant difference of the energy metabolism adapted in parasites as compared to their host cells. One of the key mitochondrial targets is the respiratory chain, also known as the electron transport chain (ETC). It includes the complex III inhibitor atovaquone, which has been widely used against *Plasmodium* (Looareesuwan *et al.*, 1999) and *Toxoplasma* (McFadden *et al.*, 2001). The specificity of this compound acting on the mitochondria has been experimentally validated (Srivastava *et al.*, 1997; Krungkrai, 2004). Further experimental results have revealed the promising antiparasitic effects from the other mitochondrial respiratory inhibitors (Omura *et al.*, 2001; Biagini *et al.*, 2006), suggesting that the enzyme complexes in the respiratory chain are the promising targets. More recent, the mitochondrial enzyme dihydroorotate dehydrogenase (DHOD) has been identified as a potential target against *Plasmodium* (Painter *et al.*, 2007). DHOD is the fourth enzyme of the essential pyrimidine *de novo* biosynthetic pathway that requires ubiquinone as electron acceptor. It demonstrated that the over-expression of ubiquinol-independent DHOD could resist to the atovaquone, suggesting that the role of complex III in *Plasmodium* is to recycle ubiquinone for DHOD. This finding once provoked a heat debate since it suggested that other mitochondrial dehydrogenases are non-essential in *Plasmodium* (Vaidya *et al.*, 2007; Fisher *et al.*, 2007). Because of the urgency of drug-resistance in malaria, it may be too early to exclude other potential targets. To combat the parasitic diseases, the current challenge is to improve the drug efficacy and the drug specificity by using combinatory treatments.

1.3.2 The Apicomplexan Mitochondrial Respiratory Chain

The importance of the mitochondrial respiratory chain in the apicomplexan parasites is evident with the antiparasitic effects by several ETC inhibitors (Srivastava *et al.*, 1997; Vercesi *et al.*, 1998; Biagini *et al.*, 2006). Previous studies demonstrated that using

this kind of inhibitors led to a dramatic collapse of $\Delta\psi_m$ in *Plasmodium* and even caused parasite deaths (Srivastava *et al.*, 1997; Biagini *et al.*, 2006). These observations clearly indicate that the mitochondrial respiratory chain is essential to maintain the mitochondrial functions. However, the importance of the respiratory chain in *Plasmodium* remains controversial since the biochemical data indicates that the ATP source in the erythrocytic stage is mainly obtained from glycolysis rather than from the respiratory chain (van Dooren *et al.*, 2006).

On the other hand, the respiratory chain in *Toxoplasma* seems to play a pivotal role in energy metabolism. *Toxoplasma* harbours the complete sets of enzymes for the glycolytic pathway and the tricarboxylic acid (TCA) cycle (Fleige *et al.*, 2007, 2008). Therefore, the respiratory chain is expected to maintain the NADH/NAD⁺ ratio since the recycled NAD⁺ is necessary to make other metabolic pathways to be functioned. Secondly, the complexes of the respiratory chain are responsible for the establishment of the electrochemical proton gradient that can provide the driving force for ATP synthase (ATPase; Vercesi *et al.*, 1998).

So far, no direct evidence has been provided about the mitochondrial activities in *Babesia* and *Theileria* (Seeber *et al.*, 2008). Moreover, *Cryptosporidium*, the much more evolutionary distant parasite as compared to *Toxoplasma*, does not encode the components for the respiratory chain due to the absence of the typical mitochondrion. Instead, this parasite possesses an organelle, called mitosome, which contains an alternative terminal oxidase for direct electron transfer from ubiquinone to O₂.

Nevertheless, the majority of the apicomplexan parasites possess the components for the respiratory transport chain. The following section will depict these common features of the respiratory chain.

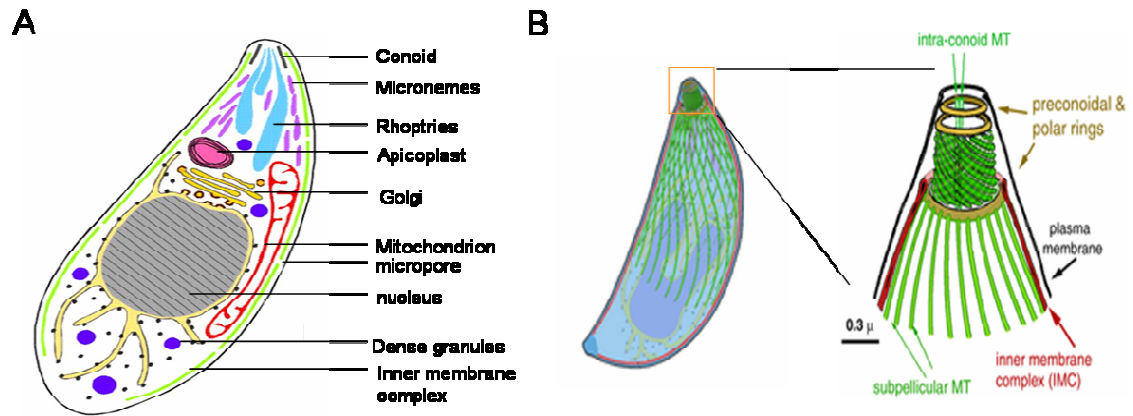


Figure 1.2 Organelles and subcellular structures of *T. gondii*. (A) Schematic representation of the organellar arrangement in tachyzoite stage (adapted from Nishi *et al.*, 2008). (B) Cytoskeletal network of *T. gondii*. MT, microtubules. (adapted from Hu *et al.*, 2006)

Table 1.3 Functions of the unique organelles in *T. gondii*
(summarized from Dubey *et al.*, 1998; Black and Boothroyd, 2000)

Organelle	Functions
Apicoplast (Roos <i>et al.</i> , 1999)	Fatty acid synthesis Heme biosynthesis Isoprenoid biosynthesis
Cytoskeleton (He <i>et al.</i> , 2006)	Including conoid, the polar rings, the microtubules (MT), and the inner membrane complex To provide the structural integrity To direct the protein secretion during invasion For gliding on host cell surfaces
Dense granules	Involved in the late invasion process
Micronemes	Host attachment in the early invasion process
Micropore	Acting as the active site of endocytosis
Rhoptries	An important role in parasite virulence Containing proteolytic enzymes for host cell penetration during invasion process

1.3.2.1 Oxidation Phosphorylation

The mitochondrial respiratory chain, also known as the electron transport chain, plays a very significant role in the production of ATP through the process called oxidation phosphorylation. This process involves two steps – the release of the free energy during the electron transport, and the generation of the electrochemical proton gradient that provides the free energy for ATPase. The whole process involves the consumption of oxygen and the catalysis of ADP to ATP. It is thus called oxidative phosphorylation (Scheffler, 2001).

The mechanism of oxidation phosphorylation is described as follows. Firstly, the electron transport starts as the high-energy electrons are converted from a hydride ion (H^-) being removed from NADH or $FADH_2$. The electrons next are passed along the enzyme complexes through a series of oxidation-reduction reaction, where the ubiquinone and cytochrome c act as mobile carriers to transfer the electrons between the complexes. The electron transport is energetically favorable so that the electrons are readily to be passed along the chain. Eventually the released energy allows the enzymes complexes III and IV (also complex I in mammalian cells) to pump the H^+ from the matrix into the intermembrane space. This pumping action eventually generates an electrochemical proton gradient across the inner mitochondrial membrane, which is composed of a gradient of proton concentration and a membrane potential. The latter component contributes the majority of the electrochemical proton gradient. Consequently, this gradient drives the flow of H^+ back to the matrix through ATPase. The ATPase uses the released energy to synthesize ATP from ADP in the matrix.

Further information about the reducing equivalents NADH and $FADH_2$ mentioned above should be described here. They can be generated from the TCA cycle in mitochondrial matrix or transferred from cytosol into mitochondrion by metabolic glycerol-3-phosphate (G3P) shuttle or/and malate/aspartate shuttle. However, it is still unclear whether these metabolic shuttles exist among the apicomplexan parasites. In *Toxoplasma*, G3P shuttle is very likely to be present, which is based on the identification of the cytosolic localized glycerol-3-phosphate dehydrogenase (G3PDH; Fleige *et al.*, 2007). Also, this shuttle is suggested to be present in *Plasmodium* (Fry

and Beesley, 1991; Uyemura *et al.*, 2004). Experiments have demonstrated that the addition of exogenous G3P could stimulate the respiratory chain (Uyemura *et al.*, 2004). Additionally, both NAD⁺-linked and FAD-linked G3PDH are predicted in the *Plasmodium* genome (van Dooren *et al.*, 2006). However, no supportive evidence exists so far for the presence of the malate/aspartate shuttle among the apicomplexan parasites. In spite of this, the reducing equivalents NADH or FADH₂ donate their high-energy electrons into the respiratory chain, which is catalyzed by several dehydrogenases. The details of the other dehydrogenases in *T. gondii* are summarized in Table 1.4.

Like the mammalian cells, the apicomplexan parasites contain the similar components in the respiratory chain, including the enzyme complexes, ubiquinone and cytochrome c (Fig. 1.4; van Dooren *et al.*, 2006; Seeber *et al.*, 2008). The apicomplexan enzyme complexes are type II NADH dehydrogenase (NDH2; single subunit), complex II (succinate: ubiquinone oxidoreductase), complex III (cytochrome bc₁ complex), complex IV (cytochrome oxidase), and complex V (ATPase). Among these enzyme complexes, the apicomplexan parasites possess NDH2 (single subunit) instead of conventional complex I present in mammalian cells. Nevertheless, they share similar function as that in the mammalian cells. Further information of the respiratory enzyme complexes is illustrated in Fig 1.3 and Table 1.5.

1.3.3 Type II NADH Dehydrogenases

NDH2, also known as the alternative complex I, has been described in prokaryotes, plants, fungi and many apicomplexan parasites, with the exception in mammals (Kerscher, 2000; Weinstein *et al.*, 2005; Biagini *et al.*, 2006; Saleh *et al.*, 2007). Compared to the conventional NADH dehydrogenase (complex I) and the prokaryotic sodium pumping NADH dehydrogenases, NDH2 does not possess any proton or sodium pumping property due to the absence of energy-transducing sites. Our current knowledge of this atypical NDH2 is still very limited. However, it is generally accepted that the main function of NDH2 is to catalyze the transfer of the electrons from NAD(P)H to quinone in the respiratory chain, which in turn contributes to the production of ATP. Up to now, it remains a mystery why these organisms favor NDH2 instead of complex I as expressed in mammalian cells, or co-express NDH2

together with the complex I. The commonly accepted hypothesis for this phenomenon is to minimize the formation of the reactive oxygen species since complex I is one of the major sources of the superoxide anion radicals in mitochondria (Fisher *et al.*, 2007; Kerschler *et al.*, 2008). Apart from that, an additional advantage for the presence of NDH2 proposed in *Plasmodium* is to balance of the proton gradient in the respiratory chain (Fisher *et al.*, 2007). As suggested, parasites adapted in a microaerophilic environment may not produce extensive ATP by oxidative phosphorylation. Therefore, they have to adjust the proton gradient either by reducing the protons to be pumped into the intermembrane space or by modifying the membrane components such as the expression of uncoupling proteins (Uyemura *et al.*, 2004) that allows the re-entry of protons to the matrix. Because of the non-proton pumping property of NDH2, this may be a possible purpose for this enzyme to reduce the proton 'back-pressure' in *Plasmodium* respiratory chain (Fisher *et al.*, 2007).

1.3.3.1 Structural Characteristics of NDH2s

NDH2s are single polypeptides usually with the molecular masses of 50-60 kDa. They possess two characteristic regions called GXGXXG motifs that consist of the $\beta\alpha\beta$ domain for the binding of NAD(P)H and the cofactor flavin adenine dinucleotide (FAD) or flavin mononucleotide (FMN). The first GXGXXG motif is located near to the N-terminus and has been predicted as the non-covalent binding site for FAD. This prediction is based on the X-ray crystallography data of the bacterial lipoamide dehydrogenase, showing that FAD binds to the first $\beta\alpha\beta$ domain. A previous study has suggested that NDH2 and lipoamide dehydrogenase in bacteria share a common ancestry (Bjorklof *et al.*, 2000). Beyond these two motifs, some NDH2s, such as *Solanum tuberosum* and *Neurospora crassa*, contain an additional Ca^{2+} -EF-hand motif, which is responsible for membrane interaction (Melo *et al.*, 2004). According to the arrangements of the binding motifs, NDH2s can be clarified into three groups A, B and C (Fig. 1.4A; Melo *et al.*, 2004). Group A containing both $\beta\alpha\beta$ domains can be found in eukaryotes, bacteria and archaea. Group B is similar to group A with an additional EF-hand motif, mainly found in eukaryotes such as plants and fungi. Group C only conserves a single $\beta\alpha\beta$ domain, which is restricted to hyperthermophilic archaea.

Table 1.4 Properties of the dehydrogenases in *T. gondii*

Dehydrogenase	Localization (expected)	Properties
Dihydroorotate dehydrogenase (DHOD)	Mitochondrion	dihydroorotate $\xrightarrow[\text{CoQH}_2]{\text{CoQ}}$ orotate
NAD ⁺ -linked glycerol-3-phosphate dehydrogenase I (G3PDH I) (Fleige <i>et al.</i> , 2007)	Cytosol	DHAP $\xrightarrow[\text{NADH}]{\text{NAD}^+}$ G3P
FAD-linked G3PDH (putative)	Mitochondrion	G3P $\xrightarrow[\text{FADH}_2]{\text{FAD}}$ DHAP
Isocitrate dehydrogenase I (Fleige <i>et al.</i> , 2008)	Mitochondrion (TCA cycle in matrix)	isocitrate $\xrightarrow[\text{NADH}_2]{\text{NAD}^+}$ α -ketoglutarate
α -ketoglutarate dehydrogenase complex	Mitochondrion (TCA cycle in matrix)	α -ketoglutarate $\xrightarrow[\text{NADH}_2]{\text{NAD}^+}$ succinyl-CoA
Branched-chain α -keto acid dehydrogenase complex (Fleige, 2006)	Mitochondrion	R-CHNH ₃ ⁺ -COO ⁻ $\xrightarrow[\text{NADH}_2]{\text{NAD}^+}$ R-CO-S-CoA end products are branched-chain acyl CoAs
Malate dehydrogenase (Fleige <i>et al.</i> , 2008)	Mitochondrion (TCA cycle in matrix)	malate $\xrightarrow[\text{NADH}]{\text{NAD}^+}$ oxaloacetate
FAD-dependent malate:ubiquinone oxidoreductase (Fleige <i>et al.</i> , 2008)	Mitochondrion	Oxidizing electrons from FADH ₂ to CoQ
Succinate:ubiquinone oxidoreductase (Saleh, 2006)	Mitochondrion (inner membrane)	succinate $\xrightarrow[\text{FADH}_2]{\text{FAD}}$ fumarate Oxidizing electrons from FADH ₂ into CoQ
Type II NADH dehydrogenases (TgNDH2-I & -II) (Lin <i>et al.</i> , 2008)	Inner mitochondrial membrane (orientation is investigated in this study)	Oxidizing electrons from NADH to CoQ

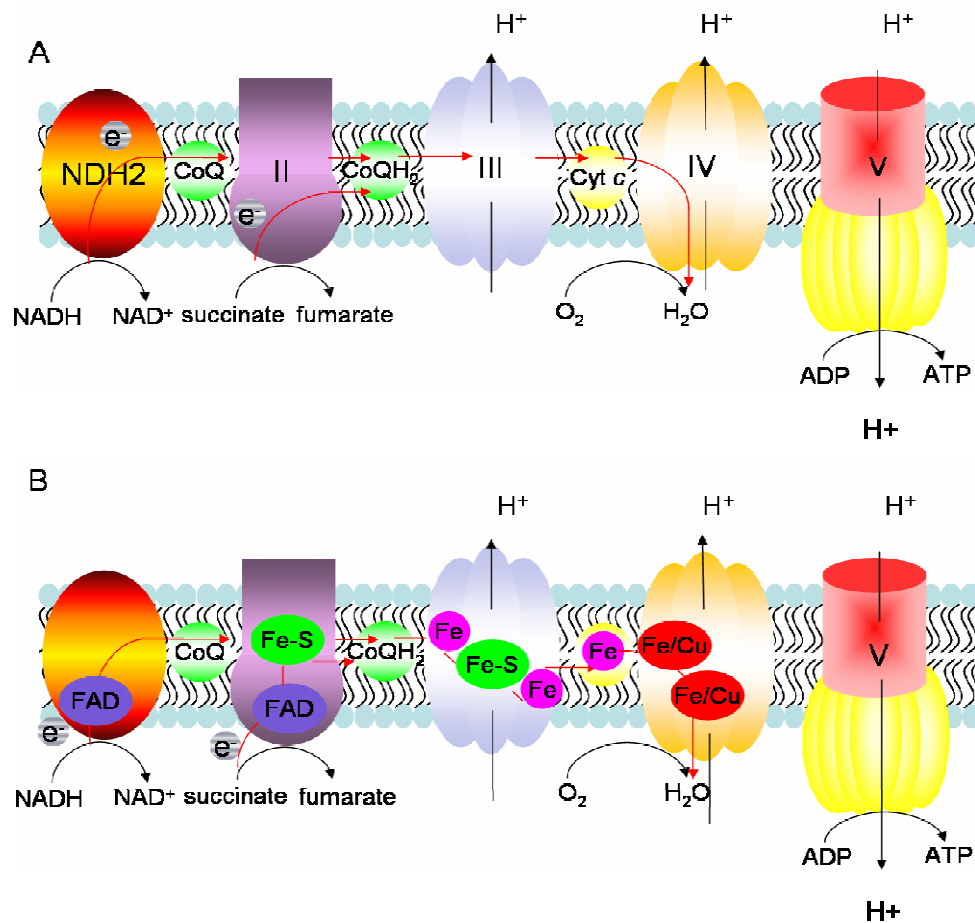


Figure 1.3 Model of the apicomplexan mitochondrial respiratory chain. (A) The major components are enzyme complexes, ubiquinone (CoQ) and cytochrome c . The enzyme complexes are type II NADH dehydrogenase (single subunit; NDH2), complex II (succinate: ubiquinone oxidoreductase), complex III (cytochrome bc_1 complex), complex IV (cytochrome oxidase), and complex V (ATPase) (B) The sequential electron carriers in the respiratory chain. The enzyme complexes may contain prosthetic group (FMN or FAD) that facilitates the catalytic reaction, and iron-sulfur (Fe-S) proteins, where a serial of oxidoreduction reaction is taking place. Cyt c , cytochrome c ; $CoQH_2$, ubiquinol (reduced CoQ).

Table 1.5 Structural and functional properties of the apicomplexan respiratory complexes
(summarized from Saraste, 1999)

Component	Structural properties	Functions
Type II NADH dehydrogenase	One single subunit Containing FAD or FMN	Transfer electrons from NADH to CoQ A role in maintaining $\Delta\psi_m$ in <i>Plasmodium</i> (Biagini <i>et al.</i> , 2006)
Complex II (Succinate: ubiquinone oxidoreductase)	~ 4 subunits Containing one FAD or FMN and several iron-sulfur center	A component in the TCA cycle Transfer electrons from FADH ₂ to CoQ
Complex III (Cytochrome bc ₁ complex)	~ 9-10 subunits Containing diheme cytochrome c, cytochrome c1 and Rieske iron-sulfur center One subunit is encoded by mitochondrial DNA (mtDNA; in mammalian cells)	Transfer electrons from ubiquinol (CoQH ₂) to cytochrome c Proton-pumping property Two active sites including Q for the oxidation of CoQH ₂ and release of protons, and Q ₁ for reduction of CoQ
Complex IV (Cytochrome oxidase)	13 subunits 3 major subunits are encoded by mtDNA Subunits contain Fe/Cu centres	Reduce oxygen to water D channel is essential for proton pumping activity
Complex V (ATPase)	F ₀ (a,b,c) and F ₁ ($\alpha,\beta,\gamma,\delta,\epsilon$) subunits (is diverged among the parasites; Seeber <i>et al.</i> , 2008) Two subunits are encoded by mtDNA (in mammalian cells)	Both ATP synthesis and hydrolysis Proton-pumping property F ₀ contains proton channel and F ₁ contains catalytic component

Although the primary structure of the NDH2s seems very highly conserved, several features such as the substrate specificity and the cofactor preference are far from our understanding. First, some NDH2s have been reported to be able to oxidize both NADH and NADPH (Rasmusson *et al.*, 2004; Geisler *et al.*, 2007) substrates. This kind of substrate specificity seems very difficult to extract from the primary structures. Although several prediction models have been proposed for the specificity for NAD(P)H, it is not widely applied (Bernard *et al.*, 1995; Melo *et al.*, 2004). Accordingly, the second β sheet in the putative NADH binding domain (second GXGXXG motif) is usually ended with an acidic residue, glutamate or aspartate. One explanation is that these negative charged amino acids will repel the negative charges of the phosphate group of NADPH, rendering NADH as the specific substrate. In *N. crassa*, the NADH dehydrogenases have conserved acidic residue GluAla (EA) or AspVal (DV), whereas the NADPH dehydrogenases encode GlnSer (QS) instead (Fig. 1.5B; Michalecka *et al.*, 2004). Additional experiments have demonstrated that a single mutation of aspartate to neutral amino acid in NADH lactate dehydrogenase and formate dehydrogenase can modify the enzyme specificity to accept NADPH in addition to their original substrates (Feeney *et al.*, 1990; Gul-Karaguler *et al.*, 2001). These are striking findings in plant biology since using NADPH as substrate may be advantageous to overcome the oxidative stress (Michalecka *et al.*, 2004). However, using primary structure to evaluate the substrate specificity is still used a reference, the ultimate step requires experimental validation. Regarding the identification of the cofactors associated within NDH2s, it is unlikely to be speculated from the primary structure. The associated cofactors are more likely to be species-dependent and only experimental results can reveal their interaction with the binding domains in NDH2s.

1.3.3.2 Membrane Interaction of NDH2s

Each single mitochondrion in eukaryotic cells contains two membrane-bounded compartments, the internal space, called matrix, and the intermembrane space. These two compartments are created by the outer and the inner mitochondrial membranes, both are comprised of a lipid bilayer. In particular, the inner mitochondrial membrane contains most of the proteins that are responsible for the respiratory chain and for metabolite exchanges.

NDH2 is known to be localized to the inner mitochondrial membrane as a component in the respiratory chain. However, the mechanism involved in the membrane anchoring in this enzyme remains unclear. Bioinformatics analyses of the primary structures of the NDH2s from different species are unable to predict any transmembrane helices (Melo *et al.*, 2004). A widely accepted model is that NDH2 attaches to the membrane using amphipathic α -helices (Bandeiras *et al.*, 2002; Melo *et al.*, 2004), where the hydrophobic and hydrophilic residues are situated on the opposite sides on the helical surface. This kind of helices is predicted to be present in the secondary structures in the majority of the NDH2s (Melo *et al.*, 2004). For instance, *Plasmodium* NDH2 is predicted with a C-terminal amphipathic α -helices (Fisher *et al.*, 2007). Additionally, the interaction of NDH2 with the membrane seems very strong based on the observation that the activity of NDH2 could be increased with a longer incubation with the lipids (Bjorklof *et al.*, 2000; Gomes *et al.*, 2001). As predicted in *Plasmodium* NDH2, some residues within the amphipathic helices can be oriented in the bilayer that the headgroups are directly interacted with the membrane. Under this circumstance, the direct electrostatic interaction between NDH2 and the bilayer can be a reasonable explanation for the importance of lipid environment for the enzyme activity.

One major function of NDH2 is to transfer electrons from NADH into quinone (including ubiquinone) in the respiratory chain. Due to the interesting combination of electron transfer between the hydrophilic NADH and the hydrophobic quinone, it is generally accepted that the quinone (Q) sites are interfaced at the membrane surface. To be more specific, the hydrophilic headgroup of the quinone is more likely to interact with the enzyme since the reduction to quinol requires the proton that is in the aqueous phase. This speculation implies that the ubiquinone-binding site in NDH2 is more specific to the ubiquinone headgroup (Eschemann *et al.*, 2005). Although Fisher and Rich have proposed two types of quinone-binding sites (Fischer and Rich, 2000) in NDH2, which is characterized by a putative conserved histidine or tyrosine residues, it is not widely applicable due to the diversity of NDH2s. The quinone-binding regions still are unpredictable from the primary structures and most of the available quinone-binding sites are based on the predictions from comparative modeling

(Fischer and Rich, 2000). X-ray crystallography data are crucial to unveil the exact quinone-binding sites for NDH2s.

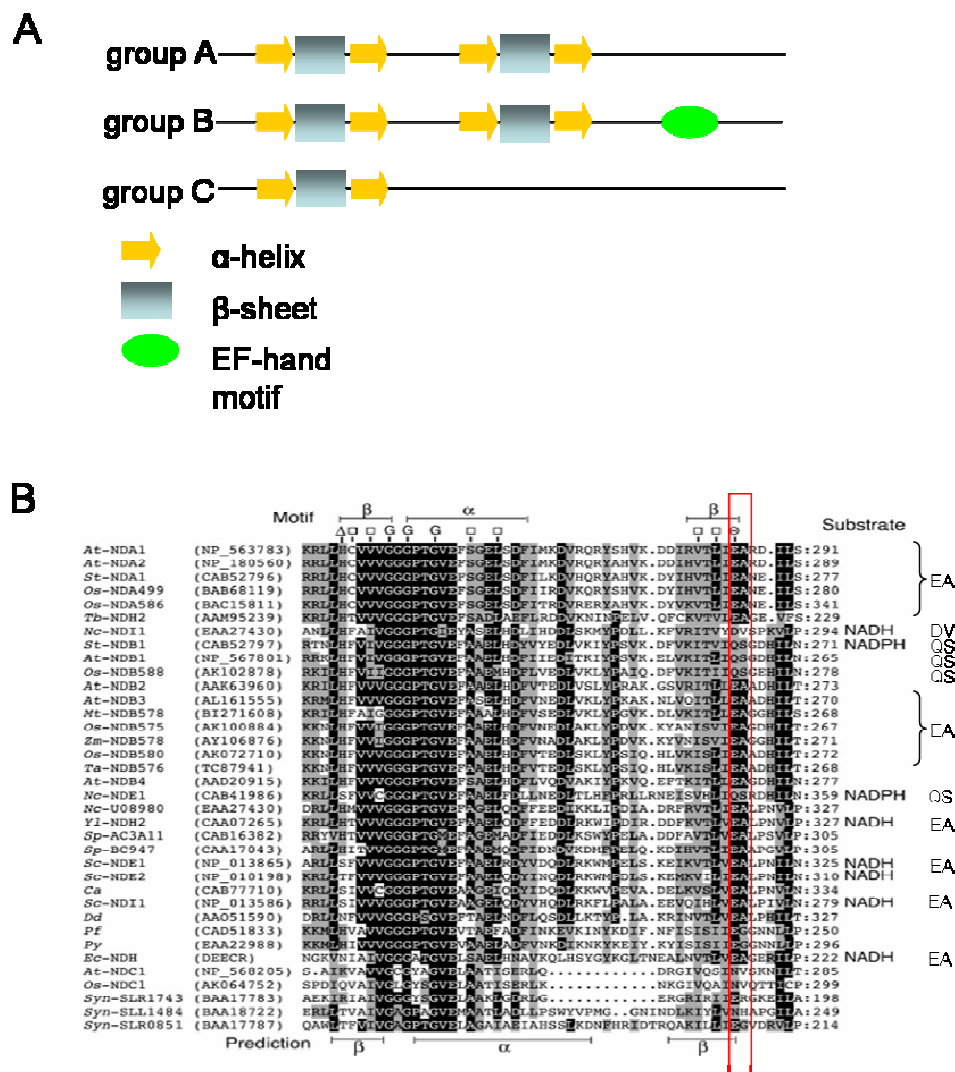


Figure 1.4 Eukaryotic type II NADH dehydrogenases. (A) Classification of NDH2s is based on the arrangement of the binding motifs. They are listed as follows: two $\beta\alpha\beta$ binding motifs for group A; two $\beta\alpha\beta$ binding motifs and one EF-hand motif for group B; and one $\beta\alpha\beta$ binding motif for group C (modified from Melo *et al.*, 2004). (B) Comparison of the substrate specificity for NAD(P)H from the putative NAD(P)H-binding domain in eukaryotic NAD(P)H dehydrogenases. The last two residues at the second β sheet showing that NADH dehydrogenases may have conserved acidic residue GluAla (EA) or AspVal (DV) but NADPH dehydrogenases have a preference for GlnSer (QS) (modified from Michalecka *et al.*, 2004).

1.3.4 Electrophysiology of Mitochondrial Membrane Potential

As mentioned above, the mitochondrial membrane potential ($\Delta\psi_m$) is the major component of the electrochemical proton gradient that is built up as a consequence of proton pumping by the respiratory chain. In mammalian cells, the proton gradient yields a total energy about 240 mV, containing of 180 mV mainly from $\Delta\psi_m$ and 60 mV from the pH gradient. Although this kind of data has not yet been available in apicomplexan parasites, the physiological impacts of the $\Delta\psi_m$ are expected to be similar to that in mammals. One of the physiological functions of the $\Delta\psi_m$ is to provide the energy stored in proton gradient for the ATPase to synthesize ATP, the energy source. Interestingly, the magnitude of the proton gradient can be varied from different cell types and differentiation stages in mammals. For instance, some cancer cells and myoblasts can adjust their membrane potentials in accordance to their needs in the differential stages (Chen *et al.*, 1988).

Indeed, the regulation of the proton gradient plays an important role in cellular functions. It affects the transport of metabolites, the import of the precursor proteins and mitochondrial protein synthesis. In particular, the importance of $\Delta\psi_m$ in mitochondrial trafficking will be addressed here. Protein import into mitochondrion can be achieved by several pathways such as the common N-terminal presequence, tail-anchor sequence and internal signal. Mitochondrial import machinery consists of the translocase of the outer membrane (TOM) complexes and the translocase of the inner membrane (TIM) complexes, which processes the proteins targeting beyond the outer membrane. Specifically, the transport of the precursor mitochondrial proteins via the TIM23 and TIM22 requires membrane potential and ATP (Truscott *et al.*, 2003). First, the membrane potential supports the transport of the positively charge presequences through the complexes pore into negatively charge matrix, Secondly, the ATP-dependent mitochondrial HSP70 drives the protein translocation into the matrix. These observations clearly implicates the role of $\Delta\psi_m$ in protein trafficking and mitochondrial function.

1.4 Objectives of the Study

The uniqueness of type II NADH dehydrogenases (NDH2s) in the apicomplexan respiratory chain defines these enzymes as a promising drug target. However, the specific roles and the importance of NDH2s (TgNDH2-I and -II) in *Toxoplasma* are still unknown.

The previous study from my current group has shown that the quinolone-like compound 1-hydroxy-2-dodecyl-4(1)quinolone (HDQ) could effectively inhibit the replication of *T. gondii* with an impressive low IC₅₀ in the nanomolar ranges (Saleh *et al.*, 2007). Although HDQ is first identified as a high affinity inhibitor for *Yarrowia* NDH2 (Eschemann *et al.*, 2005), no experimental data so far has been investigated in the apicomplexan orthologs. To follow up this observation, it is particularly important to perform biochemical assays to provide the direct evidence showing that TgNDH2s are indeed the drug targets of HDQ. In this study, the detailed enzymatic parameters including the steady-state kinetics and inhibition kinetics will be investigated.

Secondly, the physiological impact of TgNDH2s in the respiratory chain will be explored including the mitochondrial membrane potential and the parasitic ATP level. These findings will unveil the important role of TgNDH2s in the process of oxidative phosphorylation and their influences in mitochondrial functions. Additionally, the mitochondrial physiology between the tachyzoites and bradyzoites will be compared to reveal their differences in energy dependency. Moreover, this study will elucidate the orientations of both TgNDH2 isoforms in order to understand their specific integration in energy metabolism. Furthermore, this study will be in an attempt to generate conditional TgNDH2s knock-out mutants. Phenotypic differences from the depletion mutants will answer the questions about the essence and the specific roles of TgNDH2s in *T. gondii*.

Taken together, I expect this study will reveal the important role of TgNDH2s in the respiratory chain and provide the direct evidence that TgNDH2s are promising drug targets.

CHAPTER II

Materials and Methods

2.1 Materials

2.1.1 Cell Cultures

2.1.1.1 *T. gondii* Strains

RH	Wild-type
RH-TATi	RH expressing a tetracycline-inducible transactivator system (Meissner <i>et al.</i> , 2001)
TgATP- β	RH-TATi expressing <i>T. gondii</i> ATPase beta subunit with a C-terminal myc-tagged fusion (Saleh, 2006; Lin <i>et al.</i> , 2009)
TgCox19-GFP1-10	RH-TATi expressing a putative <i>T. gondii</i> cytochrome c oxidase Cox19 (TGME49_054260) fused with a C-terminal GFP1-10
TgCytoC420-GFP1-10	RH-TATi expressing a putative <i>T. gondii</i> cytochrome c (TGME49_029420) fused with a C-terminal GFP1-10
TgCytoC750-GFP1-10	RH-TATi expressing a putative <i>T. gondii</i> cytochrome c (TGME49_019750) fused with a C-terminal GFP1-10
TgCytoC750-GS-GFP1-10	RH-TATi expressing TgCyto750 fused with a linker (GS) ₄ to C-terminal GFP1-10
TgCytoC750-LS-GFP1-10	RH-TATi expressing TgCyto750 fused with a linker LS(GGGGS) ₂ AA to C-terminal GFP1-10
TgNDH2-I	RH-TATi expressing <i>T. gondii</i> type II NADH dehydrogenase isoform I with a C-terminal myc-tagged fusion (Saleh, 2006; Lin <i>et al.</i> , 2008)
TgNDH2-II	RH-TATi expressing <i>T. gondii</i> type II NADH dehydrogenase isoform II with a C-terminal myc-tagged fusion (Saleh, 2006; Lin <i>et al.</i> , 2008)
Δ TgNDH2-I	Conditional TgNDH2-I knock-out mutant
Δ TgNDH2-II	Conditional TgNDH2-II knock-out mutant
TgNDH2-I-GFP11	RH-TATi expressing TgNDH2-I fused with a C-terminal GFP11
TgNDH2-I-GS-GFP11	RH-TATi expressing TgNDH2-I fused with an additional linker (GS) ₄ to C-terminal GFP11
TgNDH2-I-LS-GFP11	RH-TATi expressing TgNDH2-I fused with an additional linker LS(GGGGS) ₂ AA to C-terminal GFP11

TgNDH2-I ₃₉₉ -GFP11	RH-TATi expressing truncated TgNDH2-I whose residues 1 to 399 are fused with GFP11 at C-terminus
TgNDH2-I ₄₈₇ -GFP11	RH-TATi expressing truncated TgNDH2-I whose residues 1 to 487 are fused with GFP11 at C-terminus
TgNDH2-II-GFP11	RH-TATi expressing TgNDH2-II fused with a C-terminal GFP11
TgS9-RFP	RH-TATi expressing a <i>T. gondii</i> mitochondrial targeting ribosomal protein S9 fused with a C-terminal RFP (Lin <i>et al.</i> , 2009)
TgSCS β -GFP1-10	RH-TATi expressing <i>T. gondii</i> succinyl-CoA synthetase beta subunit (Fleige <i>et al.</i> , 2008) fused with a C-terminal GFP1-10

2.1.1.2 Mammalian Cell Lines

HFF	Human foreskin fibroblasts (HFF)
143B	Human osteosarcoma cell line (Jacobson <i>et al.</i> , 1993; kindly provided by Dr. MP King)
143B/206	Mutant 143B cells lacking mitochondrial DNA (Jacobson <i>et al.</i> , 1993; kindly provided by Dr. MP King)

2.1.1.3 *Escherichia coli* Strains

BL21 CodonPlus-RIL	Chemically competent cells (Stratagene)
DH5 α	Chemically competent cells (Invitrogen)
TOP10	Chemically competent cells (Invitrogen)
SW103	Electrocompetent recombineering cells (Warming <i>et al.</i> , 2005; provided by NCI-Frederick); Genotype: DY380 (<i>cro-bioA</i>) \langle araC-P _{BAD} <i>Flpe gal</i> ⁺

2.1.1.4 *Yarrowia lipolytica* Strains

GB 5.2	NDH2 deletion strain (Eschemann <i>et al.</i> , 2005; kindly provided by Dr. S Kerscher); Genotype: Mat b; his-1; leu2-270; ura2; xpr2-322
--------	--------------------------------------------------------------------------------------------------------------------------------------------

2.1.2 Plasmids

pBTG11	For split GFP complementation – containing a phleomycin resistance maker used to generate a C-terminal GFP11 fusion (van Dooren <i>et al.</i> , 2008; kindly provided by Dr. B Striepen)
pCTG1-10	For split GFP complementation – containing a chloramphenicol resistance marker used to generate a C-terminal GFP1-10 fusion (van Dooren <i>et al.</i> , 2008; kindly provided by Dr. B Striepen)
pDrive	PCR cloning vector (QIAGEN PCR cloning kit)
pET-16b-TgNDH2-I24	For recombinant expression in <i>E. coli</i> - encoding TgNDH2-I mature peptide fused with 10× His-tagged at N-terminus
piBG	For cosmid recombineering – used as a template for PCR amplification of modification cassettes containing both gentamycin and phleomycin resistance markers (kindly provided by Dr. GG van Dooren)
pTetSag4-ACP-cmyc-DHFR	Expression vector for <i>T. gondii</i> - containing anhydrotetracycline (ATc)-regulatable TetO7Sag4 promoter for generating C-terminal myc-tagged parasite line (Meissner <i>et al.</i> , 2001; kindly provided by Dr. B Striepen)
ptub-FNR-RFP/sag CAT	Expression vector for <i>T. gondii</i> - encoding an apicoplast-targeting domain of ferredoxin-NADP ⁺ reductase (FNR) fused with RFP (Striepen <i>et al.</i> , 2000)
ptub-S9-GFP/sag CAT	Expression vector for <i>T. gondii</i> - encoding a mitochondrial marker S9 ribosomal protein fused with GFP (DeRocher <i>et al.</i> , 2000)
pUB30	<i>Y. lipolytica</i> / <i>E. coli</i> shuttle vector (Garofano <i>et al.</i> , 2006) for <i>Yarrowia</i> transformation
pUB38	<i>Y. lipolytica</i> / <i>E. coli</i> shuttle vector used as a template for PCR amplification of <i>Yarrowia</i> mitochondrial targeting sequence complex I NUAM subunit (Garofano <i>et al.</i> , 2006)
pUB30-NUAM-TgNDH2-I (AA24)	For <i>Y. lipolytica</i> transformation – encoding NUAM targeting sequence fused with the 24 th amino acid of TgNDH2-I mature peptide (Lin <i>et al.</i> , 2008)
pUB30-NUAM-TgNDH2-I (AA51)	For <i>Y. lipolytica</i> transformation – encoding NUAM targeting sequence fused with the 51 st amino acid of TgNDH2-I mature peptide (Lin <i>et al.</i> , 2008)
pUB30-TgNDH2-I (FL)	For <i>Y. lipolytica</i> transformation – encoding full-length TgNDH2-I (Lin <i>et al.</i> , 2008)

pUB30-NUAM-TgNDH2-II (AA62)	For <i>Y. lipolytica</i> transformation – encoding NUAM targeting sequence fused with the 62 nd amino acid of TgNDH2-II mature peptide (Lin <i>et al.</i> , 2008)
pUB30-TgNDH2-II (FL)	For <i>Y. lipolytica</i> transformation – encoding full-length TgNDH2-II (Lin <i>et al.</i> , 2008)

2.1.3 Cosmids

PSBLE59	Containing TgNDH2-I entire genome (kindly provided by Dr. LD Sibley)
PSBM942	Containing TgNDH2-II entire genome (kindly provided by Dr. LD Sibley)

2.1.4 Oligonucleotides

Table 2.1 Oligonucleotides used for cosmid recombineering

Primers	Sequences (5' → 3')
coseq2-	TTCAGCGTGATCGTATGGTC
coseq4- (for sequencing)	TGATCTACGTGCAAGCAGATTA
cosIKO+	TCCGAACGACTCCGTCAATCCTCT
cosIKO-	ACTGAGGATGCAATGCGCGCGGAA
cosIIKO+	CTCCAAAGACACTGTTTCAAGCTC
cosIIKO-	GTGCACAAATATGTATGTAAACTC
cosIRT+	ATCCTCGTCGACCAGCAAATGAAG
cosIRT-	TTCGCGGTCCTGCTCGACGCGGCGACA
cosIIRT+	GCTCGTTGACCTACCGCAACGG
cosIIRT-	ACGTGGGAACTCTGGATGCATGCTT
cosIsp-	GCCAAGTAGCGACCTGCCTGCTTC
cosIIsp-	TTGATGAAATCGGCGAACTCTGCT
gen+ (for sequencing)	ATCGCAGGTTAATTAGTGGAAGA
Ico+	ATGGCAGGGCAGTGGCTGCGGCTGCTGGCGGG GGCCTCTGTGCCTATGCTATACGACTCACTATA GGGCGAATTGG
Ico-	CGCAAGAAGTTTCACGAACTGCTCCTTTGTCAT TTGCGTTTGACGCGGCTCCTCGACTACGGCTTC CATTGGCAAC

Iico+	ATGGCGATGCTCTTCTCCAGCTCAGCAGCAGGC AGCCTGCCCTCGCGCAGATACGACTCACTATAG GGCGAATTGG
Iico-	GGCAGGGCTGCGAGTTCGAAGTTGTTCACTACT TTCTTCCGGATGGCCATCCTCGACTACGGCTTC CATTGGCAAC
NDH2-Isp+	GAAGGATCGACTGCCTTTGCGCTCT
NDH2-IIsp+	TCGGCATTCTCTTACTCTCGGTCT
WT-NDH2-I-	TGAACGTCTGCGCCAAGTAGC
WT-NDH2-II-	TACGTCCCCAGCAAACGGCTCC

Table 2.2 Oligonucleotides used for real-time PCR

Primers	Sequences (5' → 3')
Bag1+	GACCGGTCGCCTCTCAACAGC
Bag1-	CGCGCAAATAACCGGACT
Enolase1+	CGAGGGGTGGCTGAAAAGTATCC
Enolase1-	CAGCGAAGGCCACGACAAG
NDH2-I+	CTCGTCGACCAGCAAATGAAGG
NDH2-I-	TGAACGTCTGCGCCAAGTAGC
NDH2-II+	GCCGCCAGGGTGGACATTTCAA
NDH2-II-	TACGTCCCCAGCAAACGGCTCC
Tub+	CGCCACGGCCGCTACCTGACT
Tub-	TACGCGCCTTCTCTGCACCC

Table 2.3 Oligonucleotides used for split GFP complementation

Primers	Sequences (5' → 3')
GFPsp110- (for sequencing)	TGAGACTGTGTGAAATGCCACA
GS_seq+ (for sequencing)	ACTCGTTCGCCGTCCCTGAC
(GS) ₄ -AvrII+ [5' phosphate modified]	[phos]CTAGGGGCTCTGGATCGGGCTCTGGAAG CC
(GS) ₄ -AvrII- [5' phosphate modified]	[phos]CTAGGGCTTCCAGAGCCCGATCCAGAGC CC
LS(GGGGS) ₂ AA-AvrII+ [5' phosphate modified]	[phos]CTAGGCTCTCTGGCGGAGGCGGATCTGG CGGAGGCGGAAGCGCGGCGC
LS(GGGGS) ₂ AA-AvrII- [5' phosphate modified]	[phos]CTAGGCGCCGCGCTTCCGCCTCCGCCAG ATCCGCCTCCGCCAGAGAGC

SG-NDH2-I-AvrII-	TACCTAGGCTTGCGTCGGTCGCCGTACACA
SG-NDH2-I-BamHI+	TAGGATCCAAAATGGCAGGGCAGTGGCTGCG GT
SG-NDH2-I ₃₉₉ -AvrII-	TACCTAGGCTGCTGCTGAGCCTCGCGCAGCTC GG
SG-NDH2-I ₄₈₇ -AvrII-	TACCTAGGCTGCTCCTTTGTCATTTGCGTTTG AC
SG-NDH2-II-AvrII-	TACCTAGGGTGGTTGTAATATTCGTGATCC
SG-NDH2-II-BglIII+	TAAGATCTAAAATGGCGATGCTCTTCTCCAGC TA
SG-SCS β -AvrII-	TACCTAGGCGGCCGCGAAATGTGAAC
SG-SCS β -BamHI+	TAGGATCCAAAATGGCGCTCTCAGCCGCT
TgCox19-AvrII-	TACCTAGGCCGGTCTGGCGACCGGAGCGCCC CT
TgCox19-BglIII+	TAAGATCTAAAATGTCTTCGTTGGCGCTTTAC CAGT
TgCytC420-AvrII-	TACCTAGGCGAATCCTTTTCCGAGGACATGAT GTCA
TgCytC420-BglIII+	TAAAGATCTAAAATGGCGCAGAAACCTGGCT CCTCA
TgCytC750-AvrII-	TACCTAGGTTTGTGGAGGCATCAACAAGGT ACG
TgCytC750-BglIII+	TAAGATCTAAAATGTGCGGTGCTGAACCTGA CGTC

All oligonucleotides used for TgNDH2s and *Y. lipolytica* cloning are listed in Supplementary Table S1 (Lin *et al.*, 2008).

2.1.5 Antibodies

Table 2.4 Antibodies used for Western blots (WB) and immunofluorescence assays (IFA)

Antibodies (company)	Working dilution (WB; IFA)
Anti-BAG1 (7E5; Bohne <i>et al.</i> , 1994)	IFA 1:500
Anti- <i>c-myc</i> (clone 9E10; Sigma)	WB1:500; IFA 1:250
Anti-GFP (MBL)	WB 1:1000; IFA 1:250
Anti-mouse-IgG AP conjugate (Jackson ImmunoResearch Lab.)	WB1:3000
Anti-rabbit-IgG Cy2 conjugate (Jackson ImmunoResearch Lab.)	IFA 1:300
Anti-mouse-IgG Cy3 conjugate (Jackson ImmunoResearch Lab.)	IFA 1:300
Anti-mouse-IgG HRP conjugate (Jackson ImmunoResearch Lab.)	WB 1:5000
Anti-rabbit-IgG HRP conjugate (Jackson ImmunoResearch Lab.)	WB 1:5000
Anti-TgNDH2-I (Saleh 2006)	IFA 1:300
FITC-conjugated lectin (from <i>Dolichos biflorus</i> ; Sigma)	IFA 1:300

2.1.6 Enzymes

Alkaline antarctic phosphatase	New England Biolabs
DNase I	Sigma-Aldrich
Finnzymes Phusion high-fidelity DNA Polymerase	Finnzymes
KOD DNA Polymerase	Novagen
M-MLV (H minus) Reverse Transcriptase RNase, Point Mutant	Promega
Quick T4 DNA Ligase	New England Biolabs
Restriction Enzymes	New England Biolabs
RNase A	Sigma-Aldrich
<i>Taq</i> DNA Polymerase	Roche

2.1.7 Kits

BacTiter-Glo Microbial Cell Viability Assay	Promega
BCA Protein Assay Kit	Pierce
ECL detection reagent	Amersham
GenElute Mammalian Total RNA Kit	Sigma
GenElute Plasmid Mini Prep Kit	Sigma
GenElute Plasmid Maxi Prep Kit	Sigma
GenElute Mammalian Total RNA Kit	Sigma
PeqGOLD Tissue DNA Mini Kit	Peqlab
QIAGEN PCR Cloning Kit	Qiagen
QIAGEN PCR Purification Kit	Qiagen
Quick Ligation Kit	New England Biolabs

2.1.8 Molecular Weight Markers

GeneRuler 100 bp DNA Ladder	MBI Fermentas
GeneRuler 1 kb DNA Ladder	MBI Fermentas
PeqGOLD Protein-Marker IV	Peqlab
Prestained Protein Marker, Broad Range (6-175 kDa)	New England Biolabs

2.1.9 Antibiotics

Table 2.5 Working concentration used for selection

Antibiotic (dissolving solvent; company)	Working concentration
Ampicillin (ddH ₂ O; Sigma)	100 µg/ml
Chloramphenicol (ethanol; Sigma)	20 µg/ml
Gentamycin (stock solution from Biochrom)	10 µg/ml
Phleomycin (ddH ₂ O; Sigma)	50 µg/ml
Pyrimethamine (ethanol; Sigma)	1 µM

2.1.10 Fluorescent Probes

Table 2.6 Working concentration used for staining $\Delta\psi_m$ in *T. gondii*

Dye (company)	Stock solution	Working concentration
DiOC ₆ (3) (Invitrogen)	100 μ M in DMSO	5 nM
JC-1 Mitochondrial Membrane Potential Assay Kit (Cayman Chemical)	100 \times JC-1	1 \times JC-1
Reduced Mitotracker Red CM-H2XRos (Invitrogen)	100 mM in DMSO	0.5 μ M
TMEM (Invitrogen)	100 μ M in DMSO	15 nM

2.1.11 Chemicals for Substrates Complementation

Table 2.7 Working concentration used for substrate complementation

Chemical (company)	Stock solution	Working concentration
Atovaquone (Sigma)	5 mM in DMSO	1 μ M
Ascorbate (Sigma)	1 M in Ampuwa H ₂ O	1.5 mM
Digitonin (Sigma)	10 mM in DMSO	2 μ M
Dihydroorotate (Sigma)	10 M in DMSO	10 mM
Glycerol-3-phosphate (Sigma)	1 M in Ampuwa H ₂ O	1 mM
HDQ (kindly provided by Dr. W Oettmeier)	20 mM in ethanol	1 μ M
Malate (Sigma)	10 M in Ampuwa H ₂ O	10 mM
Oxaloacetate (Sigma)	10 M in Ampuwa H ₂ O	10 mM
Succinate (Sigma-Alrich)	10 M in Ampuwa H ₂ O	10 mM
Tetramethyl-phenylene-diamine (TMPD; Sigma)	100 mM in Ampuwa H ₂ O	0.2 mM
Uracil (Sigma)	1 M in DMSO	250 μ M

2.1.12 Standard Media and Buffers

2.1.12.1 Mammalian Culture Media and Reagents

ATP/GSH/Cytomix	12 mg ATP 15.2 mg glutathione (GSH) in 10 ml cytomix
Cytomix (pH 7.6)	120 mM KCl 150 μ M CaCl ₂ , 10 mM K ₂ HPO ₄ / KH ₂ PO ₄ (pH 7.6) 25 mM HEPES 2 mM EDTA 5 mM MgCl ₂ in 1L Ampuwa H ₂ O (adjust pH with KOH)
1% EDTA/PBS	1% (w/v) EDTA in 1 \times PBS (Biochrom)
10% FCS/DMEM	10% (v/v) FCS 1% (v/v) Pen/Strep (Biochrom) in DMEM (Biochrom)
Freezing medium	20% (v/v) FCS 20% (v/v) DMSO in DMEM
pH shift medium (pH 8.3 at 37°C)	50 ml 10 \times DMEM (NaHCO ₃ -free) 5 ml FCS 5 ml 100 \times Pen/Strep 10 ml 1M Tricine (pH 8.2 at 37°C) 5 ml Na ₂ CO ₃ (Biochrom) 5 ml 100 \times Glutamix (Gibco) in 500 ml Ampuwa sterile H ₂ O (adjust pH with KOH)
0.25% trypsin/PBS	0.25% (w/v) trypsin in 1 \times PBS

All chemicals not explicitly listed above were purchased from Biochrom, Gibco or Sigma.

2.1.12.2 Bacterial Culture Media and Reagents

LB (Luria Broth)	1% (w/v) Bacto Trypton (Becton Dickinson) 0.5% (w/v) Bacto yeast exact 0.5% (w/v) NaCl in ddH ₂ O
LB-plate (with antibiotics)	2% (w/v) Bacto Agar in LB (working concentration refers to Table 2.5)
TFB1 (pH 5.8)	100 mM RbCl 50 mM MnCl ₂ 30 mM potassium acetate 10 mM CaCl ₂ 15% (v/v) glycerol in ddH ₂ O
TFB2 (pH 6.8)	10 mM MOPS 10 mM RbCl 75 mM CaCl ₂ 15% (v/v) glycerol in ddH ₂ O

2.1.12.3 Standard Buffers

AP staining solution	0.05% (v/v) BCIP 0.5% (v/v) NBT in substrate solution
BCIP	5% (w/v) 5-bromo-4-chloro-3-indolyl- phosphate in ddH ₂ O
Blocking solution	5% (w/v) dry skimmed milk power 0.2% (v/v) Tween 20 0.2% (w/v) NaN ₃ in 1× PBS (pH 7.4)
Buffer P1 (home-made)	50 mM Tris-HCl, pH 8.0 10 mM EDTA, pH 8.0 100 µg/ml RNase A in ddH ₂ O
Buffer P2 (home-made)	200 mM NaOH 1% (w/v) SDS in ddH ₂ O
Buffer P3 (home-made)	3 M potassium acetate (pH 5.5)
Coomassie staining solution	0.025% (w/v) coomassie brilliant blue G 30% (v/v) methanol 10% (v/v) acetic acid in ddH ₂ O

Destaining solution	30% (v/v) methanol 10% (v/v) acetic acid in ddH ₂ O
10× DNA loading dye	40% (v/v) glycerol 1% (w/v) bromophenol blue in TE buffer (pH 8.0)
10× Electrode buffer (pH 8.3 - 8.5)	30.3 g Tris 144.41 Glycine 10 g SDS in 1L of ddH ₂ O (adjust pH with glycine)
Elution Buffer (pH 2.8) (for affinity purification)	0.2 M Glycine 1 mM EGTA (adjust pH with 1M Tris, pH 9.84)
Moviol oil	2.4 g Moviol 4-88 7.81 ml 87% glycerol 12 ml 0.2 M Tris-HCl, pH 8.5
NBT	1% (w/v) nitrotetrazolium blue chloride in ddH ₂ O
4% PFA/PBS	4% (w/v) paraformaldehyde in 1× PBS
Resolving gel (10%)	940 µl 0.5 M Tris-HCl (pH 6.8) 100 µl 10% SDS 1.67 ml 30% acrylamide/bisacrylamide 20 µl 10% (w/v) APS 10 µl TEMED 2.27 ml ddH ₂ O
5× sample buffer	5.7 ml 87% glycerol 1 g SDS 3.125 ml 1 M Tris-HCl (pH 6.8) 100 µL 0.5% (w/v) bromophenol blue 0.25 g DTT in 10 ml ddH ₂ O
Stacking gel (4.4%)	400 µl 0.5 M Tris-HCl (pH 6.8) 100 µl 10% (w/v) SDS 1.45 ml 30% acrylamide/bisacrylamide 12.5 µl 10% (w/v) APS 10 µl TEMED 10 µl 1% (w/v) Bromophenol blue 400 µl ddH ₂ O
Substrate solution	200 ml 10% (v/v) diathamoline (pH 9.6) 20 µl 5 mM MgCl ₂ 800 ml physiological NaCl (pH 7.4)
50× TAE (pH 8.0)	242 g Tris

	57.1 ml 98% acetic acid 100 ml 0.5M EDTA (pH 8.0) in 1 L ddH ₂ O
10× TBS (pH 7.6)	24.2 g Tris 80 g NaCl in 1 L ddH ₂ O
10× TE buffer (pH 8.0)	100 mM Tris 10 mM EDTA in ddH ₂ O
0.25% Triton X-100/PBS	0.25% (v/v) Triton X-100 in 1× PBS
Washing solution	0.05% (v/v) Tween 20 in 1× TBS (pH 7.4)

2.1.13 Chemicals

Acrylamide/bisacrylamide	Roth
Adenosine 5' triphosphate (ATP)	Sigma
Ammonium peroxodisulfate (APS)	Merck
Ampuwa sterile water	Fresenius kabi
Diethanolamine	Sigma-Alrich
1,4-Dithiothreitol (DTT)	Roth
Glutathione (GSH)	Sigma
Manganese Chloride (MnCl ₂)	Merck
Moviol 4-88 reagent	Fluka
Potassium dihydrogen phosphate (KH ₂ PO ₄)	Roth
Potassium phosphate monobasic (K ₂ HPO ₄)	Calbiochem
Rubidium Chloride (RbCl)	Sigma-Alrich
Sodium azide (NaN ₃)	Sigma
TEMED	Roth
Triton X-100	Sigma-Alrich
Tween 20	Sigma-Alrich

All chemicals not explicitly listed above were purchased from Calbiochem, Merck, Roth or Sigma.

2.1.14 Apparatus

Acrylamide gel cast	Modell Mini Protean II (BioRad)
Agarose gel chambers	Keutz Labortechnik (Reiskirchen)
Cell electrophoration system	Electro manipulator 600 (BTX)
Centrifuges	Megafuge 2.0 (Heraeus) Megafuge 2.0 RS (Heraeus) Modell 5417 C (Eppendorf) Modell 5417 R (Eppendorf) RC-26 Plus (Sorvall-Kendro)
Digital balances	BP 221 S (Sartorius) LP 6200 S (Sartorius)
Electrophoresis power supply	EPS 600 (Amersham Pharmacia Biotech) Standard Power Pack P25 (Biometra)
Gel documentation system	BioDoc II (Biometra)
Gel Electrophoresis	Modell Mini Protean II (BioRad)
Incubators	Heraeus
Lightcycler	Roche
Luminescent image analyzer	Image Reader LAS-4000 (Fujifilm)
Luminometry	Wallac 1420 Multilabel Counter (Perkin Elmer)
Light microscopy	Modell DM IL (Leica)
pH Meter	Modell OV5 (Biometra)
Photometer	Ultraspec 1000 (Pharmacia Biotech)
Pipette aids	Pipetboy acu (IBS Integra Biosciences) Pipetus-akku (Herschman Laborgerate)
Pipettes	Modell Research (Eppendorf)
Semi-dry transfer cell	Transfer-Blot SD cell (Bio Rad)
Shaker	SM-30 Control (Johanna Otto)
Thermocycler	Modell T3 (Biometra)
Thermomixer	Modell Compact (Eppendorf)
Time-lapse microscopy	Axiovert 200 M microscopy (Zeiss)
UV-Crosslinker	UVC-500 (Hoefer)

2.2 Methods

2.2.1 Bioinformatics

The putative *T. gondii* cytochrome c (TGME49_019750; TGME49_029420) and cytochrome c oxidase Cox19 (TGME49_054260) were identified by BLAST searches in genomic and/or cDNA sequence data via <http://ToxoDB.org>, using amino acid sequences of *S. cerevisiae* Cyc1 (NP_012582) and Cox19 (NP_013082) as queries, respectively. The TMHMM Server v. 2.0 was used for prediction of transmembrane helices in proteins (<http://www.cbs.dtu.dk/services/TMHMM/>). Multiple sequence alignments were done using the ClustalW program at the EMBL-EBI (<http://www.ebi.ac.uk/clustalw/>). Programs including MitoProt (<http://ihg2.helmholtz-muenchen.de/ihg/mitoprot.html>) and SignalP 3.0 Server (<http://cbs.dtu.dk/services/SignalP/>) were used to predict subcellular localisation.

2.2.2 Plasmid Construction

2.2.2.1. Plasmid Construction for *Y. lipolytica* Transformation

Detailed information of plasmid construction for *Yarrowia* transformation was described previously (Lin *et al.*, 2008).

2.2.2.2 Plasmid Construction for Split GFP Complementation

The complete open reading frames (ORFs) of TgSCS- β and TgNDH2-II were amplified from plasmids pTet-sag-SCSb-cmyc-DHFR (Fleige *et al.*, 2008) and pTet-sag-ndh2-II-cmyc-DHFR (Lin *et al.*, 2008) using *Phusion* polymerase with the primer sets SG-SCS β -BamHI+ and SG-SCS β -AvrII-, and SG-NDH2-II-BglIII+ and SG-NDH2-I-AvrII-, respectively. The coding sequences of TgNDH-I, TgNDH2-I₃₉₉ and TgNDH2-I₄₈₇ were amplified from pTet-sag-ndh2-I-cmyc-DHFR (Lin *et al.*, 2008) using the sense primer SG-NDH2I-BamHI+ and antisense primers SG-NDH2-I-AvrII-, SG-NDH2-I₃₉₉-AvrII- and SG-NDH2-I₄₈₇-AvrII-, accordingly. For PCR amplifying the ORFs of TgCytC750, TgCytC420 and TgCox19, cDNA of RH strain was used as a template. The primer sets used were TgCytC750-BglIII+ and TgCytC750-AvrII- for TgCytC750; TgCytC420-BglIII+ and TgCytC420-AvrII- for TgCytC420, and TgCox19-BglIII- and TgCox19-AvrII- for TgCox19. All PCR fragments were first cloned into pDrive and DNA sequenced. The BglIII/AvrII or BamHI/AvrII fragments were finally subcloned into pCTG1-10 resulting in a C-terminal GFP1-10 fusion or into pBTG11 resulting in a C-terminal GFP11 fusion (van

Dooren *et al.*, 2008). For some fusion constructs, an additional flexible linker consisting of (GS)₄ residues or LS(GGGGS)₂AA residues (Arai *et al.*, 2001) was inserted into the AvrII site of the fusion constructs, which was derived from self-annealing oligonucleotides from primer sets (GS)₄-AvrII^{+/−} and LS(GGGGS)₂AA-AvrII^{+/−}, respectively. All constructs were verified for correct sequences and orientations. All oligonucleotides mentioned above are listed in Table 2.3 in **Section 2.1.4**.

2.2.2.3 Gel Purification

DNA was extracted from agarose gel using QIAGEN PCR Purification Kit according to the manufacturer's protocol. In brief, DNA was resolved on a ~1 % agarose gel with 0.5 mg/ml ethidium bromide in 1× TAE. Each of the observed bands was visualized and excised with a scalpel under ultraviolet light. Three volumes of Buffer QG were added to 1 volume of the excised gel. Gel was completely dissolved by shaking at 50°C for 5-10 min and then mixed thoroughly with 1 gel volume of isopropanol. The mixture was applied to a QIAquick spin column placed in a 2-ml collection tube. DNA was bound by centrifugation at 13,000 ×g for 1 min and next washed with 750 µl of Buffer PE. Finally, DNA was eluted by adding 30 µl of pre-warmed ddH₂O to the centre of the column and collected by centrifugation.

2.2.2.4 PCR Cloning

The purified PCR fragments were subcloned into pDrive vector according to the manufacturer's protocol (QIAGEN PCR Cloning Kit). PCR products were added with a molar ratio of 5 times more than pDrive cloning vector (50 ng) for ligation.

2.2.2.5 Restriction Endonuclease Digestion of DNA

Restriction endonuclease digestion for subcloning was performed in 20 µl ddH₂O containing 2 µg of plasmid DNA, 1× NEB buffer, 1× BSA (optional), and 2 U of restriction endonucleases. The reaction mixture was normally incubated at 37°C (55°C for SfiI; 25°C for ApaI) for 3 h. For screening clones, reaction was done in a total volume of 10 µl ddH₂O containing 1 µg of plasmid or cosmid DNA, 1× NEB buffer, 1× BSA (optional), and 1 U of restriction endonucleases. Restriction enzyme digestion was normally incubated at 37°C for 1 h.

2.2.2.6 Alkaline Phosphatase Reaction

Vectors followed by restriction endonuclease digestion (20 μ l) were added with 2 μ l (instead of 4 μ l) of 10 \times alkaline phosphatase buffer, 2 U of alkaline phosphatase, and leveled up with ddH₂O to 40 μ l. The reaction was kept at 37°C for 15 min and inactivated at 65°C for 5 min.

2.2.2.7 Ligation of DNA

Ligation reaction was performed in a 20- μ l reaction volume containing gel-purified inserts with a molar ratio of 5 times more than vector (100 ng), 1 \times ligation buffer and 1 U of T4 DNA ligase. The ligation reaction was kept at RT (25°C) for 30 min or incubated overnight at 16°C.

2.2.2.8 Preparation of chemically Competent *E. coli* Cells

A single colony of *E. coli* cell was inoculated into 5 ml LB without antibiotics and grown overnight at 37°C with vigorous shaking. Overnight culture (2 ml) was added into 100 ml pre-warmed LB medium and grown at 37°C until an OD₆₀₀ of 0.5 was reached. The culture was transferred into 50-ml tubes and cooled on ice for 15 min. Cells were collected after centrifugation at 4000 \times g for 10 min at 4°C. The cell pellet was gently resuspended in 30 ml ice-cold TFB1 buffer and incubated on ice for 30 min. Cells then were pelleted by centrifugation as described above, resuspended in 4 ml ice-cold TFB2 buffer, and incubated on ice for another 30 min. Competent cells (100 μ l) were aliquoted in pre-chilled 1.5-ml tubes and immediately frozen at -80°C.

2.2.2.9 Cell Transformation

Transformation of plasmid DNA was performed using TOP10 or DH5 α chemically competent cells. Competent cells were first thawed on ice for 3-5 min. Total amount of 5 μ l from ligation-reaction mixture was slowly added into the cells without any vortexing. Cells were further incubated on ice for 30 min. After that, cells were heat-shocked in a 42°C water bath for 45 s followed by 2-min incubation on ice. Nine hundred μ l of LB was added to the cells and kept shaking at 37°C for 1 h at 250 rpm. Finally cells were plated on an LB-ampicillin agar plate (100 μ g/ml ampicillin). For white-blue colony selection, 40 μ l of X-gal (40 mg/ml) and 40 μ l of IPTG (1 M) were added onto the plate. Plates were incubated overnight at 37°C.

2.2.2.10 Plasmid Preparation

2.2.2.10.1 Screening Clones

The selected single colony was inoculated into 5 ml LB supplemented with antibiotics and grown overnight at 37°C with vigorous shaking. Plasmid DNA was isolated from overnight culture (3 ml) using GenElute Plasmid Mini Prep Kit according to the manufacturer's instructions. Purified plasmid DNA was digested with restriction endonucleases to screen the expected DNA insert. DNA sequencing was performed in commercial company Seqlab (www.seqlab.de). Large scale of plasmid preparation was purified by GenElute Plasmid Maxi Prep Kit.

2.2.2.10.2 Determination of DNA Concentration

DNA concentration was determined photometrically and calculated from the absorbance at 260 nm as follows: DNA concentration ($\mu\text{g/ml}$) = absorbance \times 50 \times dilution factor of the measured samples.

2.2.2.10.3 DNA Precipitation

Dissolved DNA (typically in H₂O, TE buffer or Tris-HCl, pH 7.5-8.0) was added with 1/10 volume of 3 M sodium acetate (pH 5.2) and 2.5 volumes of 100% ethanol. The sample was mixed by inverting the tube 6 times and incubated at -20°C for 30 min. Supernatant was removed from the tube after centrifugation at 14,000 rpm for 20 min. DNA was once with 1 ml of 70% ethanol and centrifuged again. After removing the ethanol, DNA pellet was air-dried under laminar flow hood for 5-10 min and resuspended with 50 μl of ddH₂O. Plasmid or cosmid DNA used for electroporation was resuspended with 45 μl of cytomix.

2.2.3. Cosmid Recombineering

2.2.3.1. Preparation of Electrocompetent Cells

SW103 (λ prophage deficient) *E. coli* strain was inoculated into 5 ml LB without antibiotics and grown overnight at 30°C with vigorous shaking. Two ml of the overnight culture was added into 100 ml pre-warmed (30°C) LB and grown at 30°C until an OD₆₀₀ of 0.4 was reached. The culture was cooled on ice for 20 min swirling every 5 min. After that, the culture was transferred into 50-ml tubes and centrifuged at 4,000 rpm for 10 min at 4°C. The cell pellet was resuspended in 50 ml ice-cold ddH₂O followed by centrifugation as described above. The cell pellet then was sequentially

washed once with 50 ml, 20 ml and 3 ml of ice-cold ddH₂O. Finally the cell pellet was resuspended with 600 µl of 10% (v/v) glycerol. Competent cells were aliquoted in ice-cold 1.5-ml microfuge tubes (50 µl per tube) and frozen immediately at -80°C.

2.2.3.2. Electroporation of Cosmid DNA

Electrocompetent SW103 cells were thawed on ice for 3-5 min. Cosmid DNA (200 ng) was added into the competent cells with slightly stirring by pipette tip and incubated on ice for 1 min. Cells were transferred into an ice-cold 2 mm gap cuvette and electroporated at 1.75 kV, 250 Ω, and 25 µF. A total of 1 ml LB was immediately added into cuvette and mixed thoroughly with the cells. Subsequently cells were transferred from cuvette into a 1.5-ml tube. Cells were shaken at 30°C for 1.5 h. An aliquot of 100 µl from the culture was spread onto an agar plate prepared with antibiotics (it depends on the vector backbone; ampicillin is used for selection of cosmids PSBLE59 and PSBM942). Several colonies were screened for the targeted genes by PCR. Selected clones were kept as glycerol stocks at -80°C.

2.2.3.3. Preparation of SW103 containing Cosmid

Glycerol stock of SW103 containing cosmid was firstly inoculated into 5 ml LB supplemented with 100 µg/ml ampicillin and grown overnight at 30°C with vigorous shaking. Two ml of overnight culture was added into 100 ml LB and grown at 30°C until OD₆₀₀ reached at 0.4. Induction of expression of recombinant proteins was done on 43°C water bath with a gentle shaking at ~100 rpm for 20 min. Afterwards the culture was cooled in wet ice for 20 min swirling every 5 min. Finally competent cells were prepared as the same procedures described in **Section 2.2.3.1**.

2.2.3.4. Cosmid Modification

Cosmid recombineering was referred to previous published protocol (Lee *et al.* 2001). Modification cassettes containing gentamycin and phleomycin resistance markers were amplified from plasmids piBG using primer sets flanking with 50 bp of gene-specific sequences (TgNDH2s). Primer sets Ico⁺ and Ico⁻, and IIco⁺ and IIco⁻ were respectively used for recombineering PSBLE59 and PSBM942 cosmids, as tabulated in **Section 2.1.4**. PCR products were purified and introduced into cells by electroporation and selected on plates supplemented with 100 µg/ml ampicillin and 10 µg/ml gentamycin. Modified cosmids were screened by PCR using primers that

amplify the flanking regions of the targeting cassette. Primer pairs used for confirming modified cosmids were NDH2-I-sp+/coseq4- and gen+/cosIsp- for PSBLE59, designated as primer Set A and B (see Figure 3.3), respectively; and NDH2-II-sp+/coseq2- (Set A) and gen+/cosIIsp- (Set B) for PSBM942. Selected clones were kept as glycerol stocks at -80°C and further confirmed by DNA sequencing.

2.2.3.5. Cosmid DNA Preparation

A single colony was inoculated into 5 ml LB supplemented with antibiotics and grown overnight at 30°C. Overnight culture (3 ml) was pelleted and lysed with 300 µl of Buffer P1 containing RNase A. Then 300 µl of Buffer P2 and P3 was sequentially added into the lysate, mixed gently and incubated at RT for 5 min each. The mixture was centrifuged at RT for 10 min. Supernatant then was transferred into a new 1.5-ml tube and mixed thoroughly with 0.7 volume of isopropanol (630 µl). After that, the mixture was incubated on ice for 5 min and the precipitated DNA was pelleted after centrifugation at 4°C for 30 min. The DNA pellet was washed with 1 ml of 70% ethanol and centrifuged at RT for 5 min. Finally supernatant was discarded, DNA pellet was air-dried and resuspended in 50 µl TE buffer. Cosmid DNA was stored at -20°C.

2.2.4 Analysis of Gene Expression

2.2.4.1 Isolation of Genomic DNA

Extracellular parasites were collected from the supernatant after centrifugation at 34 ×g for 5 min to remove host cell debris. Parasites then were pelleted at 1,314 ×g for 10 min at RT. Genomic DNA isolation was prepared using PeqGOLD Tissue DNA Mini Kit according to the manufacturer's protocol.

2.2.4.2. Total RNA Isolation

Total RNA was isolated by using GenElute Mammalian Total RNA Kit according to the manufacturer's protocol. Intracellular parasites were firstly lysed by adding 500 µl of lysis solution containing 1% (v/v) of 2-mercaptoethanol. Cell lysates then were transferred into a blue filtration column placed in a 2-ml collection tube and centrifuged at 14,000 ×g for 2 min. Equal volume of 70 % ethanol (500 µl) were added to the filtrate and thoroughly mixed. Next the mixture was transferred into a clear binding column and centrifuged at 14,000 ×g for 15 s. Afterwards flow-through

was discarded, the column was washed once with 500 μ l of Wash solution 1, twice with 500 μ l of Wash solution 2 containing ethanol, and centrifuged for 15 s each. Additional 1-min centrifugation at 14,000 \times g was done to remove residual ethanol from the washing solutions. Finally, total RNA was eluted from the column by adding 50 μ l of RNase-free H₂O and stored at -80°C until used.

2.2.4.3 Reverse Transcription – Polymerase Chain Reaction (RT-PCR)

2.2.4.3.1 Synthesis of cDNA

First-strand cDNA was reverse-transcribed in a 50- μ L RNase-free H₂O reaction containing 5 μ g of total RNA, 1 \times M-ML RT buffer, 1 μ M oligo(dT) primer, 0.5 mM dNTP, and 5 U of M-MLV reverse transcriptase at 37°C for 1.5 h. The cDNA was diluted by adding 100 μ l of RNase-free H₂O and ready for conventional PCR or real-time PCR. Samples were stored at -20°C.

2.2.4.3.2 Polymerase Chain Reaction (PCR)

PCR conditions were adjusted in accordance to following parameters: properties of DNA polymerases and templates, T_m of primer sets, and size of the PCR products. In general, PCR amplification was performed in a 25- μ l reaction for 28-30 cycles. Each PCR reaction contained 50-100 ng of DNA, 1 μ M of each upstream and downstream primer, 0.25 mM dNTP, 1 \times PCR reaction buffer, and 0.25 U of DNA polymerases. The PCR primer sets used are summarized in **Section 2.1.4**. For PCR cloning, cDNA was firstly purified by QIAquick PCR Purification Kit and PCR reaction was done in 50 μ l reaction volume for 25-28 cycles. All PCR products were analyzed on a ~1 % agarose gel with ethidium bromide and were visualized under ultraviolet light. In order to check the size of the PCR products, GeneRuler 1kb or 100 bp DNA Ladder was run along with the PCR products.

2.2.4.3.3 Real-time PCR

Real-time PCR was performed using Lightcycler according to the manufacturer's instructions. PCR amplification was carried out using these parameters: 10 min at 95°C followed by 40 cycles of denaturation (95°C, 10 s), annealing (60°C, 15 s), and extension (72°C, 20 s). All samples were tested for PCR amplification efficiencies as

described previously (Lin *et al.*, 2009). Cp values from PCR amplification were used for relative quantification. β -tubulin mRNA transcripts were used for normalization.

2.2.4.3.4 Fusion-PCR

Fusion-PCR amplification was firstly performed in a volume of 50 μ l containing 50 ng of each purified DNA fragment with 5 cycles of PCR in the absence of primers with following parameters: denaturation (98°C, 10 s), annealing (55°C, 10 s), and extension (72°C, 30 s). The PCR reaction was continued for another 7 cycles after adding the primer sets.

2.2.5 Cell Cultures

2.2.5.1 Cultivation of Human Foreskin Fibroblasts

HFF cells were maintained in DMEM supplemented with 10% FCS and 1% Pen/Strep at a 5% CO₂ humidified atmosphere. Cells were cultivated in a 175 cm² cell culture flask for 10 days to reach a confluent monolayer. Confluent cells then were split to lower cell density by re-cultivated in 175 cm², 25 cm² (T25) cell culture flasks or plates. Cells were split as follows. The culture medium was aspirated by suction and washed once with 10 ml of 1% EDTA/PBS. Then cells were added with 5 ml of 0.25% trypsin/PBS and removed most of the solution after tilting the flask several times. Monolayer cells were detached after incubation at 37°C for 1-2 min and resuspended with the same culture medium.

Human osteosarcoma 143B/206 cells, which lack mitochondrial DNA (Jacobson *et al.*, 1993), and the parental 143B cell line were maintained in DMEM supplemented with 10% FCS, 1% Pen/Strep, 1% glutamine, sodium pyruvate (110 μ g/ml) and uridine (50 μ g/ml).

2.2.5.2 *In vitro* Cultivation of *T. gondii*

Parasites were propagated in HFF cells as previously described (Roos *et al.*, 1994). In brief, tachyzoites were inoculated on a confluent HFF monolayer grown on cell culture flasks or plates with DMEM supplemented with 1% FCS and 1% Pen/Strep at 37°C in a 5% CO₂ humidified atmosphere. Extracellular parasites were released from lysed host cells after 2-3 days of post-infection. Parasites were maintained by re-infection.

2.2.5.3 *In vitro* Differentiation of Tachyzoites to Bradyzoites

Bradyzoite differentiation was induced by alkaline pH-shift (Soete *et al.*, 1994). Tachyzoites were freshly released by syringe passage and 3×10^4 parasites were inoculated onto a confluent HFF monolayer grown on a glass-bottomed 24-well imaging plate or plastic plate. Cell cultures were daily changed with a fresh pH-shift medium to remove the extracellular parasites and maintain a constant culture pH. Bradyzoite differentiation was achieved after 3-day incubation of pH-shift medium and the differentiation rate was verified by immunofluorescence assay.

2.2.5.4 Transfection of *T. gondii*

Freshly lysed tachyzoites were harvested by scrapping from the HFF (~60% of lysis) monolayer and released by syringe passage. The debris of HFF cells was pelleted by centrifugation at $34 \times g$ for 5 min. Supernatant containing the parasites were transferred into a new 50-ml tube and centrifuged at $1,314 \times g$ for 10 min. Parasites were washed once with 5 ml cytomix and centrifuged at $1,314 \times g$ for 10 min. Parasites were resuspended in filtered ATP/GSH/cytomix with a final concentration of 3×10^7 parasites/ml. A 1.5-ml tube containing linearized plasmid DNA (50 μg of DNA and 50 U of restriction endonuclease in 50 μl cytomix) was added with 350 μl of parasite suspension and gently mixed. Total volume of 400 μl of the mixture was carefully transferred into a 2 mm gap cuvette without causing gas bubbles inside and electroporation was done by using a BTX electro manipulator 600 with a setting at 1.5 kV, 25 Ω and 25 μF . After 15-min incubation at RT, the electroporated parasites were transferred into a T25 cell culture flask and immediately put under drug selection by chloramphenicol or pyrimethamine. Drug selection by phleomycin was done on extracellular parasites for 4 h. Indicated drug concentration is shown in Table 2.5 in **Section 2.1.9**.

2.2.5.5. Generation of Conditional Knock-out Mutants

Transgenic lines TgNDH2-I and TgNDH2-II each expressing an inducible copy of TgNDH2-I or -II were firstly subcloned. Modified cosmids PSBLE59 and PSBM942 were electroporated into the parental clonal line of myc-tagged TgNDH2-I and TgNDH2-II, respectively. After three rounds of drug selection, parasite lines were subcloned into 96-well plate and the isolated single plaques were first screened for the

disruption of endogenous gene locus by PCR using primer sets of cosIRT+/WT-NDH2-I- (Set 1), and cosIKO+/- for TgNDH2-I (Set 2); and cosIIRT+/WT-NDH2-I- (Set 1) and cosIIKO+/- (Set 2) for TgNDH2-II, respectively. Restriction digestion and RT-PCR and were further applied to the selected clones to confirm the knock-out pattern. Primer pairs used for RT-PCR analysis were as follows: cosIRT+/- for TgNDH2-I; and cosIIRT+/- for TgNDH2-II.

2.2.5.6. Cloning of Transgenic Lines

Medium in confluent HFF monolayer grown on 96-well plates was changed with DMEM supplemented with 1% FCS, 1% Pen/Strep and selection drugs (100 µl per well). Extracellular parasites were harvested as described in **Section 2.2.5.4**. Parasites were counted and diluted to 100 parasites per ml. One hundred µl was added into each well in the first and seventh vertical columns of a 96-well plate. Serial dilution was started from left to right by using a multi-channel pipetor. The parasites were mixed well by pipetting several times and were transferred 100 µl into next column. The medium was discarded after mixing column 6 and 12. The plates were incubated for 7 days without disturbing the cultures. Individual wells observed with a single plaque were marked and parasites of these clones were transferred into T25 flasks.

For subcloning the knock-out parasites, single plaques obtained on the 96-well plates were transferred into 12-well plates. After 5-6 days, all the clones after infecting 24-well plates, were harvested for genomic DNA isolation and subjected to PCR for knock-out screening.

2.2.5.7 Cryopreservation of *T. gondii*

Intracellular parasites were detached as described in **Section 2.2.5.1**. Detached cells were suspended in 10 ml of 10%FCS/DMEM and centrifuged at 400 ×g for 5 min. Supernatants then were discarded and the cell pellet was added with 1 ml of ice-cold 10%FCS/DMEM and quickly mixed with 1 ml of freezing medium. Cells (1 ml) were aliquoted in 2-ml cryotubes and kept in liquid nitrogen for long-term storage. For re-cultivating frozen cells, a cryotube was thawed in a 37°C water bath and the cells were immediately transferred into a cell culture flask freshly changed with 1%FCS/DMEM. Cells were incubated at 37°C in a 5% CO₂ humidified atmosphere and replaced with new medium after 12 h to remove the residual DMSO.

2.2.5.8 Immunofluorescence Assay

Samples were firstly fixed with 500 μ l of 4% PFA/PBS and permeabilized with 500 μ l of 0.25% Triton X-100/PBS for 15 min each. After blocking with 300 μ l of 1% BSA/PBS for 1 h, samples were incubated with primary antibodies followed by secondary antibodies for 1 h each. Working concentration of staining solution is summarized in Table 2.4 in **Section 2.1.5**.

2.2.5.9 Detection of $\Delta\Psi_m$

The *T. gondii* $\Delta\Psi_m$ was monitored after staining with fluorophores Mitotracker or DiOC₆(3) as described previously (Lin *et al.*, 2009). Working concentration of staining solution is summarized in Table 2.5 in **Section 2.1.10**.

2.2.5.10 Determination of Intracellular ATP Level

Parasitic ATP level was determined by using the BacTiter-Glo Microbial Cell Viability assay. Preparation, measurement and quantification of intracellular ATP level were performed as described previously (Lin *et al.*, 2009).

2.2.5.11 Time-lapse Microscopy

Live imaging of *T. gondii* $\Delta\Psi_m$ was performed with an inverted Zeiss Axiovert 200 M microscopy equipped with a XL-3 incubator and a heating unit (PeCon). Images were captured by an AxioCam MRm camera and processed with Axiovision 4.6.3 software. All live imaging experiments were performed on a black glass-bottomed 24-well imaging plate and kept at 37°C. In brief, confluent HFF monolayer seeded on an imaging plate were 16-18 h post-infected with $2-3 \times 10^5$ parasites per well. After DiOC₆(3) staining, the plate was transferred into the humidified chamber and drugs were added to the wells at the indicated concentrations.

2.2.5.12 Drug Treatment

Parasites ($3-5 \times 10^5$) were inoculated onto confluent HFF monolayer on a 24-well plate in correspondent to different time intervals. Drugs were added with the indicated concentrations and time intervals.

2.2.5.13 Cell Count

Parasites were 5-fold diluted with 1× PBS and counted using a hemocytometer. Parasites per ml = (average counted numbers × 5 × 10⁴)/ml.

2.2.5.14 Statistical Method

Statistical analysis was performed by Student's *t* test. Differences were considered statistically significant when *p* values were less than that of 0.05.

2.2.6. Analysis of Protein Expression

2.2.6.1. Growth of *E. coli* Expression Cultures

A selected positive colony was inoculated into 5 ml LB supplemented with 100 µg/ml ampicillin and 25 µg/ml chloramphenicol and grown overnight at 37°C with vigorous shaking. One ml of overnight cultures was resuspended in 30 ml of the same pre-warmed culture medium and grown at 37°C until an OD₆₀₀ of 0.6 was reached. Protein expression was induced for 1 h by adding IPTG at a final concentration of 1 mM. Cell cultures were centrifuged at 4,500 ×g for 15 min at 4°C and cell pellet was stored at -20°C.

2.2.6.2 Growth of *Y. lipolytica* Cultures

The protocol of transformation and preparation of mitochondrial membranes was described previously (Eschemann *et al.*, 2005; Lin *et al.*, 2008).

2.2.6.3 Protein Extraction

Protein fractionation for transgenic line TgATPase-β is described in detail in Lin *et al.*, 2009. For extraction of recombinant protein expressed in *E. coli*, the harvested cell pellet was resuspended in buffer B (pH 8.0; 50 ml per gram wet weight) containing 100 mM NaH₂PO₄, 10 mM Tris-HCl, 8 M urea. The cells were lysed by vortexing and stirred by a rotary at 4°C for 1 h. Supernatant (soluble protein) was collected after centrifugation at 8,000 ×g for 20 min at 4°C. Proteins were loaded with 2× sample buffer ready for SDS-PAGE analysis.

2.2.6.4 Western Blot analysis

2.2.6.4.1 Quantification of Protein Concentration

Protein concentration was determined by BCA protein assay kit according to the manufacturer's protocol.

2.2.6.4.2 Sodium Dodecyl Sulphate – Polyacrylamide Gel Electrophoresis (SDS-PAGE)

Separation of proteins was performed by SDS-PAGE. The acrylamide gel cast was set up by laying two spacers sandwiched between two rectangular glass plates. Separating gel (10% or 12.5%) was pipetted into the space. Upon the polymerization of the separating gel, a comb was inserted in the sandwich plates. Stacking gel (4.4%) was filled on top of separating gel and waited for solidifying. Equal amount of protein samples were mixed with 2× sample buffer and were boiled for 5 min. In the presence of 1× electrode buffer, electrophoresis was performed with constant current 0.3 mA.

2.2.6.4.3 Electroblotting of SDS-PAGE

The polyacrylamide gel was electroblotted using a semidry blot system onto a nitrocellulose membrane assembled in the following order: starting at anode direction with 6 Whatman filter papers soaked with 0.3 mM Tris-HCl (pH 10.4) and 20% methanol; 3 Whatman filter papers soaked with 25 mM Tris-HCl (pH 10.4) and 20% methanol; Hybond nitrocellulose membrane (Amersham Biosciences); SDS-PAGE gel and 9 Whatman filter papers soaked with 40 mM 6-aminocaproic acid (pH 7.6) and 20% methanol followed by cathode direction. Proteins were transferred at RT with constant current 0.3 mA for 1.5 h.

2.2.6.4.4 Blocking, Washing and Antibody Incubation

The electroblotted nitrocellulose membrane was first incubated with blocking solution at RT for 1 h to reduce non-specific binding of antibody. After the blocking step, the membrane was washed once with washing solution for 5 min. Bound proteins on membrane was probed with primary antibody overnight at 4°C. On the second day, membrane was washed for 30 min and washing solution was changed every 5 min. Next, the membrane was incubated with secondary antibody at RT for 1.5 h. The

membrane finally was washed again as described above. The working dilution and sources of antibodies are summarized in Table 2.4 in **Section 2.1.5**.

2.2.6.4.5 Affinity Purification of Polyclonal Antibodies

His-tagged recombinant proteins (~50 µg) were resolved by SDS-PAGE and transferred onto nitrocellulose membranes. Protein expression was visualized by Ponceau S staining and the membrane strip containing the expected protein was cut out. The membrane strip was blocked with 5% (w/v) skimmed milk at RT for 1 h and incubated overnight with 2 ml of 0.1% Triton X-100/PBS containing 40 µl of raised serum at 4°C. On the next day, the membrane strip was washed 4 times with 0.1% Triton X-100/PBS every 5 min. Afterwards the membrane strip was incubated with 150 mM NaCl at RT for 20 min and washed as described above. The membrane strip then was put into a 2-ml tube and sequentially changed with 900 µl elution buffer (pH 3.5, pH 3.0 and pH 2.5) at RT for 10 min each. Finally each elution fraction was diluted to 1:300 by adding 100 µl of 10× PBS, 10 µl of 2% sodium azide (0.02%), and 100 µl of 10% BSA.

2.2.6.4.6 Protein Detection

Methods including ECL chemiluminescent detection and alkaline phosphatase (AP) staining were used for membrane development. For ECL detection, an equal volume of detection solution 1 and 2 were mixed. The washed membrane was drained with the mixtures at RT for 1 min. The chemiluminescent signal was recorded by Image Reader. While using AP staining, the washed membrane was first incubated with 10 ml pre-warmed substrate solution at RT for 2 min, followed by 10 ml pre-warmed AP staining solution containing BCIP and NBT.

2.2.6.5 Kinetic Measurements

Measurement and analysis of enzymatic parameters are described in Lin *et al.*, 2008.

CHAPTER III

Results

3.1 Biochemical Characterization of TgNDH2s as Drug Targets for HDQ

Results of this section have been described previously (Lin *et al.*, 2008; see **Appendix I**). A summary of the findings is depicted as follows.

The quinolone-like compound HDQ, known as a high affinity inhibitor for the yeast *Y. lipolytica* NDH2 (Eschemann *et al.*, 2005), has been shown to effectively inhibit the replication rate of *T. gondii* *in vitro* (Saleh *et al.*, 2007). Thus, it is crucial to biochemically characterize *T. gondii* NDH2s to reveal whether these two isoforms, TgNDH2-I and TgNDH2-II, are indeed enzyme targets of HDQ. Given the fact that both isoforms of TgNDH2s are constitutively co-expressed in tachyzoite and bradyzoite stages, a direct biochemistry analysis of individual enzyme parameters for TgNDH2s was instead performed on recombinant proteins by using *Y. lipolytica* as a surrogate model. A *Y. lipolytica* NDH deletion strain was used to heterologously express both enzymes fused with a *Yarrowia* mitochondrial NUAM import protein. Both TgNDH2-I and TgNDH2-II were able to display oxidoreductase activities by using NADH and *n*-decylubiquinone (DBQ) as substrates. Additionally, TgNDH2-I could rescue the loss of complex I activity, implying that TgNDH2-I is functionally expressed in the yeast as an internal enzyme. Furthermore, TgNDH2-I activity was effectively inhibited by HDQ with an IC₅₀ in the nanomolar range, indicating that HDQ is a high affinity inhibitor for TgNDH2-I. Steady-state kinetics are in accordance with a ping-pong reaction mechanism for TgNDH2-I. Moreover, the mode of inhibition of HDQ on TgNDH2-I was analyzed indicating that HDQ is a non-competitive inhibitor for the NADH-binding site. Further studies on inhibition kinetics of the quinolone-like compounds showed that the derivatives with longer alkyl chains, such as C₁₂ (HDQ) and C₁₄, are high affinity inhibitors for TgNDH2-I, whereas the derivatives with shorter side chains, C₅ and C₆, yielded higher IC₅₀ values in the micromolar ranges. Collectively, this study provides evidence that type II NADH dehydrogenase isoform I is a target enzyme of HDQ in *T. gondii*.

3.2 Physiological Consequences of TgNDH2s Inhibition in *T. gondii*

Results for this section have been described previously (Lin *et al.*, 2009; see **Appendix II**). A summary of the findings is depicted as follows.

The physiological influences of TgNDH2s inhibition on mitochondrial functions were explored in this study, particularly focusing on the subject of oxidative phosphorylation. Firstly the impact of high affinity TgNDH2 inhibitor HDQ (Lin *et al.*, 2008; see **Section 3.1**) on $\Delta\Psi_m$ in *T. gondii* was determined by using the cationic fluorescent probes Mitotracker and DiOC₆(3). Observations assayed by both dyes on intracellular parasites being exposed to HDQ showed significantly depolarization of $\Delta\Psi_m$ in *T. gondii*, implying that the interferences of TgNDH2 activity attributed to HDQ inhibition directly affect oxidative phosphorylation. Intriguingly, real-time imaging revealed that intracellular parasites challenged by HDQ at nanomolar concentrations led to a dramatically collapse of $\Delta\Psi_m$ within minutes. Additionally, the collapse of $\Delta\Psi_m$ mediated by HDQ was decreased in the presence of F₀-ATPase inhibitor oligomycin, suggesting that *T. gondii* may possess a conventional-like F₀-ATPase that can be inhibited by oligomycin. As a consequence, proton translocation was prevented from entering the mitochondrial matrix and thereby $\Delta\Psi_m$ was able to be stabilized. Following that, subcellular fractionation of the lysates from a transgenic line expressing an epitope-tagged TgATPase- β , a subunit of F₁-ATPase, revealed that TgATPase- β was explicitly found on membrane fraction, indicating a mitochondrial-associated F₁-ATPase in *T. gondii*. This finding suggests that F₀F₁-ATPase in *T. gondii* is conventional-like instead of possessing a soluble F₁-ATPase as proposed in *P. falciparum* (Painter *et al.*, 2007). The influence of HDQ on intracellular ATP level was further assessed. Intracellular parasites treated with HDQ for 1 h showed a significant ATP depletion of 30%, which increased to 70% after 24 h. Taken together, these data strongly indicate that HDQ inhibition leads a fast collapse of $\Delta\Psi_m$ and eventually results in ATP depletion.

Moreover, the mode of inhibitory actions of HDQ and complex III inhibitor atovaquone were compared. HDQ-mediated but not atovaquone-mediated $\Delta\Psi_m$ depolarization was stabilized in the presence of excess substrates for the

dehydrogenases including succinate dehydrogenase, malate:ubiquinone oxidoreductase and dihydroorotate dehydrogenase. These enzymes are localized in the respiratory chain upstream of complex III, implying that additional electrons contributed from the oxidoreductase activities exerted on these dehydrogenases can feed into the ubiquinol pool and partly compensate the HDQ inhibitory effect on TgNDH2, preventing a collapse of $\Delta\Psi_m$. Finally, the long-term HDQ treatment on tachyzoites was examined showing that bradyzoite differentiation was induced as verified by quantitative RT-PCR. Interestingly, bradyzoites induced by alkaline pH-shift were detected with a lower percentage of positive- $\Delta\Psi_m$ staining, suggesting that the importance of oxidation phosphorylation in bradyzoites is different from that in tachyzoites.

3.3 Functional Analysis of TgNDH2s

3.3.1 Elucidating the Orientations of Inner Mitochondrial Membrane-associated TgNDH2s

3.3.1.1 TgNDH2-II is an Internal Enzyme

To investigate the orientations of both inner mitochondrial membrane-associated TgNDH2s, engineered self-assembling split GFP complementation was used (Cabantous *et al.*, 2005). In this approach, C-terminal fragment β -strand 1-10 of GFP (GFP1-10) and β -strand 11 of GFP (GFP11) were expressed separately. When both molecules are localized to the same compartment, these two engineered GFP fragments are able to reconstitute GFP folding and fluoresce. A transgenic parasite line expressing a mitochondrial matrix protein TgSCS- β fused with GFP1-10 (TgSCS β -GFP1-10) was first generated and the correct mitochondrial targeting was verified by co-localization with Mitotracker as illustrated in Fig. 3.1A. To test whether TgNDH2-GFP11 fusions are oriented as internal forms, constructs TgNDH2-I-GFP11 and TgNDH2-II-GFP11 were transfected into TgSCS β -GFP1-10 line. Living parasites from TgSCS β -GFP1-10 line transfected with TgNDH2-II-GFP11, but not that with TgNDH2-I-GFP11, were able to fluoresce and revealed a typical tubular mitochondrial pattern under time-lapse microscopic observation, indicating that the two C-terminal GFP fragments contributed from TgSCS- β and TgNDH2-II closely interacted and reconstituted a functional GFP molecule resulting in fluorescence (Fig.

3.1B). This observation was confirmed on fixed samples (Fig. 3.1C). To further demonstrate that the fluorescence observed in parasites is indeed due to the interaction of TgSCS- β and TgNDH2-II, individual parasite lines TgSCS β -GFP1-10, TgNDH2-I-GFP11 and TgNDH2-II-GFP11 were monitored. These parasites by themselves were unable to fluoresce (Fig. 3.1D). Thus, this finding suggests TgNDH2-II possessing an internal orientation that interacts with mitochondrial matrix protein TgSCS- β and reconstitutes GFP fluorescence.

3.3.1.2 TgNDH2-I is also an Internal Enzyme

One possible reason that TgSCS- β -GFP1-10 line transfected with TgNDH2-I-GFP11 did not fluoresce can be attributed to the inaccessibility of GFP11 that hinders a correct folding with GFP1-10. The possibility of mitochondrial mis-targeting of TgNDH2-I-GFP11 construct was ruled out, since the localization of GFP11 fusion protein at mitochondria was confirmed by IFA (Fig. 3.2A). Interestingly, a previous study has predicted that type II NADH dehydrogenase in *P. falciparum* might possess an amphipathic helix C-terminus which penetrates into the lipid bilayer (Fisher *et al.*, 2007). If this is similar in *T. gondii*, the internal inner mitochondrial membrane proteins with C-terminal GFP11 fusion would be limited by split GFP complementation approach by interacting with a mitochondrial matrix protein. To preclude this possibility, we generated two truncated constructs TgNDH2-I₃₉₉-GFP11 and TgNDH2-I₄₈₇-GFP11, where hydrophilic C-termini were fused with GFP11 (Fig. 3.2B). In addition, two constructs TgNDH2-I-GS-GFP11 and TgNDH2-I-LS-GFP11 (Fig 3.2B) were generated, which were fused with GFP11 domain with extended linkers to prevent self-aggregation or to optimize the orientation of the fusions in space that brings GFP fragments into close proximity (Remy and Michnick, 2004). The constructs were transfected into TgSCS- β line and tested whether mitochondrial GFP fluorescence was observed. Strikingly, TgSCS- β line transfected with TgNDH2-I₃₉₉-GFP11 and TgNDH2-I₄₈₇-GFP11 both resulted in GFP fluorescence as shown in fixed samples (Fig. 3.2C) and confirmed in living parasites (Fig. 3.2D). In contrast, TgNDH2-I-GFP11 even fused with additional linkers did not reveal fluorescence. Collectively, these data indicate that C-terminal GFP11 of truncated TgNDH2-I constructs were able to closely interact with TgSCS- β to reconstitute the GFP

molecules, suggesting an internal version of type II NADH dehydrogenase isoform I that might have a lipid bilayer oriented C-terminus.

To further exclude that TgNDH2-I acts as an external enzyme, identifying a protein localized at the intermembrane space was prioritized. By using sequences of Cyt1 and Cox19 from *S. cerevisiae* as queries, which are well-known to be localized at intermembrane space in *S. cerevisiae* (Lutz *et al.*, 2003), several putative proteins including cytochrome c (TGME49_019750, E-value: 5×10^{-30} ; TGME49_029420, E-value: 1×10^{-12}) and Cox19 (TGME49_054260; E-value: 4×10^{-11}) in *T. gondii* were predicted with high E-value. Parasite lines expressing each of putative cytochrome c (TgCytC750-GFP1-10; TgCytC420-GFP1-10) and Cox19 (TgCox19-GFP1-10) were generated. All constructs were fused with GFP1-10. Eventually parasite line TgCytC750-LS-GFP1-10, which includes an additional linker LS(GGGGS)₂AA between the encoding protein and GFP1-10, was targeted to the mitochondrion as detected by IFA (Fig. 3.3A). Construct TgNDH2-I-GFP11 was transfected into this line. As expected, resulting parasites were unable to fluoresce in fixed samples (Fig. 3.3B), suggesting TgNDH2-I does not interact with intermembrane space protein TgCytC750 and is thus not an external enzyme.

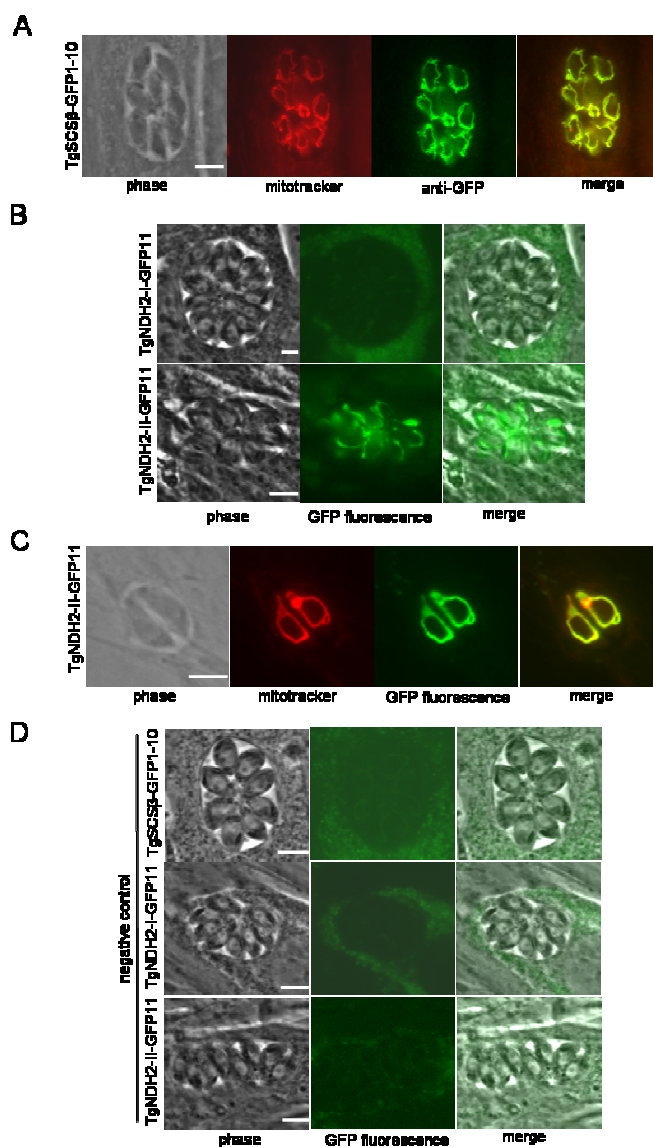


Figure 3.1 TgNDH2-II is oriented internally at inner mitochondrial membrane. (A) Mitochondrial localization of TgSCS β -GFP1-10 fusion was detected by IFA using anti-GFP antibody and confirmed by co-localization with Mitotracker in fixed samples. (B) TgNDH2-II-GFP11 transfected in TgSCS β -GFP1-10 line results GFP fluorescence in living parasites. TgSCS β -GFP1-10 line was stably transfected with TgNDH2-I-GFP1-10 (upper panel) and TgNDH2-II-GFP11 (lower panel). Living parasites from each line were observed under time-lapse microscopy. (C) Parasites from TgSCS β -GFP1-10 line being transfected with TgNDH2-II-GFP11 were co-localized with Mitotracker in fixed sample. (D) Individual living parasites from TgSCS β -GFP1-10, TgNDH2-I-GFP11 or TgNDH2-II-GFP11 line did not reveal GFP fluorescence. Scale bar, 5 μ m.

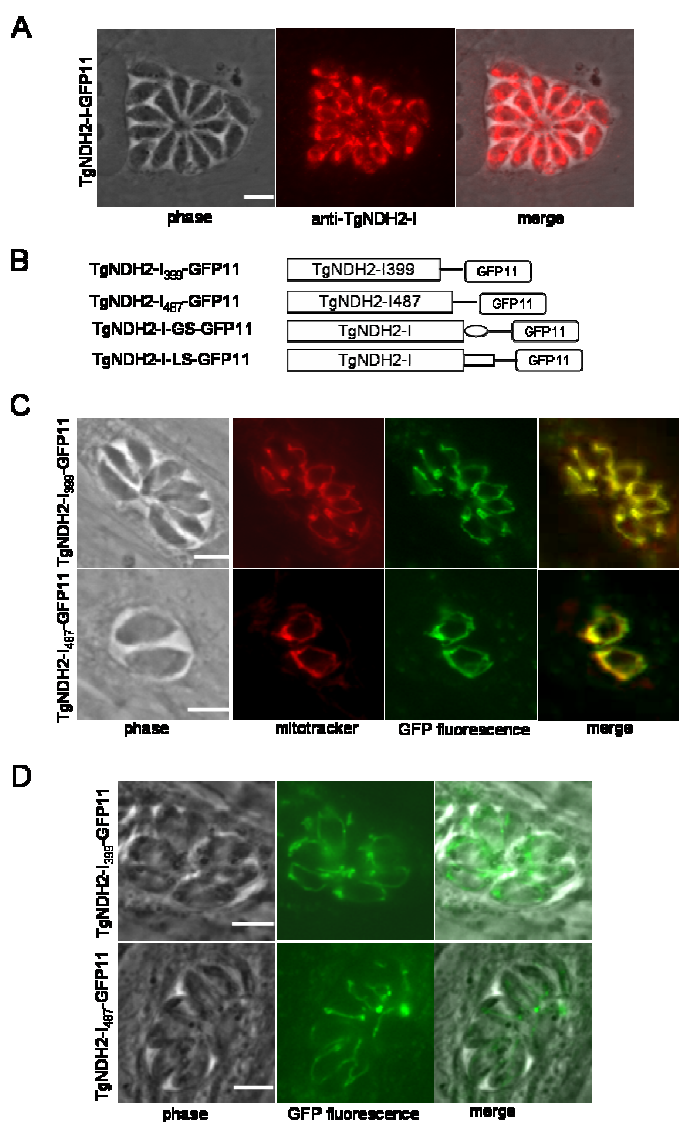


Figure 3.2 TgNDH2-I is oriented internally at inner mitochondrial membrane. (A) Mitochondrial localization of TgND2H-I-GFP11 fusion was detected by IFA using affinity-purified anti-TgNDH2-I antibody. (B) Schematic diagrams depicting the truncated constructs TgNDH2-I₃₉₉-GFP11 and TgNDH2-I₄₈₇-GFP11, and the constructs with additional amino acid residues (GS)₄ and LS(GGGGS)₄AA linking the C-terminus of TgNDH2-I and GFP11 fragment. (C) Mitochondrial localization of the parasites from TgSCSβ-GFP1-10 line being transfected with TgNDH2-I₃₉₉-GFP11 and TgNDH2-I₄₈₇-GFP11 were verified with the co-localization with Mitotracker in fixed samples and (D) in living cultures. Scale bar, 5 μm.

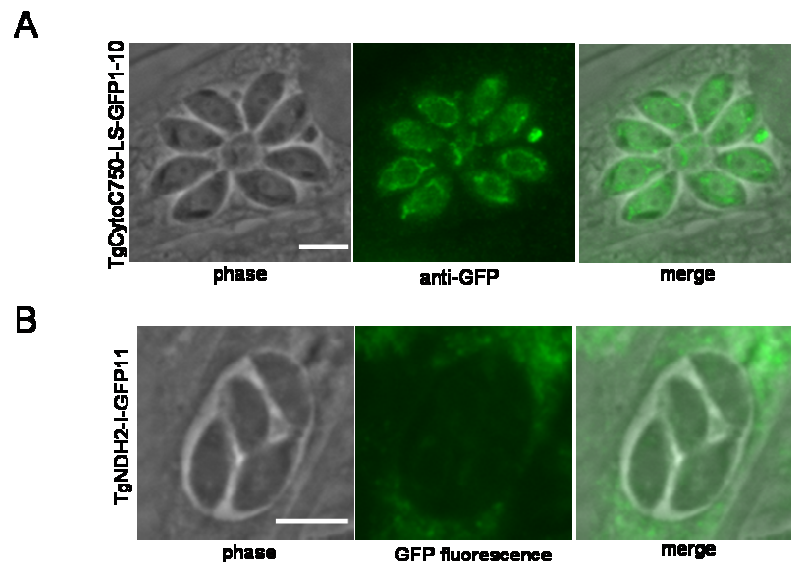


Figure 3.3 TgNDH2-I is not an external enzyme. (A) TgCytoC750-GFP1-10 fusion was localized at mitochondria. Parasites were analyzed by IFA by staining with anti-GFP antibody. (B) TgCytoC750-GFP1-10 line transfected with TgNDH2-I-GFP11 did not fluoresce. Scale bar, 5 μ m.

3.3.2 Phenotypic Analysis of TgNDH2s Depletion Mutants

3.3.2.1 Conditional TgNDH2-I and TgNDH2-II Knock-out Mutants achieved by a cosmid-based Approach

To study the phenotypes of parasites which lack one of the TgNDH2s, a logical strategy is to generate conditional TgNDH2s knock-out mutants (Meissner *et al.*, 2001), given the possibility that loss of either isoform of TgNDH2s might be deleterious for the parasites. Available approaches of gene disruption based on homologous recombination are not very efficient (Striepen and Soldati, 2007) due to the high frequency of non-homologous recombination. Therefore, a new approach by using long flanking sequences from cosmid (~ 40 kb) was applied to increase the frequency of homologous recombination (Brooks *et al.*, 2009). Fig. 3.4A has outlined the scheme of the adapted recombineering (Lee *et al.*, 2001) for cosmid modification by introducing a selection cassette that enables gene deletions. Cosmid clones PSBLE59 and PSBM942 including TgNDH2 genomic region were identified (via www.toxoDB). Modified cosmids PSBLE59 and PSBM942 were achieved and verified by PCR (Fig. 3.4B), and the insertion sites flanking the cassettes were confirmed by sequencing. To generate conditional knock-out mutants, the modified cosmids PSBLE59 and PSBM942 then were respectively transfected into myc-tagged TgNDH2-I and TgNDH2-II lines, which encode an additional copy of the target gene regulated by an ATc-dependent transactivator promoter (Meissner *et al.*, 2001). Clonal lines were tested for successful gene displacements by PCR, as shown in Fig. 3.5B. Representative knock-out clones compared to wild-type controls were detected with the expected PCR product sizes and further confirmed by restriction digestion on PCR products (Fig. 3.5C). Specific restriction site located at selection cassette or at targeted TgNDH2s genes were used to confirm the disruption of endogenous gene loci. Additionally, gene disruptions of TgNDH2s in depletion mutants (designated as Δ TgNDH2-I and Δ TgNDH2-II) at mRNA transcripts were confirmed by RT-PCR analysis (Fig. 3.5D).

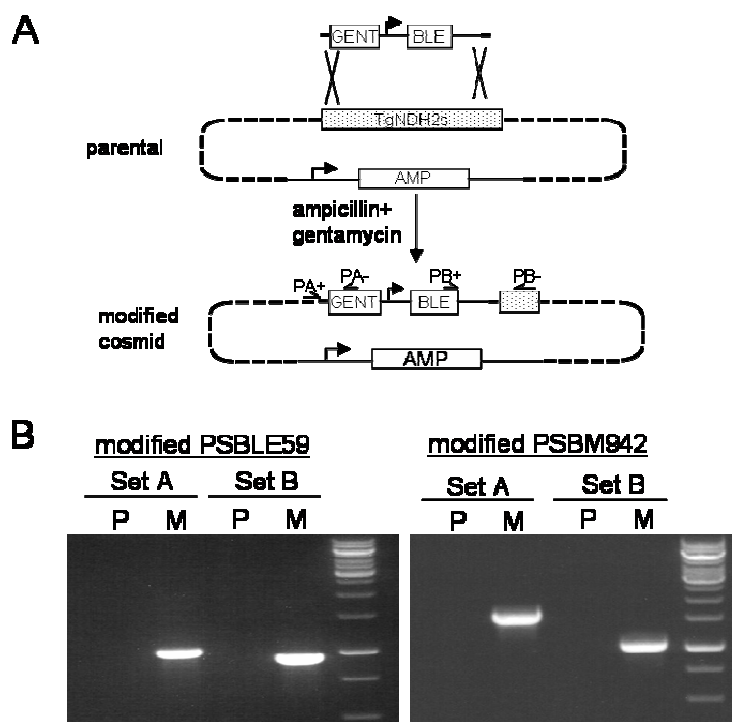


Figure 3.4 Cosmid modification by recombineering. (A) Schematic diagram of cosmid modification. Cosmids PSBLE59 and PSBM942 were modified by lambda Red-mediated homologous recombination in SW103 using PCR products containing a modification cassette with both gentamycin and phleomycin resistance markers. The primers used for PCR amplification flank with 50 bp of homology to the target genes TgNDH2s (targeting TgNDH2-I in PSBLE59 and TgNDH2-II in PSBM942) for site-directed recombination. (B) PCR amplification for verifying cosmid modification. Isolated cosmid DNA from a representative clone was subjected to PCR assay using two primer sets (Set A, primers PA+/-; Set B, primers PB+/-). Resistance markers: GENT, gentamycin; BLE, phleomycin; and AMP, ampicillin. P, parental cosmid; M: modified cosmid.

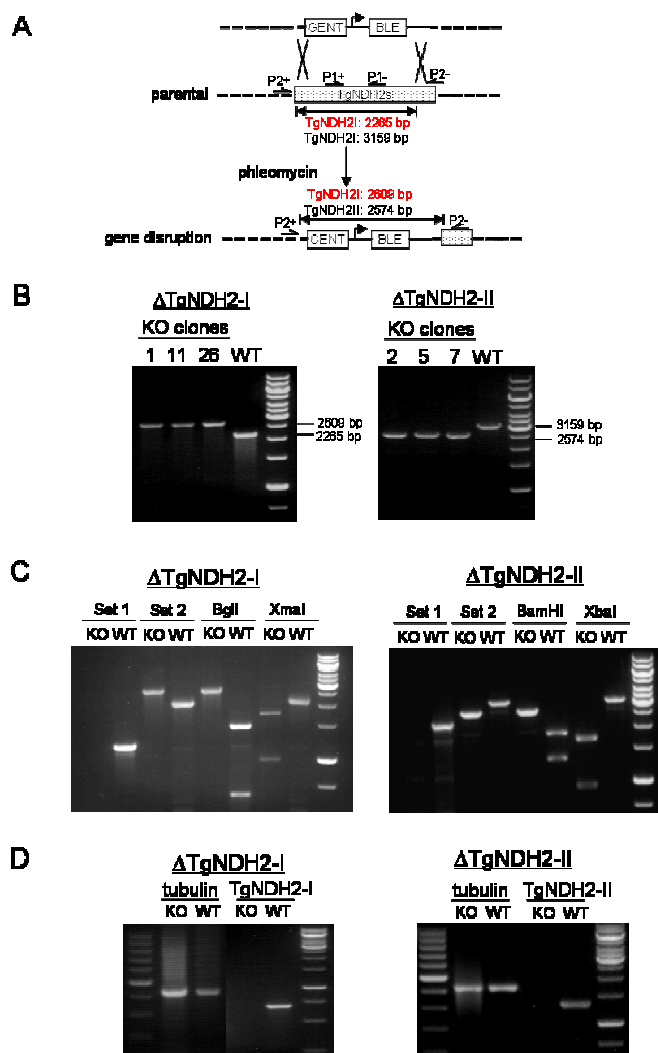


Figure 3.5 Generation of conditional knock-out mutants for TgNDH2s. (A) Schematic diagram describing a single homologous recombination event in *Toxoplasma* genome that allows the deletion of the endogenous copies of each targeted TgNDH2 gene by using long flanking sequences of modified cosmid. (B) Representative knock-out clones for TgNDH2-I (24 out of 35 are positive) and TgNDH2-II (38 out of 51 are positive). (C) Analysis of knock-out mutant by PCR and restriction digestion in a representative clone. Genomic DNA samples from the representative clones were assayed by PCR using primer Set 1 and 2. PCR products amplified by using primer Set 2 [P2+/- shown in (A)] were analyzed by restriction digestion. (D) Analysis of knock-out mutants by RT-PCR. cDNA samples from the representative knock-out clones were subjected to PCR amplification. β -tubulin was used as an internal control. All analysis includes samples (genomic DNA or cDNA) from wild-type strain. KO, knock-out; WT, wild-type.

3.3.2.2 TgNDH2-I and TgNDH2-II are non-essential for *T. gondii* Replication

Having confirmed the disruption of the endogenous gene locus in each conditional knock-out mutant (Δ TgNDH2-I and Δ TgNDH2-II, the tetracycline-inducible transactivator system was first tested in these parasites. A representative clonal line from Δ TgNDH2-I and Δ TgNDH2-II was cultivated either in the presence or absence of ATc (\pm ATc) for 72 h, and the exogenous copies of myc-tagged TgNDH2-I and TgNDH2-II were effectively suppressed as shown in Fig. 3.6A detected by IFA. Next, the growth rates of Δ TgNDH2-I and Δ TgNDH2-II parasites \pm ATc were compared after two rounds of passages in order to further dilute the residual expression of TgNDH2s from the additional ectopic copies (Fig. 3.6B). Additionally, the growth rates of the parental myc-tagged TgNDH2-I and TgNDH2-II parasites \pm ATc were also determined for comparison. These findings showed that the depletion of either TgNDH2-I (Fig. 3.6B, left panel) or TgNDH2-II (Fig. 3.6B, right panel) did not affect the intracellular replication rate, suggesting that either TgNDH2-I or TgNDH2-II is non-essential for parasite growth.

3.3.2.3 TgNDH2-I or TgNDH2-II Depletion does not affect mRNA Transcripts of the intact Isoform

In order to investigate whether the depletion of either TgNDH2-I or TgNDH2-II affects the mRNA transcript levels of the intact isoform, the steady-state mRNA transcript levels of TgNDH2-II in Δ TgNDH2-I and its parental myc-tagged TgNDH2-I parasites, and TgNDH2-I in Δ TgNDH2-II and its parental myc-tagged TgNDH2-II parasites were compared \pm ATc and quantified by real-time RT-PCR. These data revealed that the relative mRNA transcript levels of TgNDH2-II in Δ TgNDH2-I, and TgNDH2-I in Δ TgNDH2-II were unchanged (\sim 1–1.4 fold of induction \pm ATc) when compared to their parental controls (Fig. 3.7), indicating the depletion of one TgNDH2 isoform does not significantly affect the mRNA transcript level of the intact isoform.

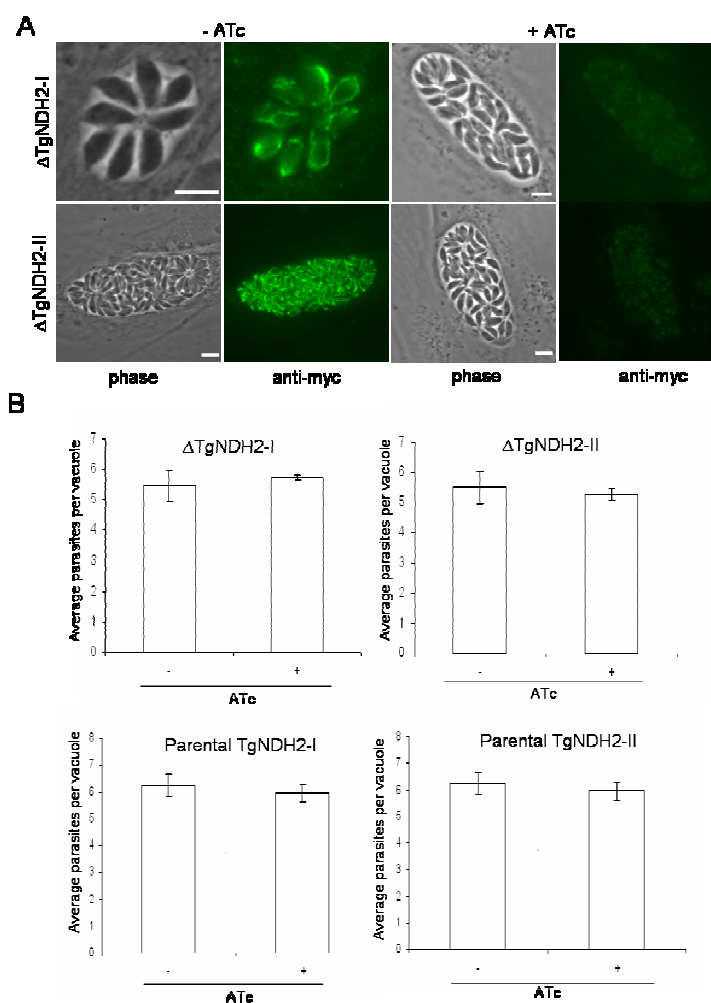


Figure 3.6 TgNDH2-I and TgNDH2-II depletion mutants display unaltered growth rates. (A) Functional ATc-regulated repression of myc-tagged TgNDH2-I and TgNDH2-II. Conditional Δ TgNDH2-I and Δ TgNDH2-II parasites were cultivated either in the presence or absence of ATc (\pm ATc) at a final concentration of 1 μ M for 72 h. Expression levels of exogenous copies of myc-tagged TgNDH2-I and TgNDH2-II were analyzed by IFA using anti-myc antibody. (B) Comparison of the growth rates of Δ TgNDH2-I and Δ TgNDH2-II. Δ TgNDH2-I (left panel) and Δ TgNDH2-II (right panel) parasites and their parental controls were grown two rounds (\pm ATc). Parasites ($\sim 1 \times 10^5$) from each clonal line were inoculated onto HFF confluent monolayer \pm ATc. Duplicate samples were fixed after 24 h and the average number of tachyzoites per vacuole was determined. At least 100 vacuoles were examined for each sample. Results were expressed as means \pm S.D. from a representative experiment, N=3.

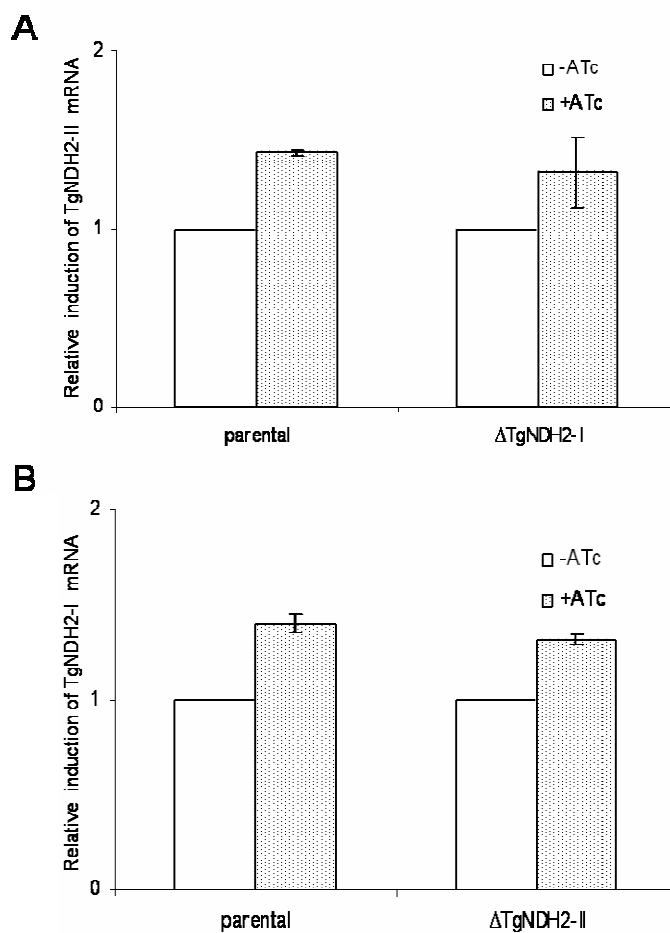


Figure 3.7 Quantitative RT-PCR for assaying mRNA transcripts of (A) TgNDH2-II in Δ TgNDH-I, and (B) TgNDH2-I in Δ TgNDH-II conditional knock-out mutants. cDNA samples from parental and Δ TgNDHs parasites cultivated \pm ATc were subjected to real-time PCR. β -tubulin was used as an internal control. Results are expressed as means \pm S.D. of the duplicate samples from a representative experiment.

3.3.2.4 TgNDH2-I or TgNDH2-II Depletion does not affect Extracellular Viability

The effects of either TgNDH2-I or TgNDH2-II depletion on the parasite's extracellular viability were further examined. Freshly released extracellular parasites from Δ TgNDH2-I and Δ TgNDH2-II, and the parental myc-tagged TgNDH2-I and TgNDH2-II lines cultivated \pm ATc were immediately infected on HFF confluent monolayer \pm ATc at 0 h or infected at 7 h that parasites were completely incubated without host cells. Samples were fixed after 24 h post-infection. Extracellular viability of the parasites was assessed by comparing the infectivity of parasites at 7 h after normalization with that at 0 h. As shown in Fig. 3.8, Δ TgNDH2-I or Δ TgNDH2-II mutant and their parental controls infected at 7 h were observed with unaltered extracellular viability \pm ATc (~75-85%), implying that either TgNDH2-I or TgNDH2-II does not play an important role in maintaining extracellular viability.

3.3.2.5 TgNDH2-I Depletion Mutant is less sensitive to HDQ Treatment

Since HDQ acts as a high affinity inhibitor for *Toxoplasma* NDH2-I in enzymatic assays (Lin *et al.*, 2008) and also inhibits the growth of *T. gondii* effectively in nanomolar concentrations (Saleh *et al.*, 2007). It was interesting to investigate whether the conditional knock-out mutants display different sensitivities against HDQ treatment. The susceptibility of Δ TgNDH2-I and Δ TgNDH2-II as well as the parental parasites to HDQ was compared \pm ATc (Fig. 3.9). Δ TgNDH2-II parasites \pm ATc showed an unchanged sensitivity to HDQ treatment at a final concentration of 10 nM. Interestingly, Δ TgNDH2-I parasites were slightly less sensitive to HDQ at 10 nM in the presence of ATc (Fig. 3.9A; bar 4). Further analysis on the sensitivity of Δ TgNDH2-I mutant in response to different HDQ concentrations (Fig. 3.9C) confirmed that the depletion of TgNDH2-I is rendering parasites slightly less sensitive to HDQ treatment.

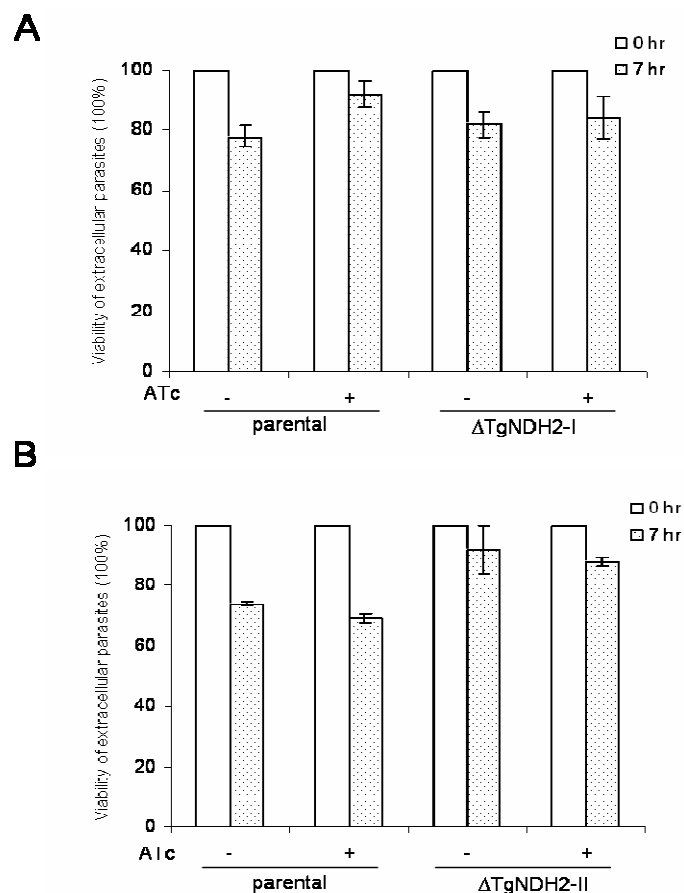


Figure 3.8 TgNDH2-I and TgNDH2-II depletion mutants show unaltered extracellular viability. Intracellular Δ TgNDH2-I and Δ TgNDH2-II, and its parental controls were mechanically released by syringe passage, followed by infection ($\sim 1 \times 10^5$) on HFF confluent monolayer at 0 h and 7 h. Samples were fixed after 24 h post-infection and the average numbers of vacuoles were calculated from 4 fields from each slide. Extracellular viability was determined by normalization the average numbers of vacuoles infected at 7 h with that calculated at 0 h. Results are expressed as means \pm S.D. from duplicate samples from a representative experiment.

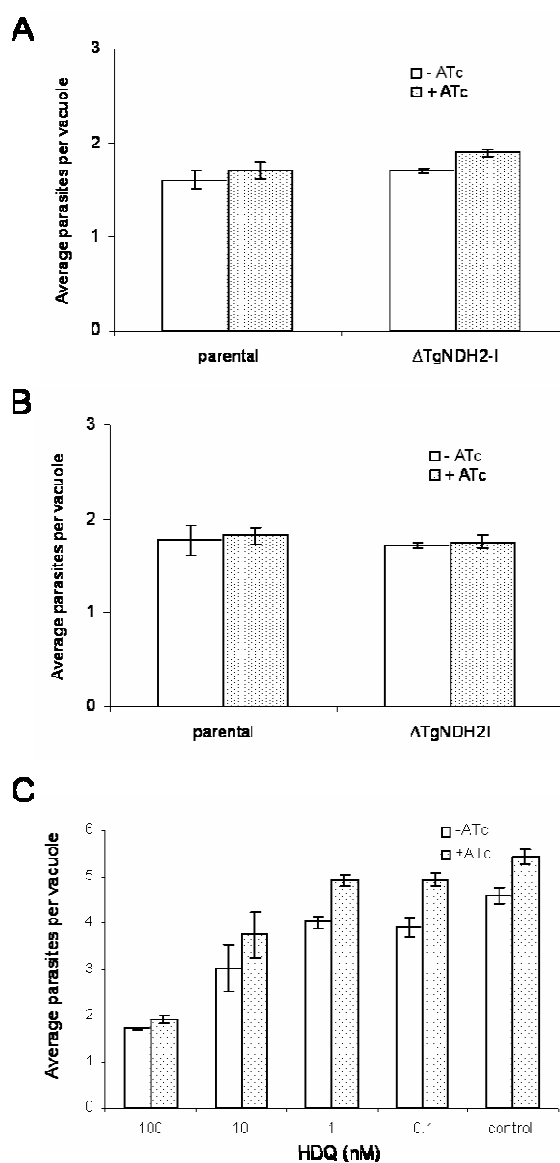


Figure 3.9 TgNDH2-I depletion is less sensitive to HDQ. The growth rates of (A) Δ TgNDH2-I and (B) Δ TgNDH2-II \pm ATc treated with HDQ was compared. Knock-out mutants and its parental controls were grown two rounds \pm ATc. Infection ($\sim 1 \times 10^5$) from each clonal line were inoculated onto HFF confluent monolayer \pm ATc exposed to HDQ at a final concentration of 10 nM. (C) Comparing the growth rates of Δ TgNDH2-I \pm ATc treated with HDQ at a final concentration of 100 nM, 10 nM, 1 nM or 0.1 nM. All samples were duplicated, fixed after 24 h, and the average number of tachyzoites per vacuole was determined. At least 100 vacuoles were examined for each sample. Results were represented as means \pm S.D.

3.3.2.6 TgNDH2-I or TgNDH2-II Depletion does not affect $\Delta\psi_m$

The impact of TgNDH2s depletion on the mitochondrial membrane potential ($\Delta\psi_m$) was further investigated based on our previous observation that TgNDH2s inhibition collapses $\Delta\psi_m$ in *T. gondii* (Lin *et al.*, 2009). Living Δ TgNDH2-I and Δ TgNDH2-II parasites cultivated \pm ATc were stained with cationic dye DiOC6(3), and $\Delta\psi_m$ of the parasites were determined (Fig. 3.10). Our data showed no significant differences of $\Delta\psi_m$ in Δ TgNDH2-I or Δ TgNDH2-II mutants \pm ATc, indicating that the depletion of either TgNDH2 isoform does not affect parasites in maintaining mitochondrial membrane potential.

3.3.2.7 Bradyzoite Differentiation is not influenced in Δ TgNDH2-I and Δ TgNDH2-II Parasites

Moreover, we tested the influence of TgNDH2-I and TgNDH2-II depletion on bradyzoite differentiation. Δ TgNDH2-I, Δ TgNDH2-II and the parental parasites were cultivated \pm ATc and bradyzoite differentiation was induced by alkaline pH-shift. The differentiation rate of the parasites was compared \pm ATc (Fig. 3.11) after 3 days of post-infection verified by IFA using bradyzoite-specific anti-BAG1 antibody as a differentiation marker (Bohne *et al.*, 1995). The fraction of bradyzoite-positive parasites (~5-10%) was similar in Δ TgNDH2-I or Δ TgNDH2-II as well as those in parental controls \pm ATc. This finding suggests the depletion of either TgNDH2-I or TgNDH2-II appearing to have no influence on the bradyzoite differentiation.

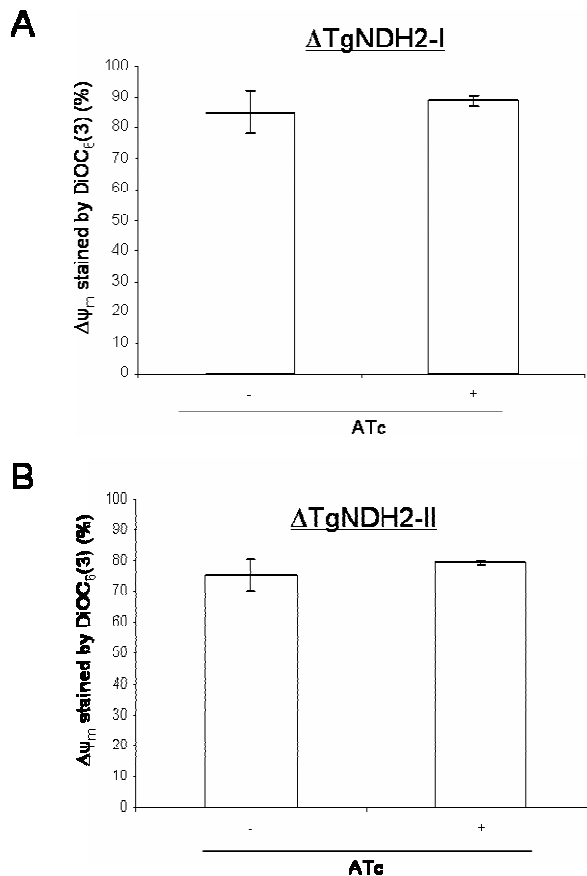


Figure 3.10 TgNDH2-I and TgNDH2-II depletion mutants show normal $\Delta\psi_m$. $\Delta\psi_m$ of living (A) Δ TgNDH2-I and (B) Δ TgNDH2-II parasites (\pm ATc) was compared. Intracellular parasites after 24 h post-infection were immediately stained with DiOC₆(3) and the numbers of vacuoles, which possess a positive- $\Delta\psi_m$ were determined by fluorescence microscopy from at least 100 vacuoles. Results were represented as means \pm S.D. from duplicate wells from a representative experiment, N=2.

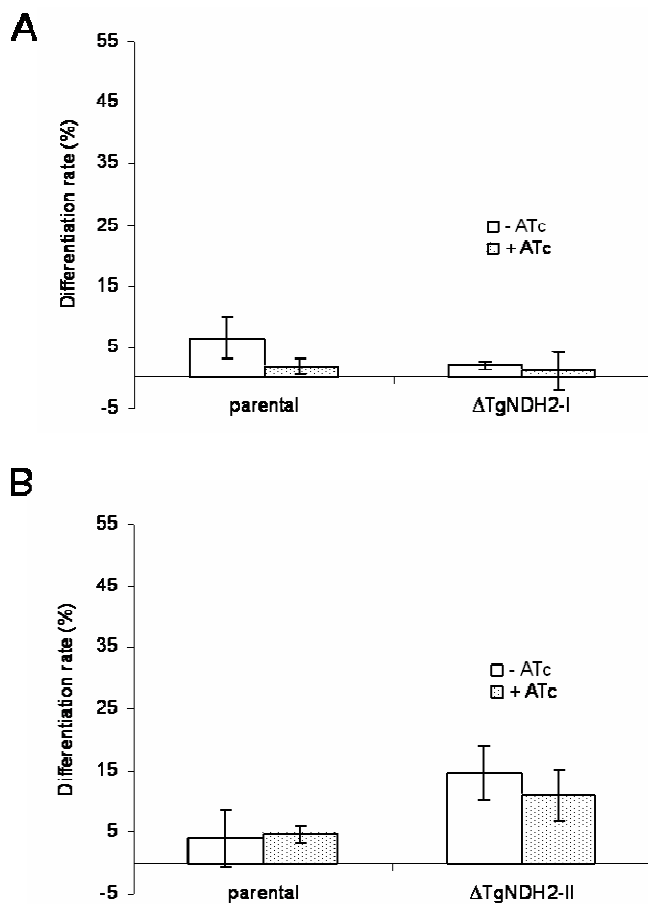


Figure 3.11 Depletion of either TgNDH2-I or TgNDH2-II does not affect bradyzoite differentiation. The differentiation rate of (A) Δ TgNDH2-I and (B) Δ TgNDH2-II \pm ATc was compared with parental parasites \pm ATc detected by IFA using bradyzoite-specific anti-BAG1 antibody. Bradyzoite differentiation was induced by alkaline pH-shift (pH 8.3) for 72 h. Results are expressed as means \pm S.D. from duplicate samples from a representative experiment, N=2.

CHAPTER IV

Discussion

4.1 Both Isoforms of TgNDH2s are Internal Enzymes

A comparative genomic study in Apicomplexa has revealed that most of the members possess type II NADH dehydrogenases instead of canonical complex I in their respiratory chains (Saleh, 2006). Although the reasons for such a preference are unclear, it is generally accepted that the crucial role of NDH2 is to maintain NADH turnover and ultimately to contribute to the production of ATP (Melo *et al.*, 2004). *Toxoplasma* encodes two isoforms of NDH2 instead of one single gene, as in other species such as *Plasmodium*, *Theileria*, *Cryptosporidium*, *Eimeria* and *Babesia*. The expression of NDH2 is not confined to Apicomplexa, but also described in bacteria, plants and fungi, however, it seems exclusively absent in mammals. Due to the absence, NDH2 has been considered as a potential drug target (Biagini *et al.*, 2006; Saleh *et al.*, 2007; Lin *et al.*, 2008) for the apicomplexan parasites.

Type II NADH dehydrogenase, known as inner mitochondrial-associated membrane protein, can be oriented as external or internal version. And it is getting more complicated in *Toxoplasma* owing to the co-existence of two isoforms. The crux of understanding the orientations of TgNDH2s is to unveil the precise functions of each isoform, which should help to interpret their roles in energy metabolism. More specifically, an external orientation implies that only cytosolic NADH, mainly produced by glycolytic enzymes, can enter the electron transport chain. In the case of an internal enzyme, the reducing equivalents are from the matrix NADH, which is mainly contributed from the TCA cycle. At the beginning of this study, the orientations of both TgNDH2s were unknown. The experimental data obtained by GFP complementation presented in this study for the first time clearly indicate that both isoforms of TgNDH2s are more likely to be internal enzymes (Fig. 3.1 and 3.2). These data are in contrast with previous suggestions in favor of external orientations (Saleh, 2006). However, it is worth to emphasize that earlier predictions are primarily based on bioinformatics approaches using phylogenetic analysis among the orthologs from apicomplexan parasites and plants. It was shown in *Plasmodium* that exogenous

NAD(P)H, which is presumably impermeable to inner mitochondrial membrane, could stimulate electron transport (Fry and Beesley, 1991; Uyemura *et al.*, 2004; Biagini *et al.*, 2006). These observations would be in agreement with an external orientation of the single PfNDH2. In contrast, the direct evidence provided from *T. gondii* supports the internal enzymes for TgNDH2s, implying that reducing equivalents from matrix NADH but not cytosolic NADH are directly utilized by these enzymes. These findings are not unexpected and correlate with the earlier identification of a cytosolic glyceraldehyde 3-phosphate dehydrogenase in *T. gondii* (Fleige *et al.*, 2007), suggesting the presence of a glycerol phosphate shuttle for the transport of electrons from cytosolic NADH to mitochondrial carrier FAD. Taken together, both reducing powers from cytosolic and matrix NADH ultimately can enter the oxidative phosphorylation pathways. Interestingly, the observations of internal TgNDH2s are in line with the earlier study in *Yarrowia* (Kerscher *et al.*, 2001) demonstrating that in the absence of essential complex I, only the internal but not external *Yarrowia* NDH2 could rescue the growth defect.

A striking property but also challenging feature of NDH2s is the complexity of membrane anchoring. Again, although they are well-known to be membrane-associated, extensive hydropathy analysis is unable to predict any transmembrane α -helices (Melo *et al.*, 2004; Fisher *et al.*, 2007). The ongoing question is how these enzymes interact with membranes that allows efficient electron transfer simultaneously among the hydrophilic NAD(P)H and hydrophobic ubiquinone substrates as well as the putative cofactors such as FMN and FAD. Available models of membrane anchoring for NDH2s are based on homology prediction and are still a matter of controversy (Melo *et al.*, 2004; Fisher *et al.*, 2007; Kerscher *et al.*, 2008). But in general, it is believed that the membrane attachment is highly relied on certain amphiphathic α -helices (Melo *et al.*, 2004), where hydrophilic headgroups and hydrophobic tails are along the α -helices with opposite sites. Such a prediction is also proposed in *P. falciparum* suggesting that a C-terminal amphiphathic α -helice is oriented in the membrane lipid bilayer (Fisher *et al.*, 2007). Surprisingly, by using GFP complementation, the truncated TgNDH2-I₃₉₉-GFP11 and TgNDH2-I₄₈₇-GFP11 but not full-length TgNDH2-I-GFP11 are able to reconstitute GFP molecules with

TgSCS β -GFP1-10 line (Fig. 3.2), suggesting that the C-terminus of TgNDH2-I may penetrate into the lipid bilayer.

Another pressing point is the identification of quinone-binding sites (ubiquinone in *T. gondii*) for NDH2s following the observations that several compounds targeting at quinone-quinol cycle have been considered as potential drug targets (Weinstein *et al.*, 2004; Eschemann *et al.*, 2005; Yano *et al.*, 2006; Biagini *et al.*, 2008). The elucidation of the quinone-binding sites would definitely illuminate invaluable information for drug design and for improving drug efficacy. However, the quinone-binding sites are unpredictable by primary structures and the majority of the structural models in hand have not yet been validated. Nevertheless, there is a consensus that the quinone-binding regions including the interactive sites of enzymes for hydrophilic quinone headgroups and hydrophobic tails, are interfaced at the membrane surface (Melo *et al.*, 2004; Fisher *et al.*, 2007; Kerscher *et al.*, 2008). For ping-pong mechanisms as described for *Yarrowia* NDH2 and TgNDH2-I (Eschemann *et al.*, 2005; Lin *et al.*, 2008), a puzzling question raised is how the hydrophilic NADH and hydrophobic ubiquinone interact with the enzyme in a common binding pocket. Despite the concerns, this kind of interaction is possible since the active site for ubiquinone is mainly at the hydrophilic headgroup rather than at the hydrophobic tail that is presumably buried at the bilayer (Fisher *et al.*, 2007). However, the exact quinone-binding sites of each individual NDH2s are variable and further analysis on X-ray structures of NDH2s together with valid substrates is necessary to draw a convincing model.

4.2 TgNDH2-I is a Drug Target for HDQ

HDQ was first identified as a high affinity inhibitor for *Yarrowia* type II NADH dehydrogenase in enzymatic assays (Eschemann *et al.*, 2005). A subsequent work clearly showed that HDQ effectively inhibited the replication rates of *T. gondii* and *P. falciparum* *in vitro* with remarkable low IC₅₀ values in nanomolar (Saleh *et al.*, 2007) ranges. By linking these observations, it seems logical to deduce that HDQ may target at the same enzymes in *Toxoplasma* and *Plasmodium*. However, without experimental validation, the drug targets of HDQ in *Toxoplasma* and *Plasmodium* remain

questionable. Here, enzyme kinetics studies on individual recombinant enzymes TgNDH2-I and TgNDH2-II being heterologously expressed in *Yarrowia* NDH2 deletion strain provide solid evidence that TgNDH2-I is a drug target of HDQ (Lin *et al.*, 2008; see **Section 3.1**). Further comparing the IC₅₀ values obtained in recombinant enzyme TgNDH2-I and in *Yarrowia* NDH2 reveals that the IC₅₀ are within similar nanomolar ranges (Eschemann *et al.*, 2005; Lin *et al.*, 2008), identifying HDQ as a high affinity inhibitor. A concern is the discrepancy of IC₅₀ values for TgNDH2-I determined in enzyme kinetics (~300 nM) and *in vitro* (2-4 nM) (also see **Discussion** described in Lin *et al.*, 2008). A key consideration is the efficiency of the interaction between the hydrophobic compound HDQ and the enzyme TgNDH2-I. Since NDH2 requires a hydrophobic environment for its activity (Bjorklof *et al.*, 2000; Melo *et al.*, 2004; see **Section 4.1**), HDQ needs to interface along the membrane surface in order to contact with NDH2-I, as proposed earlier (Lin *et al.*, 2008). In enzymatic analyses, TgNDH2-I recombinant proteins were incubated with HDQ for 5 minutes and the inhibition effect was analyzed based on electron transfer activity. For *in vitro* studies, intracellular parasites were incubated with HDQ for 24 hours and the inhibition effect was analyzed based on replication rate. By comparison of these two experimental settings, the longer incubation of HDQ with the intact enzyme inside the parasites achieves a better inhibitory effect. This could partly explain why a much lower IC₅₀ was obtained in *in vitro* studies.

A noticeable issue about the discrepancy mentioned above is the presence of additional drug targets of HDQ, which cannot be completely excluded. These enzymes include succinate dehydrogenase, isocitrate dehydrogenase, dihydroorotate dehydrogenase, glycerol-3-phosphate dehydrogenase and malate:ubiquinone oxidoreductase as well as TgNDH2-II. All of them are upstream of complex III in the respiratory chain. Although so far no direct evidence in *T. gondii* can conclude that the captioned enzymes are additional targets of HDQ, it is clear that HDQ targets differently from complex III inhibitor atovaquone. HDQ is highly probable interfering with the process of ubiquinone reduction based on previous observations from substrate supplementation experiments (Lin *et al.* 2009; see **Section 3.2**). Results showed that HDQ-mediated but not complex III inhibitor atovaquone-mediated collapse of $\Delta\psi_m$ was partly stabilized with excess substrates for the other

dehydrogenases, indicating that TgNDH2 inhibition is partly rescued by additional electrons to compensate the ubiquinol pool (Lin *et al.*, 2009; see **Section 3.2**). A more recent study in *Plasmodium* has demonstrated that diphenylene iodonium chloride (DPI) and HDQ inhibited recombinant PfDHOD instead of PfNDH2 using *E. coli* for heterologous expression (Dong *et al.*, 2009). For DPI, this finding is slightly unexpected since previous work (Biagini *et al.*, 2006) demonstrated that DPI decreased the activity of *P. falciparum* NDH2, even though a very high micromolar dosage was applied. However, several hiding points not well-mentioned on both studies need to take into consideration such as the purities of PfNDH2 described in both assay systems, the stabilities of the PfNDH2 in the absence of membrane environment (Dong *et al.*, 2009) that is important for NDH2 activity (Bjorklof *et al.*, 2000), and the specificity of DPI to PfNDH2. Without narrowing the disparities of these noticeable points, further evidence is required to make a conclusive statement. To follow up the observation of HDQ targeting at PfDHOD instead of PfNDH2, one may over-simplify that HDQ may also target at DHOD in *Toxoplasma*. Up to now, it is unlikely to support this claim unless direct evidence from functional assays on TgDHOD reveals the specificity of HDQ in *T. gondii*. Moreover, it should be noted that the importance of mitochondrial enzymes in *Plasmodium* and *Toxoplasma* are different (van Dooren *et al.*, 2006; Painter *et al.*, 2007; Seeber *et al.*, 2008). By simply shuttling the observations of *Plasmodium* and *Toxoplasma* one another can distort the understanding of the complete stories of energy metabolism in each parasite.

Despite, there were recently debates about the validity of NDH2s as a drug target, especially in *Plasmodium* (Fisher *et al.*, 2007; Vaidya *et al.*, 2007). Previous findings (Biagini *et al.*, 2006) demonstrated that low affinity inhibitors for PfNDH2 strongly decreased the activity of the *Plasmodium* ortholog, followed by the collapse of $\Delta\psi_m$ and finally lead to parasite death, suggesting an essential role of PfNDH2. On the contrary, another study showed that over-expression of type 1 *S. cerevisiae* ubiquinol independent DHOD in *P. falciparum* made parasites completely resistant to the complex III inhibitor atovaquone (Painter *et al.*, 2007). This finding argues the importance of PfNDH2 in the respiratory chain (Biagini *et al.*, 2006), suggesting that the function of *P. falciparum* complex III is to regenerate the electron acceptor for the endogenous DHOD, which is the fourth enzyme of pyrimidine biosynthetic pathway.

However, it is still early to conclude that NDH2 and other mitochondrial dehydrogenases are non-essential (Fisher *et al.*, 2008). To give an example, in the absence of essential complex I activity in *Yarrowia*, NDH2 activity in the mitochondrial matrix is essential for survival (Kerscher *et al.*, 2001). Discussion is still ongoing, but it is pertinent to point out that even within the phylum Apicomplexa, the importance of mitochondrial enzymes including NDH2 to a large extent can be species-dependent, just considering that ATP pools contributed from oxidative phosphorylation for *Plasmodium* in intraerythrocytic stage compared with *Toxoplasma* in parasitophorous vacuoles are very different (Seeber *et al.*, 2008).

Now, more than ever, DHOD has drawn the most attention among the mitochondrial dehydrogenases (Gutteridge *et al.*, 1979; Vaidya *et al.*, 2007) in Apicomplexa. Preliminary findings (Naujoks, 2008; Sternisek, 2009) in *Toxoplasma* demonstrated that a uracil phosphoribosyltransferase (UPRT)-deficient mutant was more sensitive to HDQ compared with wild-type RH strain in long-term treatments as defined by an exposure with HDQ for 48 h up to 96 h, suggesting that HDQ may target pyrimidine *de novo* biosynthetic pathway. Although these emerging data seem interesting, it is not well-supported. Uracil supplementation experiments showed that it did not lead to an increased growth rate (Lin *et al.*, 2009; Sternisek, 2009), indicating that HDQ growth inhibition is unlikely targeting at pyrimidine starvation. Uracil can rescue parasites deficient in *de novo* pyrimidine biosynthesis as shown in earlier study (Fox and Bzik, 2000) since it is converted by the parasitic UPRT to 5'-monophosphate (UMP), and UMP is further processed into nucleotides. As a rule of openness, it cannot be completely excluded that this pathway is also targeted by HDQ. However, previous postulation that DHOD is a possible target for HDQ is still unclear since no evidence has been provided. But at a circumstance, it is understandable since DHOD is the fourth enzyme in *de novo* pyrimidine biosynthetic pathway, which links to the respiratory chain concerning its role in ubiquinone recycling (Fox and Bzik, 2000). Nevertheless, much more works need to be done to unveil the underlying mechanism involved. However, without reliable data mentioning the equivalent powers actually contributed from other dehydrogenases and more critically the efficiency of the electrons from other dehydrogenases indeed fed into ETC, it may be too early to overestimate the contribution of electrons from other dehydrogenases and/or

underestimate the importance of TgNDH2s in the respiratory chain. Nevertheless, it is still a question mark about the putative drug targets for HDQ. Definitive evidence that no other targets contribute to the HDQ-mediated growth inhibition will require an analysis of resistant determinants, as described in detail previously (McFadden *et al.*, 2000).

4.3 TgNDH2-I and TgNDH2-II are non-essential for Replication Growth

It is becoming obvious that oxidation phosphorylation in *T. gondii* plays a pivotal role in energy production (Vercesi *et al.*, 1998; Lin *et al.*, 2009). The importance of this process relies on electron transport system exerted on a panel of mitochondrial enzyme complexes. Of interest, this study specifically explores the functional roles of mitochondrial TgNDH2s, which have been shown as promising drug targets (Saleh *et al.*, 2007; Lin *et al.*, 2008, 2009). NADH dehydrogenases in all aerobic organisms are known as the main entry site for reducing equivalents from the metabolism to the respiratory chain. However, the question about the essence of TgNDH2s in *Toxoplasma* has not yet been answered. To assess this point, two conditional knock-out mutants TgNDH2-I and TgNDH2-II were firstly generated based on homologous recombination by using recombiner cosmids (Fig 3.5; Lee *et al.*, 2001). Unexpectedly, phenotypic analyses of these two TgNDH2-I and TgNDH2-II depletion mutants showed that the growth rates of both isoforms were identical to parental parasites, indicating that either TgNDH2-I or TgNDH2-II is non-essential for intracellular replication in tachyzoite stage (Fig. 3.6).

Furthermore, phenotypic studies including extracellular viability (Fig. 3.8), $\Delta\Psi_m$ (Fig. 3.10) and bradyzoite differentiation (Fig. 3.11) on each depletion mutant and their parental strains did not reveal any differences, speculating that the endogenous isoform may be redundant and can compensate the loss of the second isoform to maintain their metabolic roles. Regarding to this suggestion, one criterion is that both isoforms need to be oriented with the same side in order to transfer electrons from either cytosolic or mitochondrial NADH. Noticeably, results from split GFP complementation provides clear evidence that both isoforms are oriented as internal enzymes with their active sites facing towards the mitochondrial matrix, which fulfils

this crucial criterion. Although it cannot directly prove that a redundancy indeed exists between these two isoforms, it indicates that the suggested scenario is appropriate for TgNDH2s. In an attempt to test this hypothesis, comparisons of the transcript levels of endogenous isoforms in each knock-out mutant were examined by quantitative RT-PCR. However, no significant up-regulation of each endogenous TgNDH2 isoforms was observed in knock-out mutants, which indirectly indicates that the demand of endogenous TgNDH2 transcript levels (Fig. 3.7) seems unchanged. Whether a functional redundancy is seen between these two isoforms or not seems impossible to be predicted by sequence analyses. Very little hints are derived from bioinformatics studies, which reveal that both isoforms are nearly 40% amino acid identical and can be originated from a gene duplication event (Saleh, 2006), similar to what was proposed in *S. cerevisiae* (Kerscher, 2000). Remarkably, *T. gondii* is the only organism in Apicomplexa possessing two isoforms of NDH2. Nevertheless, a detailed phenotypic analysis on the double knock-out mutant for TgNDH2s in the near future is the solution to answer this interesting question.

So far, the only phenotypic difference is the detection of a slightly lower susceptibility to HDQ in the conditional TgNDH2-I knock-out mutant in the presence of ATc (Fig. 3.9). The decreased sensitivity to HDQ in conditional TgNDH2-I knock-out mutant was consistently observed in a varied range of HDQ concentrations in the presence of ATc compared to those, which were cultivated in the absence of ATc. However, it needs to be stressed that the decreased sensitivity using the average number of parasites per parasitophorous vacuole for comparisons is only a slight difference. This indicates that, even without TgNDH2-I activity, HDQ is still able to inhibit the intracellular replication, suggesting HDQ may have additional targets. At this stage, these additional targets are still unknown, however as a logical speculation, TgNDH2-II might be the possible target due to the same internal orientation and similar function. Both enzymes were able to transfer electrons from NADH to DBQ as demonstrated in enzymatic studies (Lin *et al.*, 2008). Meanwhile, an additional interpretation for the decreased sensitivity would imply that the endogenous TgNDH2-II and also additional other possible drug targets probably possess a lower affinity for HDQ. In the near future, one feasible study is to compare the affinity of TgNDH2-I and TgNDH2-II

enzyme activities to HDQ using *Toxoplasma* lysates isolated from knock-out mutant, parental and wild-type parasites.

Using conditional knock-out mutants is an important approach to validate essential genes (Meissner *et al.*, 2002; Mital *et al.*, 2005). One major technical concern is how effective the additional copy of exogenous gene can be repressed in the tetracycline-regulatable expression system in the knock-out mutant. Although the inducible system is functional in both TgNDH2-I and TgNDH2-II mutants as shown by the suppression of exogenous copies in the presence of ATc (Fig. 3.9), it is very difficult to rule out that the residual transcript levels are sufficient to complement the loss of the knock-out genes. One possible solution to deal with this technical issue is to generate clean TgNDH2-I and TgNDH2-II knock-out mutants and compare the phenotypes.

4.4. A proposed Model explaining the Importance of TgNDH2s in *T. gondii*

This study explores the importance of TgNDH2s in the energy metabolism of *T. gondii*. Here for the first time, direct evidence from split GFP complementation has revealed that both isoforms are internal enzymes (Fig. 3.1 and 3.2). It is this becoming clear that these two enzymes utilize the reducing powers from matrix NADH but not from cytosolic NADH and the oxidized electrons are ultimately fed into the respiratory chain. In addition, this study strongly suggests that *T. gondii* possesses a conventional-like ATPase as supported by the localization of a membrane associated-ATPase-F₁ β subunit (Lin *et al.*, 2009), which is in contrast with the proposed soluble ATPase F₁ in *P. falciparum* (Painter *et al.*, 2007). Importantly, the identification of this typical-like ATPase in *T. gondii* reflects that oxidative phosphorylation may play a critical role in ATP production. Remarkably, a fast collapse of mitochondrial inner-membrane potential within minutes followed by a serious depletion of parasitic ATP level was observed with HDQ treatment (Lin *et al.*, 2009; see below). This directly reveals the physiological impact of TgNDH2 inhibition on mitochondrial functions – type II NADH dehydrogenases are indispensably important for oxidation phosphorylation in the replicative tachyzoite stage. Further investigation on the $\Delta\psi_m$ in bradyzoites revealed a significant lower frequency of $\Delta\psi_m$ -positive parasites suggesting that oxidation phosphorylation in the bradyzoite stage may be less

important compared to tachyzoites. Collectively, these important findings have advanced the understanding of the complete picture of the electron transport chain in *T. gondii* (Fig. 4.1). Overall, a model depicting the importance of type II NADH dehydrogenases *T. gondii* is proposed (Fig. 4.1). Internal enzymes TgNDH2-I and TgNDH2-II are oxidizing electrons from matrix NADH. The donated electrons including from other dehydrogenases are accepted by ubiquinone to give a reduced form ubiquinol. Electrons then are donated from ubiquinol to complex III, further passed to cytochrome c and complex IV. The energy released from electron transfer steps are used by complex III and IV to pump protons from matrix to intermembrane space and generated an electrochemical gradient. Subsequently ATP is produced by the action of ATPase using the potential energy from the proton gradient.

Type II NADH dehydrogenases in *T. gondii* have been considered as promising drug targets due to the absence in mammalian cells (Saleh *et al.*, 2007). The enzymatic analyses presented here have provided clear evidence that TgNDH2-I is indeed a drug target for HDQ (Lin *et al.*, 2008). The quinolone-like compound HDQ was first identified as a high affinity inhibitor for *Yarrowia* NDH2. Strikingly, an impressive IC_{50} for TgNDH2-I is determined in nanomolar ranges, implying that HDQ is a high affinity inhibitor for this enzyme. Bisubstrate kinetics analysis suggests a ping-pong mechanism for TgNDH2-I enzyme activity. Inhibition kinetics analysis indicates that hydrophobic HDQ is both competitive and non-competitive inhibitor for hydrophobic ubiquinone in a ping-pong mechanism. Further comparisons on the mode of action of HDQ with complex III inhibitor atovaquone in substrate supplementation experiments (Lin *et al.*, 2009) in intracellular parasites suggests that HDQ is targeting at the ubiquinone reduction level, which is different from atovaquone. Taken together, the impact of TgNDH2s inhibition in the respiratory chain is stepwise described (Fig. 4.1). First, the hydrophobic compound HDQ is reaching at the membrane interface, where it can interact with TgNDH2-I. As a ping-pong mechanism for TgNDH2-I (Lin *et al.*, 2008) activity, HDQ interferes with TgNDH2-I activity in several ways. HDQ can affect catalytic activity of TgNDH2-I by binding directly to the enzyme (non-competitive for NADH and ubiquinone) and it can compete with ubiquinone for the binding site as a competitive inhibitor. As a result of HDQ inhibition, ubiquinol turnover is reduced, eventually causing a collapse of $\Delta\psi_m$ and depletion of ATP level.

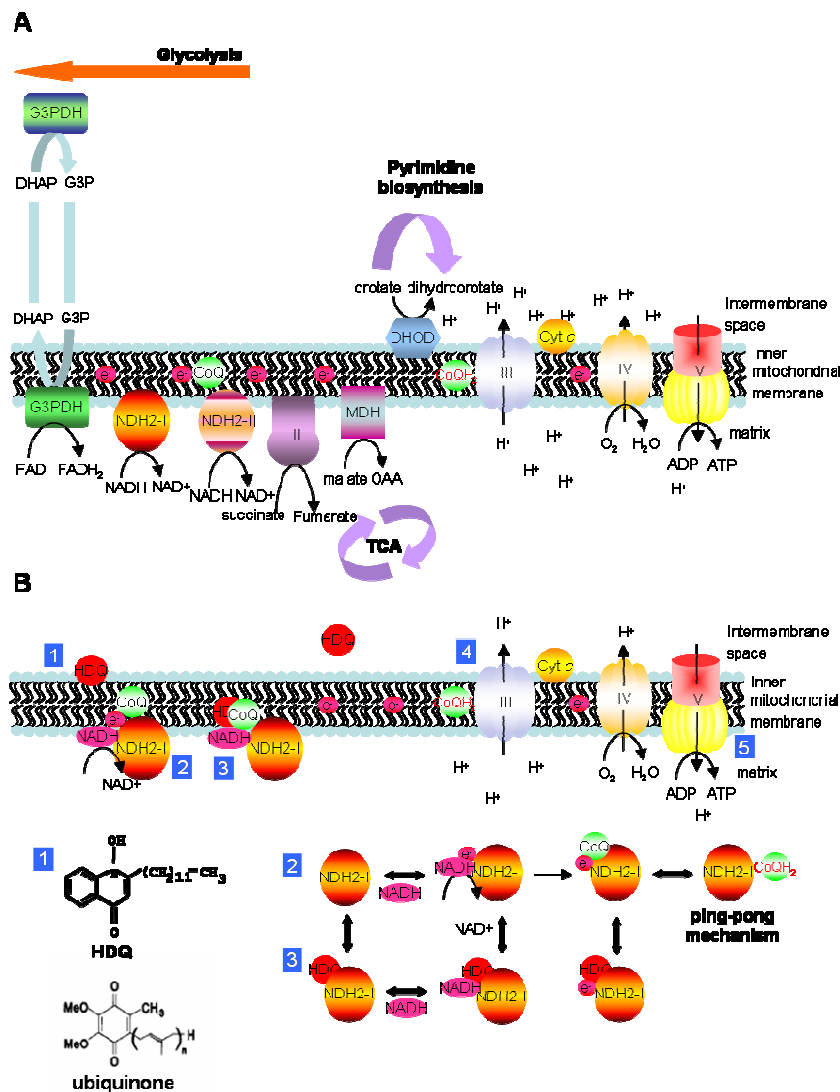


Figure 4.1 A proposed model depicting the importance of type II NADH dehydrogenases in the energy metabolism of *T. gondii* (A) Internal enzymes TgNDH2-I and TgNDH2-II transfer electrons from matrix NADH entering the respiratory chain. ATP is synthesised by the action of a conventional-like ATPase in *T. gondii*. (B) Physiological consequences of type II NADH dehydrogenases inhibition by HDQ. It comprises following steps: 1. Partition of hydrophobic quinone-like compound HDQ at membrane interface; 2. Ping-pong mechanism of TgNDH2-I electron transfer activity; 3. HDQ targeting at TgNDH2-I; 4. Collapse of $\Delta\psi_m$; and 5. ATP depletion. G3PDH, glycerol-3-phosphate dehydrogenase; DHAP, dihydroxyacetone phosphate; G-3P, glycerol-3-phosphate; NDH2, type II NADH dehydrogenase; MDH, malate:ubiquinone oxidoreductase; OAA, oxaloacetate; DHOD, dihydroorotate dehydrogenase; Cyt *c*, cytochrome *c*; CoQ: ubiquinol; CoQH₂, ubiquinol.

Summary

The single subunit mitochondrial type II NADH dehydrogenases (NDH2s) in apicomplexan parasites have been considered as potential drug targets due to the absence in mammalian cells. *Toxoplasma gondii* encodes two isoforms of NDH2s, TgNDH2-I and TgNDH2-II, whose functions are not known. Therefore, this study is explicitly focusing on drug target validation of these enzymes as well as revealing their specific roles in both mitochondrial functions and energy metabolism in *T. gondii*.

The validity of TgNDH2s as putative targets was firstly addressed in this study. Previously, the quinolone-like compound 1-hydroxy-2-alkyl-4(1)quinolone (HDQ), known as a high affinity inhibitor for *Yarrowia lipolytica* NDH2, has been shown to effectively inhibit the replication of *T. gondii*. To obtain biochemical evidence that TgNDH2s are the targets for HDQ, both TgNDH2 isoforms were heterologously expressed in a *Yarrowia* NDH2 deletion strain. TgNDH2-I was able to display oxidoreductase activities by using NADH and *n*-decylubiquinone as substrates. Additionally, TgNDH2-I could rescue the loss of complex I activity in *Yarrowia*, indicating that TgNDH2-I is expressed as an active enzyme. Furthermore, TgNDH2-I activity was effectively inhibited by HDQ with an IC₅₀ at nanomolar concentration. Steady-state kinetics analyses for TgNDH2-I are in accordance with a ping-pong mechanism. Moreover, the mode of inhibition of HDQ on TgNDH2-I revealed that HDQ is a non-competitive inhibitor for NADH. Collectively, these biochemical data provide direct evidence that TgNDH2-I is a target enzyme of HDQ in *T. gondii*.

Having validated TgNDH2 activity as a target of HDQ, the physiological impact of HDQ activity on mitochondrial functions was examined next. Intracellular parasites exposed to HDQ displayed a significant collapse of the mitochondrial membrane potential ($\Delta\psi_m$). Strikingly, $\Delta\psi_m$ in living parasites was depolarized within minutes, as recorded by time-lapse microscopy. The effect was diminished by adding substrates for mitochondrial dehydrogenases located downstream in the respiratory chain, which is in agreement with a specific inhibition of TgNDH2 activity by HDQ. Further experiments demonstrated that $\Delta\psi_m$ in the presence of HDQ was stabilized with the F₀-ATPase inhibitor oligomycin, indicating that *T. gondii* is likely to possess a

conventional-like mitochondrial F_0F_1 -ATPase. Additional subcellular localization of a membrane-associated F_1 -ATPase β subunit strongly supports this location, which is different to the location previously suggested to *Plasmodium* as a soluble matrix protein. Moreover, the collapse of $\Delta\psi_m$ mediated by HDQ is followed by a significant depletion of the intracellular parasitic ATP level. Taken together, these findings indicate that HDQ is an effective inhibitor of oxidative phosphorylation in tachyzoites. Interestingly, the percentage of $\Delta\psi_m$ -positive bradyzoites is significantly lower as compared to tachyzoites, implying that the importance of oxidative phosphorylation varies in these two stages.

Moreover, the integration of TgNDH2s in the parasitic energy metabolism was explored. A split GFP complementation approach was used in order to determine whether the active sites of the TgNDH2 isoforms are facing to the mitochondrial matrix or to the intermembrane space. A parasite line expressing a matrix-localized succinyl-CoA synthetase beta subunit (TgSCS β)-GFP1-10 fusion protein was generated and transfected with TgNDH2-I-GFP11 or TgNDH2-II-GFP11 fusion constructs. Full-length constructs of TgNDH2-II and truncated versions of TgNDH2-I were able to reconstitute GFP fluorescence, suggesting an internal, matrix-oriented localization of both enzymes. This indicates that both enzymes are specifically using NADH contributed from the matrix but not from the cytosol. Further investigations on the specific functional roles of TgNDH2s were focused on phenotypic analyses of conditional TgNDH2-I and TgNDH2-II depletion mutants. Unexpectedly, the phenotypic studies on these mutants showed that either TgNDH2-I or TgNDH2II is non-essential for replication, suggesting that TgNDH2s may be highly functional redundant and in turn complement each other.

The mode of action of HDQ together with the biochemical and molecular findings on TgNDH2s presented here may contribute to the ongoing strategic drug development to combat the emerging drug resistance of apicomplexan parasites.

References

- Al-Anouti F, Ananvoranich S. (2002). Comparative analysis of antisense RNA, double-stranded RNA, and delta ribozyme-mediated gene regulation in *Toxoplasma gondii*. *Antisense Nucleic Acid Drug Dev.* **12**: 275-281.
- Al-Anouti F, Quach T, Ananvoranich S. (2003). Double-stranded RNA can mediate the suppression of uracil phosphoribosyltransferase expression in *Toxoplasma gondii*. *Biochem Biophys Res Commun.* **302**: 316-323.
- Arai R, Ueda H, Kitayama A, Kamiya N, Nagamune T. (2001). Design of the linkers which effectively separate domains of a bifunctional fusion protein. *Protein Eng.* **14**: 529-532.
- Armstrong CM, Goldberg DE. (2007). An FKBP destabilization domain modulates protein levels in *Plasmodium falciparum*. *Nat Methods.* **4**: 1007-1009.
- Banaszynski LA, Chen LC, Maynard-Smith LA, Ooi AG, Wandles TJ. (2006). A rapid reversible, and tunable method to regulate protein function in living cells using synthetic small molecules. *Cell.***126**: 995-1004.
- Bandeiras TM, Salgueiro C, Kletzin C, Gomes M, Teixeira M. (2002). *Acidianus ambivalens* type-II NADH dehydrogenase: genetic characterisation and identification of the flavin moiety as FMN. *FEBS Lett.* **531**: 273-277.
- Beckers CJ, Roos DS, Donald RG, Luft BJ, Schwab JC, Cao Y, Joiner KA. (1995). Inhibition of cytoplasmic and organellar protein synthesis in *Toxoplasma gondii*. Implications for the targets of macrolide antibiotics. *J Clin Invest.* **95**: 367-376.
- Bernard N, Johnsen K, Holbrook JJ, Delcour J. (1995). D175 discriminates between NADH and NADPH in the coenzyme binding-site of *Lactobacillus delbrueckii subsp. Bulgaricus* D-lactate dehydrogenase. *Biochem Biophys Res Commun.* **208**: 895-900.
- Biagini GA, Fisher N, Berry N, Stocks PA, Meunier B, Williams DP, Bonar-Law R, Bray PG, Owen A, O'Neill PM, Ward SA. (2008). Acridinediones: selective and

potent inhibitors of the malaria parasite mitochondrial bc1 complex. *Mol Pharmacol.* **73**: 1347-1355.

Biagini GA, Viriyavejakul PO, O'Neill PM, Bray PG, Ward SA. (2006). Functional characterization and target validation of alternative complex I of *Plasmodium falciparum* mitochondria. *Antimicrob Agents Chemother.* **50**: 1841-1851.

Björklöf K, Zickermann V, Finel M. (2000). Purification of the 45 kDA, membrane bound NADH dehydrogenase of *Escherichia coli* (NDH-2) and analysis of its interaction with ubiquinone analogues. *FEBS Lett.* **467**: 105-110.

Black MW, Boothroyd JC. (2000). Lytic Cycle of *Toxoplasma gondii*. *Mol Biol Rev.* **64**: 607-623.

Bohne W, Heesemann J, Gross U. (1994). Reduced replication of *Toxoplasma gondii* is necessary for induction of bradyzoite-specific antigens: a possible role for nitric oxide in triggering stage conversion. *Infect Immun.* **62**:1761-1767.

Brecht S, Erdhart H, Soete M, Soldati D. (1999). Genome engineering of *Toxoplasma gondii* using the site-specific recombinase Cre. *Gene.* **234**: 239-247.

Cabantous S, Terwilliger TC, Waldo GS. (2005). Protein tagging and detection with engineered self-assembling fragments of green fluorescent protein. *Nat Biotechnol.* **23**: 102-107.

Carlton JM, Escalante AA, Neafsey D, Volkman SA. (2008). Comparative evolutionary genomics of human malaria parasites. *Trends Parasitol.* **24**: 545-549.

Carruthers VB, Sibley LD. (1997). Sequential protein secretion from three distinct organelles of *Toxoplasma gondii* accompanies invasion of human fibroblast. *Eur J Cell Biol.* **73**:114-123.

Carvalho TG, Thilberge S, Sakamoto H, Menard R. (2004). Conditional mutagenesis using site-specific recombination in *Plasmodium berghei*. *Proc Natl Acad Sci USA.* **101**: 14931-14936.

- Chen LB. (1988). Mitochondrial membrane potential in living cells. *Ann Rev Cell Biol.* **4**: 155-181.
- DeRocher A, Hagen CB, Froehlich JE, Feagin JE, Parsons M. (2000). Analysis of targeting sequences demonstrates that trafficking to the *Toxoplasma gondii* plastid branches off the secretory system. *J Cell Sci.* **113**: 3969-3977.
- Divo AA, Geary TG, Jensen JB. (1985). Oxygen- and time- dependent effects of antibiotics and selected mitochondrial inhibitors on Plasmodium falciparum in culture. *Antimicrob Agents Chemother.* **27**: 21-27.
- Doerig C, Billker O, Haystead T, Sharma P, Tobin AB, Waters NC. (2008). Protein Kinases of malaria parasites: an update. *Trends Parasitol.* **24**: 570-577.
- Donald RGK. (2007). *Toxoplasma* as a model system for apicomplexan drug discovery. In: Weiss LM, Kim K. eds. *Toxoplasma gondii: The Model Apicomplexan – Perspective and Methods*. 1st ed. London: Elsevier. pp. 391-415.
- Donald RG, Allocco J, Singh SB, Nare B, Salowe SP, Wiltsie J, Liberator PA. (2002). *Toxoplasma gondii* cyclic GMP-dependent kinase: chemotherapeutic targeting of an essential parasite protein kinase. *Eukaryot Cell.* **1**: 317-328.
- Donald RG, Liberator PA. (2002). Molecular characterization of a coccidian parasite cGMP dependent protein kinase. *Mol Biochem Parasitol.* **120**:165-175.
- Donald RG, Roos DS. (1993). Stable molecular transformation of *Toxoplasma gondii*: a selectable dihydrofolate reductase-thymidylate synthase marker based on drug-resistance mutation in malaria. *Proc Natl Acad Sci USA.* **90**: 11703-11707.
- Donald RG, Roos DS. (1994). Homologous recombination and gene replacement at the dihydrofolate reductase-thymidylate synthase locus in *Toxoplasma gondii*. *Mol Biochem Parasitol.* **63**: 243-253.
- Dong CK, Patel V, Yang JC, Dvorin JD, Duraisingh MT, Clardy J, Wirth DF. (2009). Type II NADH dehydrogenase of the respiratory chain of *Plasmodium falciparum* and its inhibitors. *Bioorg Med Chem Lett.* **19**: 972-975.

- Dubey JP, Lindsay DS, Speer CA. (1998). Structures of *Toxoplasma gondii* Tachyzoites, Bradyzoites, and Sporozoites and Biology and Development of Tissue Cysts. *Clin Microbiol Rev.* **11**: 267-299.
- Eschemann A, Galkin A, Oettmeier W, Brandt U, Kerscher S. (2005). HDQ (1-Hydroxy-2-dodecyl-4(1H)quinolone), a high affinity inhibitor for mitochondrial alternative NADH dehydrogenase. *J Biol Chem.* **280**: 3138-3142.
- Feeney R, Clarke AR, Holbrook JJ. (1990). A single amino-acid substitution in lactate-dehydrogenase improves the catalytic efficiency with an alternative coenzyme. *Biochem Biophys Res Commun.* **166**: 667-672.
- Fidock DF, Eastman RT, Ward SA, Meshnick SR. (2008). Recent highlights in antimalarial drug resistance and chemotherapy research. *Trends Parasitol.* **24**: 537-544.
- Fichera ME, Bhopale MK, Roos DS. (1995). *In vitro* assays elucidate peculiar kinetics of clindamycin action against *Toxoplasma gondii*. *Antimicrob Agents Chemother.* **39**: 1530-1507.
- Fichera ME, Roos DS. (1997). A plastid organelle as a drug target in apicomplexan parasites. *Nature.* **390**: 407-409.
- Fisher N, Bray PG, Ward SA, Biagini GA. (2007). The malaria parasite type II NADH:quinone oxidoreductase: an alternative enzyme for an alternative lifestyle. *Trends Parasitol.* **23**: 305-310.
- Fisher N, Bray PG, Ward SA, Biagini GA. (2007). Malaria-parasite mitochondrial dehydrogenases as drug targets: too early to write the obituary. *Trends Parasitol.* **24**: 9-10.
- Fisher N, Rich PR. (2000). A motif for quinone binding sites in respiratory and photosynthetic system. *J Mol Biol.* **296**: 1153-1162.

- Fleige T, Fischer K, Ferguson DJ, Gross U, Bohne W. (2007). Carbohydrate metabolism in the *Toxoplasma gondii* apicoplast: localization of three glycolytic isoenzymes, the single pyruvate dehydrogenase complex and a plastid phosphate translocator. *Eukaryot Cell*. **6**: 984-996.
- Fleige T, Pfaff N, Gross U, Bohne W. (2008). Localisation of gluconeogenesis and tricarboylic acid (TCA)-cycle enzymes and first functional analysis of the TCA cycle in *Toxoplasma gondii*. *Int J Parasitol*. **38**: 1121-1132.
- Fleige T. (2006). Compartmentalization of carbohydrate metabolism in *Toxoplasma gondii*. *PhD Thesis*.
- Fox BA, Bzik DJ. (2002). *De novo* pyrimidine biosynthesis is required for virulence of *Toxoplasma gondii*. *Nature*. **415**: 926-929.
- Fox BA, Ristuccia JG, Gigley JP, Bzik DJ. (2009). Efficient gene replacements in *Toxoplasma gondii* strains deficient for nonhomologous end-joining. *Eukaryot Cell*. **8**: 520-529.
- Fry M, Beesley JE. (1991). Mitochondria of mammalian Plasmodium spp. *Parasitology*. **102**: 17-26.
- Fry M, Pudney M. (1992). Effect of mitochondrial inhibitors on adenosinetriphosphate levels in *Plasmodium falciparum*. *Biochem Pharmacol*. **43**: 1545-1553.
- Garofano A, Eschemann A, Brandt U, Kerscher S. (2006). Substrate-inducible versions of internal alternative NADH:ubiquinone oxidoreductase from *Yarrowia lipolytica*. *Yeast*. **23**: 1129-1136.
- Geisler DA, Broselid C, Hederstedt L, Rasmusson AG. (2007). Ca²⁺-binding and Ca²⁺-independent respiratory NADH and NADPH dehydrogenases of *Arabidopsis thaliana*. *J Biol Chem*. **282**: 28455-28464.
- Gomes CM, Bandejas TM, Teixeira M. (2001). A new type-II NADH dehydrogenase from the archaeon *Acidianus ambivalens*: characterization and in vitro reconstitution of the respiratory chain. *J Bioenerg Biomembr*. **33**: 1-8.

- Gul-Karaguler N, Sessions RB, Clarke AR, Holbrook JJ. (2001). A single mutation in NAD-specific formate dehydrogenase from *Candida methylica* allows the enzyme to use NADP. *Biotechn Lett.* **23**: 283-287.
- Gubbels MJ, Mazumdar J, van Dooren GG, Striepen B. (2007). Manipulating the *Toxoplasma* Genome. In: Ajika JW, Soldati D. eds. *Toxoplasma: Molecular and Cellular Biology*. 1st ed. Norfolk: Horizon Bioscience. pp. 241-262.
- Gurnett AM, Liberator PA, Dulski PM, Salowe SP, Donald RG, Anderson JW, Wiltsie J, Diaz CA, Harris G, Chang B, Barkin-Rattray SJ, Nare B, Crumley T, Blum PS, Misura AS, Tamas T, Sardana MK, Yuan J, Biftu T, Schmatz DM. (2002). Purification and molecular characterization of cGMP-dependent protein kinase from Apicomplexan parasites. A novel chemotherapeutic target. *J Bio Chem.* **277**: 15913-15922.
- Gutteridge WE, Dave D, Richards WH. (1979). Conversion of dihydroorotate to orotate in parasitic protozoan. *Biochim Biophys Acta.* **582**: 390-401.
- Herm-Gotz A, Agop-Nersesian C, Munter S, Grimley JS, Wandless TJ, Frischknecht F, Meissner M. (2007). Rapid control of protein level in the apicomplexan *Toxoplasma gondii*. *Nat Methods.* **4**: 1003-1005.
- Hu K, Johnson J, Florens L, Fraunholz M, Suravajjala S, Dilullo C, Yates J, Roos DS, Murray JM. (2006). Cytoskeletal components of an invasion machine: the apical complex of *Toxoplasma gondii*. *PLos Pathogens.* **2**: e13.
- Huynh MH, Carruthers VB. (2009). Tagging of endogenous genes in a *Toxoplasma gondii* strain lacking Ku80. *Eukaryot Cell.* **8**: 530-539.
- Jacobson MD, Burne JF, King MP, Miyashita T, Reed JC, Raff MC. (1993). Bcl-2 blocks apoptosis in cells lacking mitochondrial DNA. *Nature.* **361**: 365-369.
- Kerscher S. (2000). Diversity and origin of alternative NADH:ubiquinone oxidoreductase. *Biochim Biophys Acta* **1459**: 274-283.
- Kerscher S, Eschemann A, Okun PM, Brandt U. (2001). External alternative NADH: ubiquinone oxidoreductase redirected to the internal face of the mitochondrial inner

- membrane rescues complex I deficiency in *Yarrowia lipolytica*. *J Cell Sci.* **114**: 3915-3921.
- Kerscher S, Dröse S, Zickermann V, Brandt U. (2008). The three families of respiratory NADH dehydrogenases. *Results Probl Cell Differ.* **45**: 185-222.
- Kim K, Soldati D, Boothroyd JC. (1993). Gene replacement in *Toxoplasma gondii* with chloramphenicol acetyltransferase as selection marker. *Science.* **262**: 911-914.
- Kim K, Weiss LM. (2004). *Toxoplasma gondii*: the model apicomplexan. *Int J parasitol.* **34**: 423-432.
- Krungkrai J. (2004). The multiple roles of the mitochondrion of the malaria parasite. *Parasitology.* **129**: 511-524.
- Lee EC, Yu D, Martinez de Velasco J, Tessarollo L, Swing DA, Court DL, Jenkins NA, Copland NG. (2001). A highly efficient *Escherichia coli*-based chromosome engineering system adapted for recombinogenic targeting and subcloning of BAC DNA. *Genomics.* **73**: 56-65.
- Lin SS, Kerscher S, Saleh A, Brandt U, Gross U, Bohne W. (2008). The *Toxoplasma gondii* type-II NADH dehydrogenase TgNDH2-I is inhibited by 1-Hydroxy-2-Alkyl-4(1H)Quinolones. *Biochim Biophys Acta Bioenerg.* **1777**: 1455-1462.
- Lin SS, Gross U, Bohne W. (2009). Type II NADH dehydrogenase inhibitor 1-hydroxy-2-dodecyl-4(1H)quinolone leads to collapse of mitochondrial inner-membrane potential and ATP depletion in *Toxoplasma gondii*. *Eukaryot Cell.* **8**: 877-887.
- Looareesuwan S, Chulay JD, Canfield CJ, Hutchinson DB. (1999). Malarone (atovaquone and proguanil hydrochloride): a review of its clinical development for treatment of malaria. Malarone Clinical Trials Study Group. *Am J Trop Med Hyg.* **60**: 533-541.
- Luft BJ, Remington JS. (1988). AIDS commentary. Toxoplasmic encephalitis. *J Infect Dis.* **157**: 1-6.

- Luft BJ, Remington JS. (1992). Toxoplasmic encephalitis in AIDS. *Clin Inf Dis.* **15**: 211-222.
- Lutz T, Neupert W, Herrmann JM. (2003). Import of small Tim protein into the mitochondrial intermembrane space. *EMBO J.* **22**: 4400-4008.
- Mazumdar J, Wilson E, Masek K, Hunter C, Striepen B. (2006). Apicoplast fatty acid synthesis is essential for organelle biogenesis and parasite survival in *Toxoplasma gondii*. *Proc Natl Acad Sci USA.* **103**: 13192-13197.
- McFadden DC, Boothroyd JC. (1999). Cytochrome b mutation identified in a decoquinone-resistance mutant of *Toxoplasma gondii*. *J Eukaryot Microbiol.* **46**: 81S-82S.
- McFadden DC, Camps M, Boothroyd JC. (2001). Resistance as a tool in the study of old and new drug targets in *Toxoplasma*. *Drug Resist Updat.* **4**: 79-84.
- McFadden DC, Tomavo S, Berry EA, Boothroyd JC. (2000). Characterization of cytochrome b from *Toxoplasma gondii* and Q(o) domain mutations as a mechanism of atovaquone-resistance. *Mol Biochem Parasitol.* **108**: 1-12.
- Meissner M, Schluter D, Soldatic D. (2002). Role of *Toxoplasma gondii* myosin A in powering parasites gliding and host cell invasion. *Science.* **298**: 837-840.
- Meissner M, Breinich MS, Gilson PR, Crabb BS. (2007). Molecular genetic tools in *Toxoplasma* and *Plasmodium*: achievements and future needs. *Curr Opin Microbiol.* **10**: 349-356.
- Meissner M, Brecht S, Bujard H, Soldati D. (2001). Modulation of myosin A expression by a newly established tetracycline repressor-based inducible system in *Toxoplasma gondii*. *Nucleic Acid Res.* **29**: E115.
- Melo AM, Bandejas TM, Teixeira M. (2004). New insights into type II NAD(P)H:quinone oxidoreductases. *Microbiol Mol Biol Rev.* **68**: 603-616.

- Michalecka AM, Agius SC, Møller IM, Rasmusson AG. (2004). Identification of a mitochondrial external NADPH dehydrogenase by overexpression in transgenic *Nicotiana sylvestris*. *Plant J.* **37**: 415-425.
- Mital J, Meissner M, Soldati D, Ward GE. (2005). Conditional expression of *Toxoplasma gondii* apical membrane antigen-1 (TgAMA1) demonstrates that TgAMA1 plays a critical role in host cell invasion. *Mol Biol Cell.* **16**: 4341-4349.
- Montoya JG, Rosso F. (2005). Diagnosis and management of toxoplasmosis. *Clin Perinatol.* **32**: 705-726.
- Naujoks B. (2008). Inhibierung der *Toxoplasma-gondii*-Replikation durch Hemmung der mitochondrialen Atmungskette. *MD Thesis*.
- Nicolle C, Manceaux L. (1908). Sur une infection a corps de Leishman (ou organisms voisins) du gondi. *CR Acad Sci.* **147**: 763.
- Nishi M, Hu K, Murray JM, Roos DS. (2008). Organellar dynamics during the cell cycle of *Toxoplasma gondii*. *J Cell Sci.* **121**: 1559-1568.
- Omura S, Miyadera H, Ui H, Shiomi K, Yamaguchi Y, Masuma R, Nagamitsu T, Takano D, Sunazuka T, Harder A, Kölbl H, Namikoshi M, Miyoshi H, Sakamoto K, Kita K. (2001). An anthelmintic compound, nafuredin, shows selective inhibition of complex I in helminth mitochondria. *Proc Natl Acad Sci USA.* **98**: 60-62.
- Painter HJ, Morrisey JM, Mather MW, Vaidya AB. (2007). Specific role of mitochondrial electron transport in blood-stage *Plasmodium falciparum*. *Nature.* **446**: 88-91.
- Pfefferkorn ER, Borotz SE, Nothnagel RF. (1993). Mutant of *Toxoplasma gondii* resistant to atovaquone (566C80) or decoquinat. *J Parasitol.* **79**: 559-564.
- Ralph SA, van Dooren GG, Walker RF, Crawford MJ, Fraunholz MJ, Foth BJ, Tonkin CJ,
- Remy I, Michnick SW. (2004). A cDNA library functional screening strategy based on fluorescent protein complementation assays to identify novel components of signaling pathways. *Methods.* **32**: 381-388.

- Rasmusson AG, Soole KL, Elthon TE. (2004). Alternative NAD(P)H dehydrogenases of plant mitochondria. *Annu Rev Plant Biol.* **55**: 23-39.
- Roos DS, Crawford MJ, Donald RG, Kissinger JC, Klimczak LJ, Striepen B. (1999). Origin, targeting, and function of the apicomplexan plastid. *Curr Opin Microbiol.* **2**: 426-432.
- Roos DS, Donald RG, Morrisette NS, Moulton AL. (1994). Molecular tools for genetic dissection of the protozoan parasite *Toxoplasma gondii*. *Methods Cell Biol.* **45**: 27-63.
- Saleh A. (2006). Characterization of alternative NADH dehydrogenases in the respiratory chain of *Toxoplasma gondii* as a novel drug targets. *PhD Dissertation*.
- Saleh A, Friesen J, Baumeister S, Gross U, Bohne W. (2007). Growth inhibition of *Toxoplasma gondii* and *Plasmodium falciparum* by nanomolar concentrations of 1-hydroxy-2-dodecyl-4(1H)quinolone, a high-affinity inhibitor of alternative (type II) NADH dehydrogenases. *Antimicrob Agents Chemother.* **51**: 1217-1222.
- Saraste M. (1999). Oxidation Phosphorylation at the fin de siècle. *Science.* **283**: 1488-1493.
- Scheffler IE. (2001). Mitochondria make a come back. *Adv Drug Deliv Rev.* **49**: 3-26.
- Seeber F, Limenitakis J, Soldati-Favre D. (2008). Apicomplexan mitochondrial metabolism: a story of gains, losses and retentions. *Trends Parasitol.* **24**: 468-478.
- Soete M, Camus D, Dubremetz JF. (1994). Experimental induction of bradyzoite-specific antigen expression and cyst formation by the RH strain of *Toxoplasma gondii* in vitro. *Exp Parasitol.* **78**: 361-370.
- Soldati D, Boothroyd JC. (1993). Transient transfection and expression in the obligate intracellular parasite *Toxoplasma gondii*. *Science.* **260**: 349-352.
- Splendore A. (1908). Un nuovo parassita deconigli incontrato nelle lesioni anatomiche d' una malattia che ricorda in molti punti il Kala-azar dell'uomo Nota preliminare pel. *Rev Soc Sci Sao Paulo.* **3**: 109-112.

- Srivastava IK, Rottenberg H, Vaidya AB. (1997). Atovaquone, a broad spectrum antiparasitic drug, collapses mitochondrial membrane potential in a malaria parasite. *J Biol Chem.* **272**: 3961-3966.
- Sternisek P. (2009). Einfluss des Pyrimidin *Salvage Pathway* Enzyms UPRT auf die Sensitivität von *Toxoplasma gondii* gegenüber Inhibitoren der Atmungskette. *Diploma Thesis*.
- Striepen B, Crawford MJ, Shaw MK, Tilney LG, Seeber F, Roos DS. (2000). The plastid of *Toxoplasma gondii* is divided by association with the centrosomes. *J Cell Biol.* **151**: 1423-1434.
- Striepen B, Pruijssers AJP, Huang J Li C, Gubbels MJ, Umeijiego NN, Hedstrom L, Kissinger JC. (2004). Gene transfer in the evolution of parasite nucleotide biosynthesis. *Proc Natl Acad Sci USA.* **101**: 354-359.
- Striepen B, Soldati B. (2007). Genetic manipulation of *Toxoplasma gondii*. In: Weiss LM, Kim K. eds. *Toxoplasma gondii: The Model Apicomplexan – Perspective and Methods*. 1st ed. London: Elsevier. pp. 391-415.
- Striepen B, White MW, Li C, Guerini MN, Malik SB, Logsdon, JM Jr, Liu C, Abrahamsen MS. (2002). Genetic complementation in apicomplexan parasites. *Proc Natl Acad Sci USA.* **99**: 6304-6309.
- Truscott KN, Brandner K, Pfanner N. (2003). Mechanisms of Protein Import into Mitochondria. *Curr Biol.* **13**: 326-337.
- Ullu E., Tschudi C, Charkraborty T. (2004). RNA interference in protozoan parasites. *Cell Microbiol.* **6**: 509-519.
- Uyemura SA, Luo S, Vieira M, Moreno SN, Docampo R. (2004). Oxidative phosphorylation and rotenone-insensitive malate- and NADH-quinone oxidoreductases in *Plasmodium yoelii yoelii* mitochondria in situ. *J Biol Chem.* **279**: 385-393.
- Vaidya AB, Painter HJ, Morrisey JM, Mather MW. (2007). The validity of mitochondrial dehydrogenases as antimalarial drug targets. *Trends Parasitol.* **2**: 8-9.

van Dooren GG, Stimmler LM, McFadden GI. (2006). Metabolic maps and functions of the *Plasmodium* mitochondrion. *FEMS Microbiol Rev.* **30**: 596-630.

van Dooren GG, Tomova C, Agrawal S, Humbel BM, Striepen B. (2008). *Toxoplasma gondii* Tic20 is essential for apicoplast protein import. *Proc Natl Acad Sci U S A.* **105**: 13574-13579.

Vercesi AE, Rodrigues CO, Uyemura SA, Zhong L, Moreno SN. (1998). Respiration and oxidative phosphorylation in the apicomplexan parasite *Toxoplasma gondii*. *J Biol Chem.* **273**: 31040-31047.

Warming S, Castantino N, Court DL, Jenkins NA, Copeland NG. (2005). Simple and highly efficiency BAC recombineering using galK selection. *Nucleic Acids Res.* **33**: e36.

Weinstein EA, Yano T, Li LS, Avarbock D, Avarbock A, Helm D, McColm AA, Duncan K, Lonsdale JT, Rubin H. (2005). Inhibitors of type II NADH:menaquinone oxidoreductase represent a class of antitubercular drugs. *Proc Natl Acad Sci U S A.* **102**: 4548-4553.

Yano T., Li LS, Weinstein E, Teh JS, Rubin H. (2006). Steady-state kinetics and inhibitory action of antitubercular phenothiazines on *Mycobacterium tuberculosis* type-II NADH-menaquinone oxidoreductase (NDH-2). *J Bio Chem.* **281**: 11456-11463.



Contents lists available at ScienceDirect

Biochimica et Biophysica Acta

journal homepage: www.elsevier.com/locate/bba



The *Toxoplasma gondii* type-II NADH dehydrogenase TgNDH2-I is inhibited by 1-hydroxy-2-alkyl-4(1H)quinolones

San San Lin^a, Stefan Kerscher^b, Ahmad Saleh^a, Ulrich Brandt^b, Uwe Groß^a, Wolfgang Böhne^{a,*}

^a Institute of Medical Microbiology University of Göttingen, Kreuzbergweg 57, Göttingen D-37075, Germany

^b Johann Wolfgang Goethe-Universität, Fachbereich Medizin, Zentrum der Biologischen Chemie, Molekulare Bioenergetik, Centre of Excellence Frankfurt "Macromolecular Complexes", Frankfurt am Main, Germany

ARTICLE INFO

Article history:

Received 27 June 2008

Received in revised form 11 August 2008

Accepted 12 August 2008

Available online 22 August 2008

Keywords:

Alternative (type-II) NADH dehydrogenase

(NDH2)

Toxoplasma gondii

Inhibition kinetics

Ping-pong mechanism

1-Hydroxy-2-alkyl-4(1H)quinolone

HQ

ABSTRACT

The apicomplexan parasite *Toxoplasma gondii* does not possess complex I of the mitochondrial respiratory chain, but has two genes encoding rotenone-insensitive, non-proton pumping type-II NADH dehydrogenases (NDH2s). The absence of such "alternative" NADH dehydrogenases in the human host defines these enzymes as potential drug targets. TgNDH2-I and TgNDH2-II are constitutively expressed in tachyzoites and bradyzoites and are localized to the mitochondrion as shown by epitope tagging. Functional expression of TgNDH2-I in the yeast *Hansenula polymorpha* as an internal enzyme, with the active site facing the mitochondrial matrix, permitted growth in the presence of the complex I inhibitor DQA. Bisubstrate kinetics of TgNDH2-I measured within *H. polymorpha* mitochondrial membrane preparations were in accordance with a ping-pong mechanism. Using inhibition kinetics we demonstrate here that 1-hydroxy-2-alkyl-4(1H)quinolones with long alkyl chains of C₁₂ (HQ) and C₁₄ are high affinity inhibitors for TgNDH2-I, while compounds with shorter side chains (C₈ and C₆) displayed significantly higher IC₅₀ values. The efficiency of the various quinolone derivatives to inhibit TgNDH2-I enzyme activity mirrors their inhibitory potency *in vivo*, suggesting that a long acyl side chain is critical for the inhibitory potential of these compounds.

© 2008 Elsevier B.V. All rights reserved.

1. Introduction

NADH:ubiquinone oxidoreductases, also known as NADH dehydrogenases constitute one of the electron entry points into the respiratory chain, oxidizing NADH and generating ubiquinol. In eukaryotes, this class of enzymes is divided into two major subfamilies, which can be discriminated on the basis of cofactor content and sensitivity towards rotenone into type-I NADH dehydrogenases (complex I) and type-II NADH dehydrogenases (NDH2s) [1]. Proton-pumping complex I is a nearly ubiquitous enzyme that couples the rotenone-sensitive transfer of electrons from NADH to ubiquinone with the active transport of protons across the inner mitochondrial membrane [2]. Bacterial complex I typically consists of fourteen subunits that are homologous to the seven mitochondrially coded and the seven nuclear coded "central" subunits of the eukaryotic enzyme. Although eukaryotic complex I contains a variable number of so-called accessory subunits, with a total of 45 subunits and

a molecular mass of roughly 1 MDa in mammals, the bioenergetic function and the overall structure are conserved [3,4].

In contrast to complex I, type-II NADH dehydrogenases are non-proton-pumping, rotenone-insensitive, single polypeptides. Their active site can face either to the cytosol (external enzymes) thereby oxidizing cytosolic NADH, or to the mitochondrial matrix (internal enzymes) thereby oxidizing mitochondrial NADH. Seven NDH2 isoforms are expressed in *Arabidopsis*; three of them are identified as internal enzymes, whereas the other four are external [5]. In *Saccharomyces cerevisiae* mitochondria lacking complex I, one internal and two external enzymes have been described [6].

Type-II NADH dehydrogenases have been described in plants, fungi, protozoa and bacteria [1,7], but appear to be absent in mammals, which qualifies them as attractive drug targets. The apicomplexan parasites *Plasmodium falciparum* and *Toxoplasma gondii*, which are the causative agents of malaria and toxoplasmosis respectively, both lack complex I. Instead, the genome of *P. falciparum* is predicted to encode a single NDH2 of unknown orientation, while the *T. gondii* genome encodes two NDH2 isoforms. Treatment of *P. falciparum* with micromolar concentrations of diphenylene iodonium chloride, a low affinity inhibitor of NDH2, resulted in an inhibition of PfNDH2 activity, in a collapse of the parasite's mitochondrial membrane potential and finally in parasite death [8].

Abbreviations: HPQ, human forokin fibroblasts; HQ, 1-Hydroxy-2-Octyl-4(1H) Quinolone; HBQ, 1-Hydroxy-2-Hexyl-4(1H) Quinolone; HPQ, 1-Hydroxy-2-Pentyl-4(1H) Quinolone; HTQ, 1-Hydroxy-2-Tetradecyl-4(1H) Quinolone

* Corresponding author. Tel.: +49 551 393989; fax: +49 551 395361.

E-mail address: wboehne@gwdg.de (W. Böhne).

0005-2728/\$ – see front matter © 2008 Elsevier B.V. All rights reserved.
doi:10.1016/j.bba.2008.08.006

The quinolone-like compound 1-hydroxy-2-dodecyl-4(1)quinolone (HDQ) was described as the first high affinity inhibitor of type-II NADH dehydrogenases that inhibits NDH2 activity in mitochondrial membranes of the yeast *Yarrowia lipolytica* with an IC_{50} of 200 nM [9]. We have recently shown that HDQ is highly effective against *T. gondii* and inhibits parasite replication with an IC_{50} in the nanomolar range [10]. Moreover, a combined treatment of HDQ with the complex III inhibitor atovaquone resulted in synergism [10].

To further elucidate the suitability of type-II NADH dehydrogenases as drug targets it is crucial to obtain functional data from pathogen orthologs and to determine their interaction with putative inhibitors. We here report functional expression of TgNDH2-I in the yeast *Y. lipolytica*. This allowed us to study the kinetics of this enzyme and to demonstrate that 1-hydroxy-2-alkyl-4(1)quinolones with long alkyl side chains are high affinity inhibitors for TgNDH2-I.

2. Materials and methods

2.1. Genome data mining and sequence analyses

Preliminary genomic and/or cDNA sequence data were accessed via <http://Toodb.org> (version 3.0) [11] and/or http://tig.org/tdb/t_gondii/. Genomic data were provided by the Institute for Genomic Research (NIH grant #A05093), and by the Sanger Center (Wellcome Trust). EST sequences were generated by Washington University (NIH grant #1R01AI045806-01A1). Bioinformatics programs including MitoProt II 3.0 (<http://ihg.gsf.de/ihg/mitoprot.htm>) and SignalP 3.0 (<http://www.cbs.dtu.dk/services/SignalP/>) were used to predict subcellular location of Tgndh-1 and Tgndh-2.

2.2. Determination of the ATC initiation codons

An in-frame stop codon is present at 783 and 51 nt upstream of the presumed initiation ATC codons of tgnhd2-1 and tgnhd2-2 respectively. The deduced amino acid sequences coded by these regions have no other in-frame methionine residues and no similarity to NDHs nor to other proteins when blasted using NCBI BLAST. For tgnhd2-1 the next methionine residue is located 177 nt downstream of the first one. However, only the amino acid sequence deduced from the first ATC has characteristics of a mitochondrial targeting sequence. For tgnhd2-2, a putative second start ATC is located 6 nt downstream of the first.

2.3. RNA extraction, RT-PCR and fusion-PCR

Total RNA was isolated using the GenElute Mammalian Total RNA Kit (Sigma) and treated with DNase I (Sigma). Reverse transcription (RT) was done on 5 µg of total RNA, Oligo(dT) primer (Sigma) and M-MLV reverse transcriptase (RNase H minus, Sigma) according to the manufacturer's instructions. For PCR amplification, the reaction mixture was cycled in a thermal cycler. Fusion-PCR amplification was firstly performed in a volume of 50 µl containing 50 ng of each purified DNA fragment (QIAquick PCR purification kit, Qiagen) with 5 cycles of PCR in the absence of primers. The PCR reaction was continued for another 7 cycles after adding the primer sets (BamHI-NUAM-Fusion+ with NDH2-I-FL- or NDH2-II-FL-).

2.4. Real-time PCR

Light cycler PCR (Roche) was performed to amplify cDNA of tgnhd2-1, tgnhd2-2 and β -tubulin with the following primer sets RT-AND1/1+ and 2-, RT-AND2/1+ and 2-, and RT-Tub/3+ and 4-, as listed in Supplementary Table 1. A control sample without reverse transcriptase was incubated in parallel. The threshold crossing-point values of tgnhd2-1 and tgnhd2-2 were normalized to that of β -tubulin.

2.5. Immunofluorescence microscopy

Samples were fixed with 4% paraformaldehyde/PBS for 10 min and permeabilized with 0.25% Triton X-100/PBS for 15 min. After blocking for 1 h with 1% BSA/PBS, samples were incubated with a 1:250 dilution of anti-myc mAb 9E10 (Sigma) followed by incubation with a 1:500 dilution of Cy3-conjugated anti-mouse IgG (Dianova) in 1% BSA/PBS for 1 h each.

2.6. *T. gondii* strains, cultivation and in vitro stage conversion

Parasites were propagated in human foreskin fibroblasts (HFF) as previously described [12]. A clonal isolate of the RH strain was used for in vitro stage conversion and preparation of cDNA for real time RT-PCR analysis. Transactivator expressing *T. gondii* of strain RH TAT1-1 [13] were kindly provided by Dr. D. Soldati and Dr. M. Meissner and used for transfection experiments. Bradyzoites obtained by in vitro stage conversion were prepared as follows. *T. gondii* infected HFFs were firstly cultivated in 1% FCS/DMEM for 3 h at 37 °C in a 5% CO₂ humidified atmosphere. The medium was subsequently replaced with pH-shift medium (pH 8.3) to induce bradyzoite differentiation [14] and the cultures were incubated at 37 °C without CO₂. The medium was changed daily with fresh pH-shift medium to remove the extracellular parasites and maintain a constant culture pH. After 4-day incubation, cells were detached and harvested for RNA isolation.

2.7. Generation of myc-tagged Tgndh2-1 and Tgndh2-2 for expression in parasites

The complete open reading frames (ORF) of Tgndh2-1 and Tgndh2-2 were amplified from cDNA of the RH strain using *Hfu* polymerase (Promega) with the primer sets AND1/ORF1+_{AflII} and AND1/ORF2-_{AvrII}, and AND2/ORF1+_{NotI} and AND2/ORF2-_{AvrII}, respectively. The PCR fragments were cloned into pCR40-TOPO (Invitrogen) and DNA sequenced. The AflII/AvrII and NotI/AvrII fragments were finally subcloned into pTetO7Sag4-acyl carrier protein (ACP)-*cmyc*-DHFR vector (kindly provided by Dr. B. Striepen), thereby replacing the ACP ORF with the Tgndh2-1 and Tgndh2-2 ORFs. The final constructs pTetSag4-ndh2-1-*cmyc*-DHFR and pTetSag4-ndh2-2-*cmyc*-DHFR consisted of the anhydrotetracycline (Anr)-regulable TetO7Sag4 promoter element [15], which controls the expression of the complete Tgndh2-1 and Tgndh2-2 ORFs with a C-terminal myc-tag, and additionally includes a pyrimethamine resistance cassette for selection [16]. Parasites (2×10^7) were electroporated with 50 µg of NotI-linearized constructs as previously described [12]. NotI (25 U) was added to the cytomix before electroporation in order to increase the frequency of stable transfectants [17]. Stably transfected parasites were selected with 1 µM pyrimethamine.

2.8. Plasmid construction and *Y. lipolytica* transformation

The NUAM-Tgndh2s fusion constructs were generated as translational fusions comprising the *Y. lipolytica* mitochondrial targeting sequence of the complex I NUAM subunit [18] and the corresponding Tgndh2-1 or Tgndh2-2 mature peptides. The NUAM DNA fragments were amplified by PCR from plasmid pUB38 [19] using proof-reading Phusion DNA polymerase (Finnzymes' Phusion high-fidelity DNA polymerase, NEB) with sense primer BamHI-NUAM-Fusion+ and the corresponding anti-sense primers YL-NDH2-I-24-, YL-NDH2-I-51- and YL-NDH2-II-62- (Supplementary Table S1). For obtaining DNA fragments for the mature parts of the Tgndh2-1(AA24), Tgndh2-1(AA51) and Tgndh2-2(AA62) constructs, cDNA isolated from the RH strain was used as a template for PCR amplification with the following primer sets: YL-NDH2-I-24+ and NDH2-I-FL-, YL-NDH2-I-51+ and NDH2-I-FL, and YL-NDH2-II-62+ and NDH2-II-FL-, respectively. The NUAM-Tgndh2 fusions were achieved by fusion-PCR. To create the

Tgndh2s full-length constructs, primer sets NDH2-I-FL+ and NDH2-I-FL- for Tgndh2-I, and NDH2-II-FL+ and NDH2-II-FL- for Tgndh2-II were used as shown in Supplementary Table S1. All PCR fragments were cloned into pDrive vector (PCR cloning kit, Qiagen) according to the manufacturer's protocol, and then subcloned into the BamHI and EcoRI sites of the *Y. lipolytica*/E. coli shuttle vector pUB30 [19], behind the pPOX2 promoter. All clones were sequenced and confirmed with correct orientation. *Y. lipolytica* haploid NDH2 deletion strain CBS2 [20] was used for transformation with pUB30 constructs encoding TgNDH2-I and TgNDH2-II full-length, or NUAM-TgNDH2-I and NUAM-TgNDH2-II fusion constructs. Transformants were grown in rich glucose medium in the presence of 100 µg/ml Hygromycin B.

2.9. Preparation of mitochondrial membranes

Mitochondrial membranes were isolated as previously described [9]. In brief, cells were harvested and resuspended in ice-cold buffer containing 600 mM sucrose, 20 mM Na⁺Mops, pH 7.4, 1 mM EDTA, and 2 mM phenyl-methylsulfonyl fluoride, and disrupted by glass beads. Mitochondrial membranes were collected from the supernatant and further homogenized, shock-frozen and stored at -80 °C. Samples were aliquoted for kinetic measurements and protein determination.

2.10. Kinetic measurements

NADH:DBQ oxidoreductase activity of mitochondrial membranes from *Y. lipolytica* expressing Tgndh2-I and Tgndh2-II was measured at 30 °C in a reaction mixture containing 20 mM Na⁺Mops (pH 7.4), 50 mM NaCl, 2 mM KCN, 0.1 µM NADH, 60 µM DBQ, and 100 µg/ml mitochondrial membranes in the presence of 27 µM complex I inhibitor DQA. The reaction was initiated by adding DBQ and monitored using a plate reader spectrophotometer (SPECTRAMax PLUS 384, Molecular Devices). Enzyme activities were recorded in terms of velocity (*v*, unit: µM·min⁻¹·mg⁻¹). The applied DBQ concentrations were in the range from 2.5–300 µM (at 100 µM NADH) and the NADH concentrations were in the range from 10–100 µM (at 60 µM DBQ). Data were analysed according to the equations detailed in [9]. Determination of

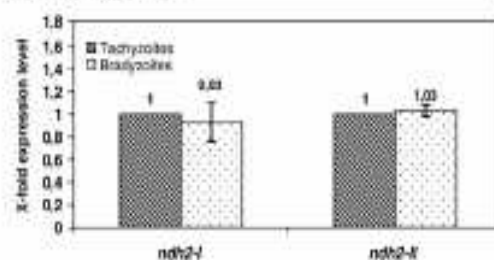


Fig. 2. Real-time PCR analysis for TgNDH2-I and TgNDH2-II mRNA transcripts. HTfs were infected with RH strain tachyzoites in alkaline medium of pH 8.3 to induce bradyzoite differentiation. Total RNA was isolated from tachyzoites at 24 h post-infection and from bradyzoites at 4 days post-infection. Light cycle PCR was performed to amplify cDNAs of TgNDH2-I and TgNDH2-II. β -tubulin was used as an internal control. Values are represented in terms of x-fold increase in the mRNA transcripts of TgNDH2-I and TgNDH2-II in tachyzoites compared to that in bradyzoites after normalization to β -tubulin mRNA transcripts. Results are expressed as mean \pm S.D. of the duplicate wells of two independent experiments.

Michaelis–Menten parameters was by direct fit using the ENZFITTER software package (Biosoft, Cambridge). HDQ and HDQ analogues were kindly provided by Dr. W. Oettmeier and were dissolved in tissue culture grade DMSO (Sigma).

2.11. Nucleotide sequence accession numbers of Tgndh2-I and Tgndh2-II genes

Sequence data of Tgndh2-I and Tgndh2-II were submitted to GenBank with accession numbers DQ211932 and DQ228957, respectively.

3. Results

3.1. *T. gondii* expresses two mitochondrial NDH2 isoforms but no complex I

Based on BLAST homology searches, the genome of *T. gondii* is predicted to encode conventional respiratory chain components, with the exception of the multi-subunit, proton-translocating NADH

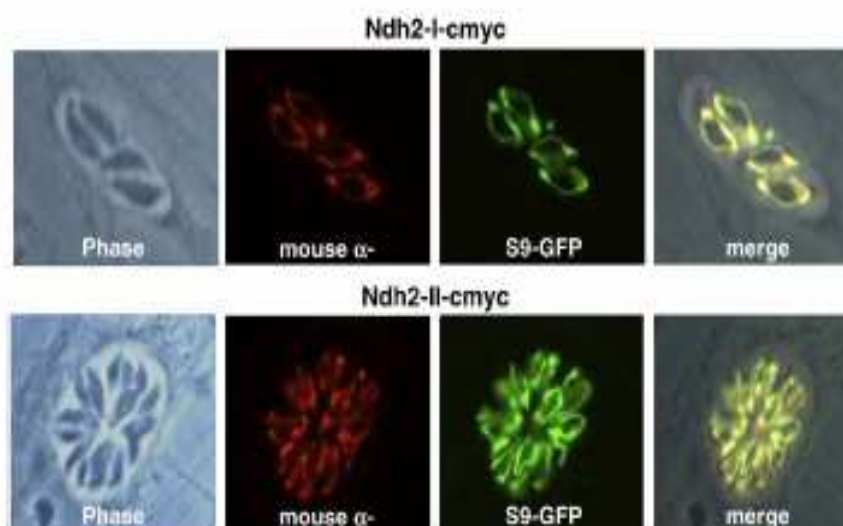


Fig. 1. Mitochondrial localization of myo-tagged TgNDH2-I and TgNDH2-II in parasites. RH strain tachyzoites were transfected with expression plasmids (pTetO75ag4-NDH2-I/-II-cmyc-DHFR), harboring the complete OMPs of TgNDH2-I and TgNDH2-II. The myc-tagged fusion proteins were detected by immunofluorescence staining using anti-myc mAb 9E10. For co-localization experiments, stably transfected parasites expressing the endopic TgNDH2-I and TgNDH2-II genes were co-transfected with pCAT S9-GFP, which encodes a mitochondrially targeted GFP fusion.

dehydrogenase known as complex I. Instead, two contigs (TCC_994254 and TCC_994290) with high similarities to type-II NADH dehydrogenases were identified in the ToxoDB. The complete open reading frames of both genes were amplified, subcloned and sequenced from *T. gondii* RH strain cDNA. The two genes encoding the type-II NADH dehydrogenases were designated as *tgndh2-I* (accession#: DQ211932) and *tgndh2-II* (accession#: DQ228957). They encode precursor polypeptides of 619 and 657 amino acids with predicted masses of 67.1 and 72.1 kDa, respectively. Information on gene structures is given in Supplementary Fig. S1. The deduced primary structure of both proteins includes N-terminal mitochondrial targeting sequences as predicted by

MitoProt II and SignalP 3.0. To verify the mitochondrial localization of *TgNDH2-I* and *TgNDH2-II*, we performed epitope tagging experiments. The complete open reading frames (ORF) of both genes were fused to a C-terminally located c-myc epitope and the resulting expression plasmids (pTerO7Sag4-NDH2-I/II-cmyc-DHFR) were introduced into RH strain parasites of the TAT1-1 line by electroporation. Immunofluorescence analysis of stably transfected parasite populations revealed that both isoforms were targeted to the single *T. gondii* mitochondrion as confirmed by co-localization with the mitochondrial marker 39-C19 [21] that had been co-transfected into NDH2-myc expressing parasites (Fig. 1). We examined *tgndh2-I* and *tgndh2-II* transcript levels in the two

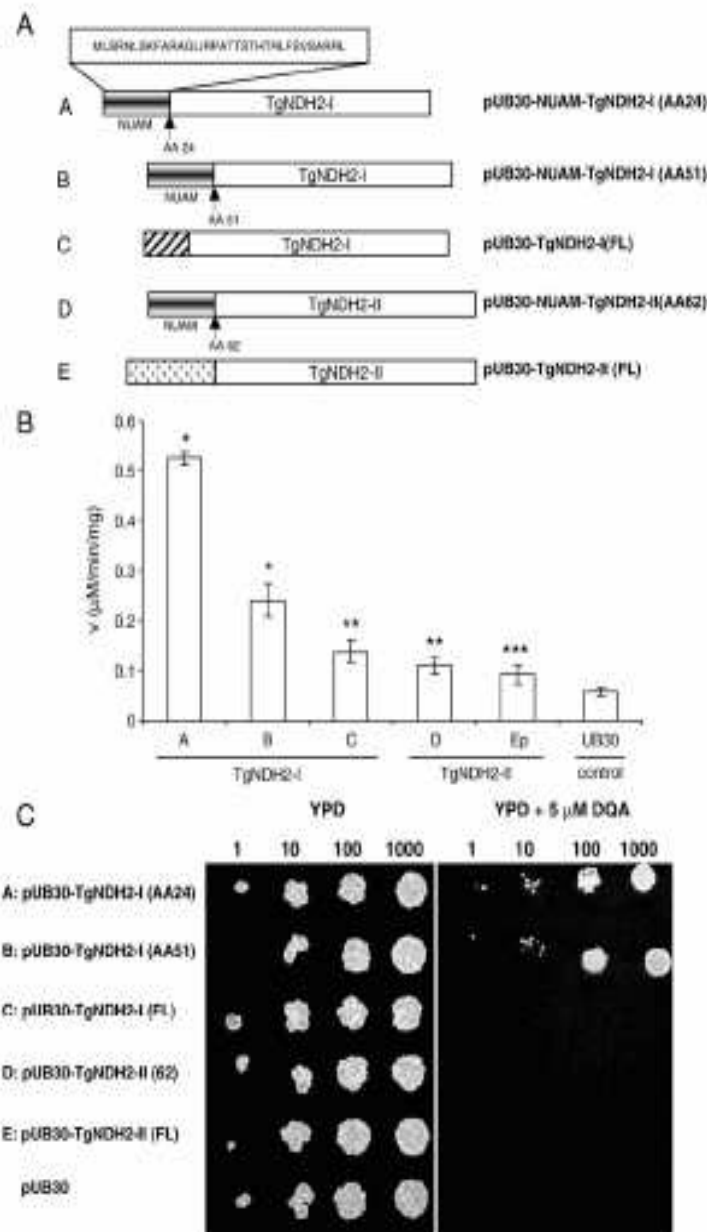


Fig. 3. *TgNDH2-I* displays NADH:DQA oxidoreductase activity. (A) Schematic diagram depicting the constructs established for *Y. lipolytica* transformation. The arrows indicate the coding position for the mature parts of *TgNDH2-I* and *TgNDH2-II*. AA, amino acid; FL, full-length. (B) Oxidoreductase activity was measured in a reaction mixture containing 100 $\mu\text{g/ml}$ mitochondrial membranes from *Y. lipolytica* strain G15.2 containing pUB30-*TgNDH2-I*, *TgNDH2-II* or control pUB30 vector, 100 μM NADH and 60 μM DQA as substrate in the presence or of the complex I inhibitor DQA. Student's *t*-test; **p* < 0.0001; ***p* < 0.001; ****p* < 0.02 versus control pUB30 vector. (C) *TgNDH2-I* confers resistance to the complex I inhibitor DQA. As series of dilutions including 1, 10, 100 and 1000 cells/ml were plated on complete media in the absence or presence of 5 μM DQA.

parasitic stages (tachyzoites and bradyzoites), which are present in the human host by quantitative real time RT-PCR. Both genes displayed comparable mRNA levels in the analyzed stages (Fig. 2), suggesting that they were constitutively expressed rather than stage specifically regulated.

3.2. Functional expression of *TgNDH2-I* in *Y. lipolytica*

The yeast *Y. lipolytica* expresses a single, external, non-essential NDH2 and has been established as a model organism for studying the biochemistry of alternative NADH dehydrogenases [22] and of respiratory chain complex I [23]. We used *Y. lipolytica* strain CB 5.2, in which the external NDH2 was deleted, for heterologous expression of *TgNDH2-I* and *TgNDH2-II*. It is not known whether a mitochondrial import sequence from a *T. gondii* protein is sufficient for accurate targeting into *Y. lipolytica* mitochondria. Thus, in addition to full-length *T. gondii* constructs, we also employed fusions of the N-terminal part of the *Y. lipolytica* mitochondrial NUAM protein and mature versions of *TgNDH2-I* and *TgNDH2-II*. The predicted start position for mature *TgNDH2-I* is at amino acid 24 and for mature *TgNDH2-II* at amino acid 62 (Fig. 3A). The predicted presequence for *TgNDH2-I* is relatively short and after a manual sequence alignment with *TgNDH2-II*, a second, although less likely start position for mature *TgNDH2-I* was identified at position 51 and used for NUAM fusion. It has been demonstrated previously that the addition of the NUAM mitochondrial import signal to the external *Y. lipolytica* NDH2 is sufficient to convert this enzyme into an internal, enzymatically active isoform [18]. All constructs were placed under the control of the *pPOX2* promoter in the replicative vector *pJB30* [19]. Mitochondrial membrane preparations of *Y. lipolytica* transformants were analyzed

for NADH dehydrogenase activity in an enzymatic assay using DBQ as electron acceptor. The NUAM-*TgNDH2-I* fusions displayed electron transfer activities that were 10-fold (construct A: AA24) and 5-fold (construct B: AA51) higher than controls, demonstrating that this isoform can be expressed as an active enzyme in *Y. lipolytica* (Fig. 3B). Both *TgNDH2-II* constructs displayed electron transfer activities that were less than 2-fold above controls, and the activity of full-length *TgNDH2-I* was less than 2.5-fold above controls.

Complex I, the proton-translocating multi-subunit NADH dehydrogenase of the mitochondrial respiratory chain, is essential for growth of *Y. lipolytica*. The ability of the five expression constructs to compensate for the loss of complex I activity was tested in a *Y. lipolytica* growth assay on YPD agar plates in the presence of the complex I inhibitor DQA. Expression of *TgNDH2-I* as NUAM fusion proteins conferred DQA resistance (Fig. 3C), in line with the results obtained from the enzyme activity assay. This demonstrated that both NUAM-*TgNDH2-I* fusions were expressed as functional, internal enzymes with their active site oriented towards the mitochondrial matrix. NUAM-*TgNDH2-I* expressed from construct A which displayed the highest activity and was used in all kinetic assays and is termed *TgNDH2i* in the following.

3.3. *TgNDH2i* activity is effectively inhibited by 1-hydroxy-2-alkyl-4(1H) quinolones

The quinolone-like compound HDQ is a potent inhibitor of *Y. lipolytica* NDH2 [9] and our recent findings have shown that HDQ could effectively inhibit *T. gondii* replication [10]. We thus investigated the inhibitory effect of HDQ on the NADH dehydrogenase activity of *TgNDH2i* in unsealed *Y. lipolytica* mitochondrial membranes. Using

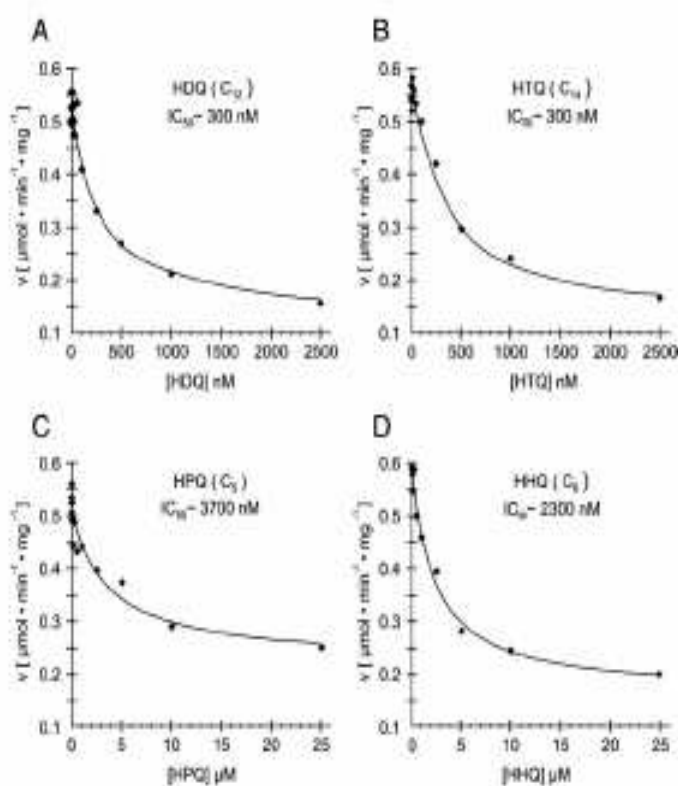


Fig. 4. Inhibition of *TgNDH2i* by HDQ derivatives differing in side chain length. The concentration of inhibitor required for half-maximal inhibition (IC_{50}) of *TgNDH2i* in *Y. lipolytica* mitochondrial membranes was determined at a total protein concentration of 100 $\mu\text{g}/\text{ml}$ in the presence of 60 μM DBQ and 100 μM NADH. (A–D) HDQ with C_{10} , C_{14} , C_{16} and C_{18} alkyl side chains, respectively.

DBQ as a substrate, inhibition of NADH:ubiquinone oxidoreductase activity by HDQ was dose dependent with a concentration required for half-maximal inhibition (K_{50}) of about 300 nM (Fig. 4A). A 1-hydroxy-2-alkyl-4(1H)quinoline compound with a C_{14} alkyl side chain (HTQ, Fig. 4B) displayed a similar K_{50} as HDQ (C_{12}), while derivatives with shorter alkyl side chains (C_5 =HPQ and C_6 =HHQ) were less effective with significantly higher K_{50} values of about 3700 nM and 2300 nM, respectively (Fig. 4C, D).

3.4. TgNDH2 substrate kinetics suggest a ping-pong reaction mechanism

Mitochondrial membrane preparations from *Y. lipolytica* expressing TgNDH2i were used to determine bisubstrate kinetics for NADH and DBQ. K_m values of 76 μ M for NADH and 34 μ M for DBQ were obtained. In a Hanes plot ($[S]/v$ over $[S]$) of the kinetic data, the obtained lines crossed close to the y-axis (Fig. 5) which is in accordance with a ping-pong reaction mechanism for TgNDH2i [9]. A (random or ordered) sequential mechanism could be excluded since in that case the lines would cross in the fourth quadrant. This result suggests that the enzyme forms binary complexes with each of the substrates, but is unable to form a ternary complex with both substrates. Most likely, both substrates interact with a common binding site in a mutually exclusive fashion.

3.5. HDQ inhibition follows a non-competitive pattern for both substrates

To determine the mode of inhibition of HDQ on TgNDH2i in mitochondrial membrane preparations from *Y. lipolytica*, we performed steady-state inhibition kinetics for both NADH and DBQ. Double reciprocal plots of the kinetic data obtained in the presence of 0, 60 and 300 nM HDQ are depicted in Fig. 6. With increasing HDQ concentrations, the slopes increased, and the lines intersected close to the y-axis. Similar as found with *Y. lipolytica* NDH2 [9], these results formally follow the pattern of non-competitive inhibition for both substrates and similar values for the two inhibition constants (see

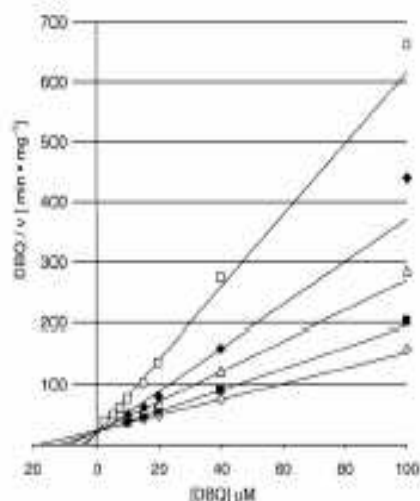


Fig. 5. TgNDH2i employs a ping-pong reaction mechanism. Hanes plots of steady-state kinetics with TgNDH2i in *Y. lipolytica* mitochondrial membranes, assayed at a total protein concentration of 100 μ g/ml. V_{max} and apparent K_m values for DBQ in the presence of five different NADH concentrations were obtained from direct fits to the Michaelis–Menten equation and used to draw the lines. NADH concentrations were 10 (\square), 15 (\blacklozenge), 30 (Δ), 50 (\blacksquare) and 100 μ M (\circ). V_{max} values were 0.7 \pm 0.01 (\square), 0.28 \pm 0.04 (\blacklozenge), 0.40 \pm 0.04 (Δ), 0.57 \pm 0.06 (\blacksquare) and 0.77 \pm 0.07 (\circ) U/mg. Apparent K_m values were 3.5 \pm 0.5 (\square), 5.3 \pm 2.9 (\blacklozenge), 9.1 \pm 2.8 (Δ), 11.9 \pm 4.1 (\blacksquare) and 18.0 \pm 5.0 μ M (\circ). Each data point represents the mean of five independent measurements.

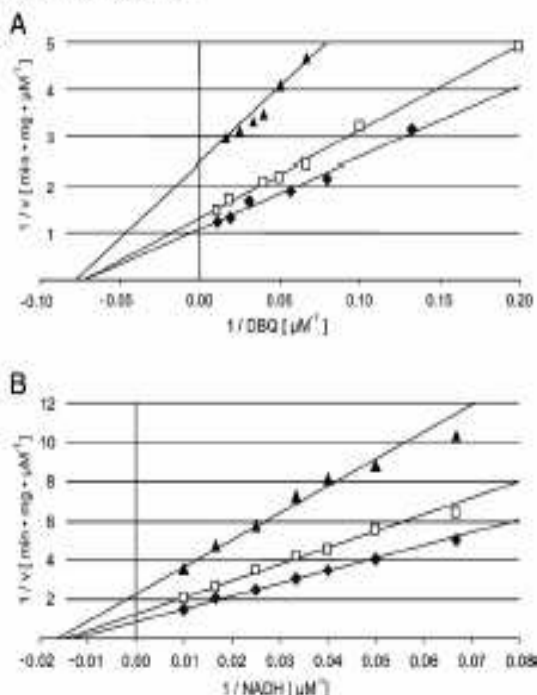


Fig. 6. Double reciprocal plots of HDQ inhibition kinetics of TgNDH2i in *Y. lipolytica* mitochondrial membranes were measured at a total protein concentration of 100 μ g/ml for A, DBQ (at 100 μ M NADH) and B, NADH (at 60 μ M DBQ) in the absence (\bullet) and in the presence of 60 nM (\square) and 300 nM (\blacktriangle) C_{12} -HDQ. The lines for the diagrams were calculated using parameters obtained from direct fits to the Michaelis–Menten equation. In A, V_{max} values were 0.52 \pm 0.06 (\bullet), 0.76 \pm 0.03 (\square) and 0.41 \pm 0.02 (\blacktriangle) U/mg. Apparent K_m values for DBQ were 3.3 \pm 2.4 (\bullet), 13.8 \pm 2.0 (\square) and 12.9 \pm 2.5 μ M (\blacktriangle). In B, V_{max} values were 1.16 \pm 0.07 (\bullet), 0.80 \pm 0.04 (\square) and 0.44 \pm 0.03 (\blacktriangle) U/mg. Apparent K_m values for NADH were 76 \pm 7 (\bullet), 6.8 \pm 5 (\square) and 61 \pm 8 μ M (\blacktriangle). Each data point represents the mean of five independent measurements.

Supplementary Fig. S2). Using linear secondary plots of the slopes and y-axis intercepts of the lines in Fig. 6 against the HDQ concentrations used, numeric values for the inhibition constants could be derived from the points of intersection with the x-axis (see Supplementary Fig. S3). Secondary plots of the slopes thus gave $K_i = 283$ nM and $K_i = 292$ nM, and secondary plots of the intercepts gave $K_i = 234$ nM and $K_i = 298$ nM. Within experimental error, these results are in excellent agreement with the directly determined K_{50} value for HDQ on TgNDH2i and with the assumption that K_i equals K_p .

4. Discussion

In this study we have determined enzymatic parameters from heterologously expressed, functionally active *T. gondii* NDH2-i and could show that 1-hydroxy-2-alkyl-4(1H)quinolones with long alkyl chains are high affinity inhibitors for this enzyme. *T. gondii* lacks complex I but possesses two mitochondrial type-II NADH dehydrogenases. Both are constitutively expressed, hampering direct determination of individual enzymatic parameters in *T. gondii* lysates. Thus, for *in vitro* characterization, we have expressed TgNDH2-i in a strain of the yeast *Y. lipolytica* that lacks endogenous alternative NADH dehydrogenase activity. Functional expression of TgNDH2-i as an internal NADH dehydrogenase, capable of electron transfer from matrix NADH to membrane bound ubiquinone, was achieved by fusing the TgNDH2-i open reading frame without the endogenous mitochondrial targeting sequence to the N-terminal part of the NUAM subunit of *Y. lipolytica* mitochondrial complex I. Direct evidence for *in vivo* function of TgNDH2i was provided by the observation that expression of the transgene allowed cells of *Y. lipolytica* to survive in

the presence of the complex I inhibitor DQA. Thus we were able to achieve heterologous expression of a protozoan type-II NADH dehydrogenase in an active form. Functional expression of protozoan type-II NADH dehydrogenases in *Y. lipolytica* should facilitate future comparative studies of apicomplexan orthologs. In addition, expression of protozoan type-II enzymes in *Y. lipolytica* could be used for the development of a screening assay to identify novel, specific inhibitors for this class of enzymes.

The steady-state inhibition kinetics of TgNDH2-I for the quinolone derivative HDQ were found to be very similar to those of *Y. lipolytica* NDH2 [9] and formally follow the pattern of non-competitive inhibition for both substrates, NADH and DBQ. In the case of a ping-pong reaction mechanism, this inhibition pattern is predicted when the inhibitor blocks both the enzyme, here TgNDH2-FAD and the intermediate form, here TgNDH2-FADH₂ [24]. As with *Y. lipolytica* NDH2 [9], our data thus support a model in which the inhibitor can interact with a complex consisting of the enzyme and one of its substrates, presumably NADH, as depicted in Supplementary Fig. S2.

Bisubstrate kinetics revealed that the NADH:DBQ oxidoreductase activity of TgNDH2 followed a ping-pong reaction mechanism, a mode of action that was also shown for the *Y. lipolytica* ortholog [9] and proposed for the *S. cerevisiae* and *T. brucei* enzymes [25,26]. The determined K_m (NADH) of 76 μ M was significantly higher than the K_m of most other eukaryotic enzymes, for example from *S. tuberosum*, *N. crassa* and *S. cerevisiae*, which were in the range of 11–32 μ M [7]. Only the *T. brucei* enzyme with 120 μ M displayed a higher K_m than the *T. gondii* ortholog [26]. Also, the K_m (DBQ) of 14 μ M observed for TgNDH2 was higher than the K_m (DBQ) of 7.0 μ M for *Y. lipolytica* NDH2 [9]. However, differences in K_m values have to be interpreted with caution, since different electron acceptors were used in these studies and specific reaction conditions as the volume of the lipid phase could influence activities. Since the activity of TgNDH2 was about 4-fold lower than the activity of NDH2, the external alternative NADH dehydrogenase of *Y. lipolytica* parental strains, we had to double the amount of total mitochondrial proteins used in the assays. Lower effective concentrations of DBQ in the lipid phase would explain the elevated K_m (DBQ) values observed in the present study. In contrast, the K_m (NADH) is not expected to depend on the volume of the lipid phase.

The K_{50} value of about 300 nM obtained for HDQ indicates that this compound is a high affinity inhibitor for TgNDH2-I. The only other NDH2 enzyme for which the K_{50} value for HDQ is known is the *N. rowleyi* orthologue, which with 200 nM is in the same range [9]. In the future, it will be important to determine K_{50} values for further orthologues from pathogenic and non-pathogenic microorganisms, in order to classify HDQ as a broad spectrum NDH2 inhibitor or as an inhibitor with a selected inhibitory potential. An example for a respiratory chain inhibitor with a selected inhibitory potential is the clinically approved antimalaria drug atovaquone. This drug is a complex III inhibitor that interferes with the ubiquinol oxidation site of the cytochrome *bc*₁ complex by acting as a competitive inhibitor for ubiquinol. Atovaquone possesses antimicrobial activity against certain apicomplexan parasites such as *Plasmodium* and *Toxoplasma* and the opportunistic fungal pathogen *Pneumocystis carinii*, whereas the human and bovine cytochrome *bc*₁ complexes are insensitive towards atovaquone [27].

For HDQ, the *in vitro* K_{50} of ~300 nM for inhibition of TgNDH2-I activity is significantly higher than the *in vivo* K_{50} of 2–4 nM for static effects on *T. gondii* parasites, determined in tissue culture after a 24 h treatment period [10]. Apparent differences in K_{50} values should not be overinterpreted since these are strongly dependent on the fractional volume of the lipid phase. Assuming that a highly hydrophobic substance like HDQ will partition to the hydrophobic phase, the effective HDQ concentration for interaction with type-II NADH dehydrogenase may well differ by two orders of magnitude between the two assay systems. However, we can not exclude at present that HDQ inhibits other ubiquinone dependent NADH

oxidoreductases such as succinate dehydrogenase, dihydroorotate dehydrogenase, glycerol-3-phosphate dehydrogenase and the malate:quinone oxidoreductase, in addition to type-II NADH dehydrogenases.

A long alkyl side chain of C₁₂ or C₁₄ at position 2 is critical for the inhibition of NADH:DBQ oxidoreductase activity. Compounds with short alkyl side chains of C₅ (HPQ) and C₆ (HHQ) with 3700 nM and 2300 nM displayed significantly higher K_{50} values as compounds with long alkyl side chains of C₁₂ (HDQ, K_{50} =300 nM) and C₁₄ (HTQ, K_{50} =300 nM). On the basis of structural similarities, it is tempting to speculate that 1-hydroxy-2-alkyl-4(1H)quinolones are likely to compete with ubiquinone for the same binding site. A long alkyl side chain leads to a higher hydrophobicity and is likely to render the physicochemical properties and the structure of 1-hydroxy-2-alkyl-4(1H)quinolones more similar to ubiquinone. Another aspect is the partition of the compounds between aqueous and membrane lipid phase. Highly hydrophobic 1-hydroxy-2-alkyl-4(1H)quinolones as HDQ and HTQ, in contrast to those with smaller alkyl side chains, can be expected to partition almost quantitatively into the membrane lipid phase. The correlation between K_{50} values and length of the alkyl side chain mirrored the *in vivo*-efficiency of these drugs to inhibit parasite replication: HPQ (C₅) did not show any inhibitory effect at 10 nM, while parasite growth was reduced to more than 50% by HDQ and HTQ at this concentration [20]. A reevaluation of the efficiency of HHQ (C₆) to inhibit *T. gondii* replication yielded an I_{C50} of 220 nM for HHQ (C₆), which is more than 50-fold higher than the K_{50} for HDQ (data not shown). Together, these data reveal that only 1-hydroxy-2-alkyl-4(1H)quinolones with long alkyl side chains are effective TgNDH2-I inhibitors and antiparasitic drugs.

Acknowledgments

This study has been supported by grants from the Deutsche Forschungsgemeinschaft, DFG to WB (BO 1557/3-1) and UB (SFB472, Teilprojekt P2 and EXC115). S.S. Lin is supported by a scholarship from the Croucher foundation.

Appendix A. Supplementary data

Supplementary data associated with this article can be found, in the online version, at doi:10.1016/j.bbabs.2008.08.006.

References

- [1] S. Kerscher, V. Zickermann, U. Brandt, The three families of respiratory NADH dehydrogenases, *Res. Probl. Cell Different.* 46 (2008) 185–222.
- [2] U. Brandt, Energy converting NADH:quinone oxidoreductases, *Annu. Rev. Biochem.* 75 (2006) 69–92.
- [3] J. Gero, I.M. Burnley, R.J. Shannon, J. Hirst, J.R. Walker, Analysis of the subunit composition of complex I from bovine heart mitochondria, *Mol. Cell. Proteomics* 2 (2003) 117–126.
- [4] M. Radermacher, T. Ilak, T. Claus, S. Benjamin, U. Brandt, V. Zickermann, The three-dimensional structure of complex I from *Narrowsia lipolytica*: a highly dynamic enzyme, *J. Struct. Biol.* 154 (2006) 269–279.
- [5] D. Elshafiq, M.W. Manda, R. Clifton, K.L. Soole, D.A. Day, J. Whelan, Characterization of mitochondrial alternative NAD(P)H dehydrogenases in *Arabidopsis*: intraspecific location and expression, *Plant Cell Physiol.* 47 (2006) 143–54.
- [6] K.M. Overkamp, B. Bakken, P. Köster, A. van Tuji, S. de Vries, J.P. van Dijken, J.T. Pronk, *In vivo* analysis of the mechanisms for oxidation of cytosolic NADH by *Saccharomyces cerevisiae* mitochondria, *J. Bacteriol.* 182 (2000) 2823–2830.
- [7] A.M. Meib, T.M. Bandejas, M. Teixeira, New insights into type II NAD(P)H:quinone oxidoreductases, *Microbiol. Mol. Biol. Rev.* 68 (2004) 603–616.
- [8] G.A. Bugni, P.O. Virjavajjala, P.M. O'Neill, P.G. Bray, S.A. Ward, Functional characterization and target validation of alternative complex I of *Plasmodium falciparum* mitochondria, *Antimicrob. Agents Chemother.* 50 (2006) 1841–1851.
- [9] A. Zickermann, A. Gallin, W. Oettermier, U. Brandt, S. Kerscher, HDQ(1-hydroxy-2-dodecyl-4(1H)quinolone) a high affinity inhibitor for mitochondrial alternative NADH dehydrogenase, *J. Biol. Chem.* 280 (2005) 3138–3142.
- [10] A. Sühb, J. Priesm, S. Baumwieser, U. Gross, W. Böling, Growth inhibition of *Koexizans gondii* and *Plasmodium falciparum* by nanomolar concentrations of 1-hydroxy-2-dodecyl-4(1H)quinolone a high-affinity inhibitor of alternative (type II) NADH dehydrogenase, *Antimicrob. Agents Chemother.* 51 (2007) 1217–1222.

- [11] J.C. Kissinger, B. Gajria, I.T. Paulsen, D.S. Roos, Tox0DB: accessing the *Toxoplasma gondii* genome. *Nucleic Acids Res.* 31 (2003) 234–236.
- [12] D.S. Roos, R.G. Donald, N.S. Morrisette, A.L. Moulton, Molecular tools for genetic dissection of the protozoan parasite *Toxoplasma gondii*. *Methods Cell Biol.* 45 (1994) 27–63.
- [13] M. Meissner, D. Schlüter, D. Soldati, Role of *Toxoplasma gondii* myosin A in powering parasite gliding and host cell invasion. *Science* 298 (2002) 837–840.
- [14] M. Soete, D. Gernis, J.F. Dubremetz, Experimental induction of bradyzoite-specific antigen expression and cyst formation by the RH strain of *Toxoplasma gondii* in vitro. *Exp. Parasitol.* 78 (1994) 361–370.
- [15] M. Méresse, S. Brecht, H. Bujard, D. Soldati, Modulation of myosin A expression by a newly established tetracycline repressor-based inducible system in *Toxoplasma gondii*. *Nucleic Acids Res.* 29 (2001) E115.
- [16] R.G. Donald, D.S. Roos, Stable molecular transformation of *Toxoplasma gondii*: a selectable dihydrofolate reductase-thymidylate synthase marker based on drug-resistance mutations in malaria. *Proc. Natl. Acad. Sci. U. S. A.* 90 (1993) 11703–11707.
- [17] M.T. Black, P. Seiber, D. Soldati, K. Kim, J.C. Boothroyd, Restriction enzyme-mediated integration elevates transformation frequency and enables co-transfection of *Toxoplasma gondii*. *Mol. Biochem. Parasitol.* 74 (1995) 55–63.
- [18] S. Krescher, A. Eschenmann, P.M. Olson, U. Brandt, External alternative NADH:ubiquinone oxidoreductase redirected to the internal face of the mitochondrial inner membrane rescues complex I deficiency in *Yarrowia lipolytica*. *J. Cell Sci.* 114 (2001) 3915–3921.
- [19] A. Garofano, A. Eschenmann, U. Brandt, S. Krescher, Substrate-inducible versions of internal alternative NADH:ubiquinone oxidoreductase from *Yarrowia lipolytica*. *Yeast* 23 (2006) 1129–1136.
- [20] S. Krescher, J.G. Olson, U. Brandt, A single external enzyme confers alternative NADH:ubiquinone oxidoreductase activity in *Yarrowia lipolytica*. *J. Cell Sci.* 112 (1999) 2347–2354.
- [21] A. DeRoover, C.B. Hagen, J.E. Froehlich, J.E. Peagin, M. Parsons, Analysis of targeting sequences demonstrates that trafficking to the *Toxoplasma gondii* plastid branches off the secretory system. *J. Cell Sci.* 113 (2000) 3969–3977.
- [22] S. Krescher, Diversity and origin of alternative NADH:ubiquinone oxidoreductases. *Biochim. Biophys. Acta* 1459 (2000) 274–283.
- [23] S. Krescher, S. Deise, K. Zwicker, V. Zickermann, U. Brandt, *Yarrowia lipolytica* a yeast genetic system to study mitochondrial complex I. *Biochim. Biophys. Acta* 1555 (2002) 83–91.
- [24] W.W. Odland, The kinetics of enzyme-catalyzed reactions with two or more substrates or products. II. Prediction of initial velocity and inhibition patterns by inspection. *Biochim. Biophys. Acta* 67 (1963) 188–216.
- [25] I. Velasco, J.R. Pardo, Kinetic characterization of the rotenone-insensitive internal NADH:ubiquinone oxidoreductase of mitochondria from *Saccharomyces cerevisiae*. *Arch. Biochem. Biophys.* 389 (2001) 7–14.
- [26] J. Bing, D.S. Beattie, Novel FMN-containing rotenone-insensitive NADH dehydrogenase from *Trypanosoma brucei* mitochondria: isolation and characterization. *Biochemistry* 41 (2002) 3005–3072.
- [27] A.L. Baggish, D.R. Hill, Antiparasitic agent atovaquone. *Antimicrob. Agents Chemother.* 46 (2002) 1163–1173.

Type II NADH Dehydrogenase Inhibitor 1-Hydroxy-2-Dodecyl-4(1H)Quinolone Leads to Collapse of Mitochondrial Inner-Membrane Potential and ATP Depletion in *Toxoplasma gondii*[†]

San San Lin, Uwe Groß, and Wolfgang Böhne*

Institute of Medical Microbiology, University of Göttingen, Kreuzbergring 57, D-37075 Göttingen, Germany

Received 4 December 2008/Accepted 2 March 2009

The apicomplexan parasite *Toxoplasma gondii* expresses type II NADH dehydrogenases (NDH2s) instead of canonical complex I at the inner mitochondrial membrane. These non-proton-pumping enzymes are considered to be promising drug targets due to their absence in mammalian cells. We recently showed by inhibition kinetics that *T. gondii* NDH2-I is a target of the quinolone-like compound 1-hydroxy-2-dodecyl-4(1H)quinolone (HDQ), which inhibits *T. gondii* replication in the nanomolar range. In this study, the cationic fluorescent probes Mitotracker and DiOC₆(3) (3,3'-dihexyloxacarbocyanine iodine) were used to monitor the influence of HDQ on the mitochondrial inner membrane potential ($\Delta\Psi_m$) in *T. gondii*. Real-time imaging revealed that nanomolar HDQ concentrations led to a $\Delta\Psi_m$ collapse within minutes, which is followed by severe ATP depletions of 30% after 1 h and 70% after 24 h. $\Delta\Psi_m$ depolarization was attenuated when substrates for other dehydrogenases that can donate electrons to ubiquinone were added to digitonin-permeabilized cells or when infected cultures were treated with the F₀-ATPase inhibitor oligomycin. A prolonged treatment with sublethal concentrations of HDQ induced differentiation into bradyzoites. This dormant stage is likely to be less dependent on the $\Delta\Psi_m$, since $\Delta\Psi_m$ -positive parasites were found at a significantly lower frequency in alkaline-pH-induced bradyzoites than in tachyzoites. Together, our studies reveal that oxidative phosphorylation is essential for maintaining the ATP level in the fast-growing tachyzoite stage and that HDQ interferes with this pathway by inhibiting the electron transport chain at the level of ubiquinone reduction.

The apicomplexan parasite *Toxoplasma gondii* contains a single mitochondrion of an elongated tubular structure (28, 32), which shows several significant metabolic differences from the mammalian counterpart (see references 24 and 33 for review). Although the *T. gondii* mitochondrion harbors the complete set of enzymes for the tricarboxylic acid cycle (15), it lacks the pyruvate dehydrogenase complex (7, 14, 18), which is typically a central enzyme in carbohydrate metabolism that catalyzes the decarboxylation from pyruvate to acetyl coenzyme A. Other mitochondrial pathways for mitochondrial acetyl coenzyme A generation, such as the 2-methylcitrate cycle, are currently under investigation (33). The *T. gondii* genome predicts the presence of all components necessary for a respiratory chain. Biochemical evidence for oxidative phosphorylation was provided by extracellular *T. gondii* tachyzoites that were permeabilized with digitonin (39). However, the overall contribution of oxidative phosphorylation to energy production in relation to other ATP-generating pathways has not been satisfactorily clarified for intracellular *T. gondii* so far.

A fundamental difference of the *T. gondii* and also the *Plasmodium falciparum* electron transport chains (ETCs) as opposed to the mammalian ETC is the lack of multisubunit complex I, which couples the transfer of electrons from NADH to

ubiquinone with the translocation of protons (6). Instead, *P. falciparum* expresses one isoform (2) and *T. gondii* expresses two isoforms (22) of so-called “alternative” or type II NADH dehydrogenases (NDH2s). These single-subunit enzymes do not transport protons across the membrane, and they are, in contrast to the NADH-oxidizing activity of complex I, not rotenone sensitive (21, 27). NDH2s can occur in two topological orientations with respect to the inner mitochondrial membrane. Internal enzymes are facing with their active site toward the mitochondrial matrix and use mitochondrial NAD(P)H as the electron donor, while external enzymes use cytosolic NAD(P)H. Up to now, the orientation of the apicomplexan isoforms is unknown.

Due to their absence in the mammalian host, NDH2s were proposed to be promising drug targets against *Mycobacterium tuberculosis* (40). Their suitability as a drug target in *Plasmodium* is controversial and has been the subject of discussion (16, 17, 38). Previously, it was demonstrated that low-affinity NDH2 inhibitors in micromolar concentrations were able to inhibit the activity of the *P. falciparum* NDH2 and led to a collapse of the mitochondrial membrane potential ($\Delta\Psi_m$) (2). The only high-affinity NDH2 inhibitors described so far are 1-hydroxy-2-alkyl-4(1H)quinolones with long alkyl-site chains, for example, 1-hydroxy-2-dodecyl-4(1H)quinolone (HDQ) (C₁₂), which possesses structural similarity to ubiquinone. These compounds were shown to inhibit the activities of *Yarrowia lipolytica* NDH2 (13) and *T. gondii* NDH2-I (22) with 50% inhibitory concentrations of between 200 and 300 nM. HDQ was also shown to effectively inhibit *T. gondii* and *P.*

* Corresponding author. Mailing address: Institute of Medical Microbiology, University of Göttingen, Kreuzbergring 57, D-37075 Göttingen, Germany. Phone: 49-551-395869. Fax: 49-551-395861. E-mail: wboehne@gwdg.de.

[†] Published ahead of print on 13 March 2009.

falciparum replication in nanomolar concentrations in tissue cultures (31).

We demonstrate in this study that HDQ treatment in nanomolar concentrations leads to a depolarization of the *T. gondii* $\Delta\Psi_m$ within minutes. The subsequent lack of oxidative phosphorylation leads to a ~70% reduction of the intracellular ATP level within 24 h. This suggests an indispensable role of NDH2 activity in the maintenance of the $\Delta\Psi_m$ and in energy metabolism in the tachyzoite stage.

MATERIALS AND METHODS

***T. gondii* cultivation, in vitro stage conversion, and cell lines.** Tachyzoites were propagated in human foreskin fibroblasts (HFFs) as previously described (30). Bradyzoite differentiation was induced by an alkaline-pH shift (34). In brief, tachyzoites were freshly released by syringe passage, and 3×10^6 parasites were inoculated onto a confluent HFF monolayer grown on a 24-well imaging plate. The pH shift medium (pH 8.3) was exchanged daily to maintain a constant pH. 143B/206 cells, which lack mitochondrial DNA (20), and the parental 143B cell line were maintained in Dulbecco's modified Eagle's medium (DMEM) supplemented with 10% fetal calf serum (FCS), penicillin (100 U/ml), streptomycin (100 µg/ml), 1% glutamine, sodium pyruvate (110 µg/ml), and uridine (50 µg/ml).

Chemicals. HDQ was kindly provided by W. Oettmeier and was dissolved in dimethyl sulfoxide or ethanol. Oligomycin, atovaquone, tetramethyl-p-phenylenediamine (TMPD), ascorbate, malate, succinate, glycerol-3-phosphate, dithiothreosulfate, coenzyme, urea, and digitonin were purchased from Sigma.

Plasmids. Plasmid *pub-S9-RFP*/*tag-CAT* was constructed by replacing the FNR fragment from *BglIII*/*AvrII*-digested *pub-FNR-RFP*/*tag-CAT* (36) with a *BglIII*/*AvrII* 59 fragment from *pub-S9-GFP*/*tag-CAT* (8). For generating *pTetO7Sag4-TgATP-β-emyc-DHFR*, the complete open reading frame (ORF) of the *T. gondii* ATPase β subunit (*TgATP-β*) (GenBank accession number DQ228960) was amplified from RH cDNA using *Pfu* polymerase (Promega) with the primer set consisting of primers 5'-TAATGCATAAAATGGCGTCTCCCGCACTC (Nail) and 5'-TACCTAGGCTTTCCGCTCCGCCCTTCTCTG (AvrII). The PCR fragment was cloned into *pCR40-TOP0* (Invitrogen), and the DNA was sequenced. Finally, the Nail/AvrII fragment was subcloned into vector *pTetO7Sag4-ACP-emyc-DHFR* (kindly provide by B. Striepen), thereby replacing the acyl carrier protein ORF with the *ATP-β* ORF. The final construct consists of the anhydrotetracycline-regulable *TetO7Sag4* promoter element (25), which controls the expression of the complete *TgATP-β* ORF with a C-terminal myc tag, and additionally includes a pyrimethamine resistance cassette for selection (9).

Generation of transgenic parasites. The transfection of *T. gondii* strain RH TAT-1 (26) was carried out based on previously reported protocols (30, 35). Stable transgenic parasite lines expressing *TgATP-β* and S9-red fluorescent protein (RFP) were selected with 1 µM pyrimethamine and 20 µM chloramphenicol, respectively.

Detection of $\Delta\Psi_m$ in *T. gondii*. The *T. gondii* $\Delta\Psi_m$ was monitored after staining with the fluorophore Mitotracker or DiOC₂(3) (3,3'-dihexyloxacarbocyanine iodide; Invitrogen). Both fluorescent dyes were dissolved in tissue-culture-grade dimethyl sulfoxide. For Mitotracker, the staining solution was prepared by adding the dye to 1% FCS-DMEM at a final concentration of 0.5 µM. For $\Delta\Psi_m$ detection of intracellular parasites, infected HFFs in a 24-well plate were incubated with staining solution (1 ml per well) at 37°C for 45 min. Afterwards, samples were washed with 1% FCS-DMEM, fixed with 4% paraformaldehyde-phosphate-buffered saline (PBS) for 10 min, and mounted with Mowiol. In experiments using 143B/206 cells, parasites were mechanically released by syringe passage before Mitotracker staining. Freshly released parasites were harvested and immediately stained in suspension with Mitotracker solution (see above), supplemented with 25 mM HEPES (pH 7.4), for 45 min at 37°C. Parasites were fixed with 4% paraformaldehyde-PBS for 10 min after washing, and a 10-µl aliquot of the parasite suspension was air dried on a glass slide and mounted with Mowiol. DiOC₂(3) staining was applied for live imaging of the *T. gondii* $\Delta\Psi_m$. The staining solution consists of 1% FCS-DMEM with a final concentration of 5 nM DiOC₂(3). After incubation at 37°C for 30 min, samples were ready for real-time $\Delta\Psi_m$ monitoring.

Time-lapse microscopy. Live imaging of the *T. gondii* $\Delta\Psi_m$ was performed with an inverted Zeiss Axiovert 200 M microscope equipped with an XL-3 incubator and a heating unit (PeCon). Images were captured by using an AxioCam MRm camera and processed with Axiovision 4.6.3 software. All live-imag-

ing experiments were performed on a black glass-bottomed 24-well imaging plate (Greiner Bio-One) kept at 37°C. In brief, confluent HFFs seeded onto an imaging plate were infected with 2×10^6 to 3×10^6 parasites per well. After DiOC₂(3) staining, the plate was transferred to the humidified chamber, and drugs were added to the wells at the indicated concentrations.

Digitonin permeabilization. Substrate supplementation was performed on digitonin-permeabilized intracellular parasites using a modification of a previously described protocol that was established for extracellular parasites (39). Various concentrations (2 to 64 µM) of digitonin were tested on intracellular parasites, and a final concentration of 2 µM was selected, which did not cause HFF detachment and left the intensity of DiOC₂(3) staining intact over a time period of 35 to 45 min. DiOC₂(3)-stained intracellular parasites were digitonin permeabilized and incubated with HDQ or atovaquone, either alone or in combination with different substrates, for 15 to 25 min at the indicated concentrations. Samples were analyzed by fluorescence microscopy, and the percentage of parasites possessing a detectable $\Delta\Psi_m$ was determined from duplicates.

Determination of the intracellular ATP level. The parasite ATP level was determined by using the BacTiter-Glo microbial cell viability assay (Promega). Samples were prepared as follows. Infected HFFs were washed once with PBS supplemented with protease inhibition (protease inhibitor cocktail; Roche) to remove extracellular parasites. Parasitized cells were then resuspended in 5 ml of 1% FCS-DMEM (phenol red free) supplemented with the same protease inhibitors and freshly released by syringe passage. Afterwards, a centrifugation step at $34 \times g$ was performed in order to remove host cell debris. Parasites in the supernatant were harvested by centrifugation and resuspended in 250 µl of 1% FCS-DMEM. An aliquot of 20 µl of parasites was used for counting, and the remaining parasites were immediately frozen in liquid nitrogen for later measurement. ATP levels from each sample were measured as duplicates in a flat-bottomed 96-well plate. One hundred microliters of the parasite suspension, containing 4×10^6 parasites, was mixed thoroughly with the same volume of BacTiter-Glo reagent and incubated at room temperature for 5 min. Luminescence was detected using luminometry (Wallac 1420; Perkin-Elmer) and quantified as photon counts per second. The relative parasitic ATP levels for each sample were normalized with the number of parasites counted previously.

Immunofluorescence assay. Samples were first fixed with 4% paraformaldehyde-PBS for 10 min and then permeabilized with 0.25% Triton X-100-PBS for another 15 min. After blocking with 1% bovine serum albumin-PBS for 1 h, samples were incubated with an anti-myc monoclonal antibody (MAb) (clone 9E10; Sigma) (1:250), followed by a Cy2-conjugated anti-mouse immunoglobulin G (IgG) antibody (1:300; Dianova) for 1 h each. To detect bradyzoites, a bradyzoite-specific anti-BAG1 MAb (7E5) (1:500) (3) and a Cy3-conjugated anti-mouse IgG antibody (1:300; Dianova) were used instead. Lectin staining was performed with the same procedures by using a fluorescein isothiocyanate-conjugated lectin from *Dolichos biflorus* (1:300; Sigma).

RNA extraction and real-time PCR. Total RNA was isolated using the GenElute mammalian total RNA kit (Sigma), and reverse transcription was done using 5 µg of total RNA, oligo(dT) primer (Sigma), and Moloney murine leukemia virus reverse transcriptase (RNase H minus; Sigma) according to the manufacturer's instructions. Real-time PCR was performed using LightCycler PCR (Roche) to amplify cDNA for the mRNA transcript levels of the bradyzoite-specific genes *enolase 1* and *hsp70* as well as β -tubulin. The primer sets used for cDNA amplification were 5'-CGAGGGGTGGCTGAAAAGATATCC-3' and 5'-CAGCGAAGGCCACGACAAG-3' for *enolase 1*, 5'-GACCGGTCCCTCTCAACAGC-3' and 5'-CGCGCAAAATACCGGACACT for *hsp70*, and 5'-CGCCAGGGCCGCTACTGACT-3' and 5'-TACCGGCTTCTCTCTG CACCC-3' for β -tubulin, respectively. PCR amplification was carried out using the following parameters: 10 min at 95°C followed by 40 cycles of denaturation (95°C for 10 s), annealing (60°C for 5 s), and extension (72°C for 15 s). All samples were tested for PCR amplification efficiencies according to manufacturer's protocols and software (Roche). Serial dilutions of cDNAs were subjected to real-time PCR amplification in duplicates using the β -tubulin primer pair. Crossing points were plotted against the log of cDNA dilutions, and amplification efficiencies (*E*) were calculated from the slopes of the obtained lines by the following formula: $E = 10^{-1/\text{slope}}$. The difference of amplification efficiencies (ΔE) of HDQ-treated samples and the untreated control was less than 0.05 ($\Delta E_{\text{Enolase 1, 200 ng total RNA}} = 0.019$; $\Delta E_{\text{Hsp70, 1,000 ng total RNA}} = 0.015$), and crossing-point values from PCR amplification could thus be used for relative quantification. β -Tubulin mRNA levels were used for the normalization of *enolase 1* and *hsp70* transcript levels in HDQ-treated and -untreated samples.

Protein fractionation and immunoblotting. Protein extracts were prepared at 4°C throughout. Extracellular tachyzoites (3×10^7 to 4×10^7 tachyzoites) from a stable transgenic line expressing *TgATPase-β* were harvested and resuspended in ice-cold PBS containing protease inhibitors. Parasites were lysed by repetitive

freeze-and-thaw steps and sonicated five times for 10 s each. Subsequently, the lysates were separated after centrifugation at $13,000 \times g$ for 45 min. The supernatant comprising the membrane-soluble fraction was collected, precipitated by trichloroacetic acid, and resuspended in $2 \times$ sodium dodecyl sulfate (SDS)-polyacrylamide gel electrophoresis (PAGE) sample buffer containing 0.09 M Tris-Cl (pH 6.8), 30% glycerol, 2% SDS, 0.02% bromophenol blue, and 0.1 M dithiothreitol. The pellet fraction was also resuspended in the same buffer. Protein fractions were resolved on an SDS-polyacrylamide gel and electroblotted onto a Hybond nitrocellulose membrane (Amersham Biosciences). Bound proteins were probed with an anti-myc MAbs (1:500), followed by a secondary antibody with goat anti-mouse IgG coupled to alkaline phosphatase (12,000; Dianova). Reactive proteins were detected by alkaline phosphatase staining solution containing 0.05% bromo-4-chloro-3-indolyl phosphate and 0.5% nitroblue tetrazolium (Sigma) as substrates.

RESULTS

HDQ treatment leads to a collapse of the $\Delta\Psi_m$. The influence of the high-affinity NDH2 inhibitor HDQ (13, 22) on the $\Delta\Psi_m$ was investigated with the aid of the cationic fluorescent dye Mitotracker. When mock controls were stained with Mitotracker at different time points from 7 to 32 h postinfection, 75 to 80% of all intracellular parasites showed the typical intense staining of the single *T. gondii* mitochondrion (Fig. 1A) and were thus categorized as being $\Delta\Psi_m$ positive. The frequencies of $\Delta\Psi_m$ -positive parasites were similar in all samples and unrelated to the size of the parasitophorous vacuoles, suggesting that the majority of tachyzoites possess a $\Delta\Psi_m$ throughout their intracellular life span. In contrast, mitochondrial staining was absent in more than 85% of the parasites when cultures were incubated with 100 nM HDQ (Fig. 1A and B) for the last 6 h. In the remaining parasites, which were classified as being $\Delta\Psi_m$ positive, the intensity of the staining appeared to be less than that for the untreated controls. This suggests that HDQ treatment leads to a collapse of the $\Delta\Psi_m$. Furthermore, it indicates that the susceptibility to membrane depolarization is independent from the size of the parasitophorous vacuole.

Real-time monitoring of the *T. gondii* $\Delta\Psi_m$. Mitotracker comprises a chloromethyl moiety that forms covalent bonds with the SH groups of mitochondrial membrane proteins, which allows the fixation of the stained samples before microscopic analysis. A drawback of this feature is that Mitotracker cannot be reliably used to monitor changes in the $\Delta\Psi_m$ in living cells, since the thiol bond formation is nonreversible. In order to determine the kinetics of an HDQ-mediated $\Delta\Psi_m$ collapse in intracellular *T. gondii*, we first searched for a $\Delta\Psi_m$ -sensitive dye that allows real-time imaging of the *T. gondii* $\Delta\Psi_m$. We compared the cationic fluorophores TMRE (tetramethylrhodamine ethyl ester), JC-1 (3,3'-tetraethylbenzimidazolcarbocyanine iodine), and DiOC₆(3) for their abilities to specifically stain the mitochondrion of intracellular tachyzoites with no or only weak staining of the plasma membrane. DiOC₆(3) was found to be the most suitable dye for this purpose, since it resulted in an intense and specific mitochondrial staining pattern, which perfectly colocalized with a mitochondrially targeted RFP (S9-RFP) (Fig. 2A). When intracellular parasites were treated with 10 nM of the well-established complex III inhibitor atovaquone (1), the intensity of the DiOC₆(3) staining decreased gradually over time, leading to a complete depolarization of the $\Delta\Psi_m$ within 40 min in >60% of the parasites (Fig. 2B and C). These results are consistent with

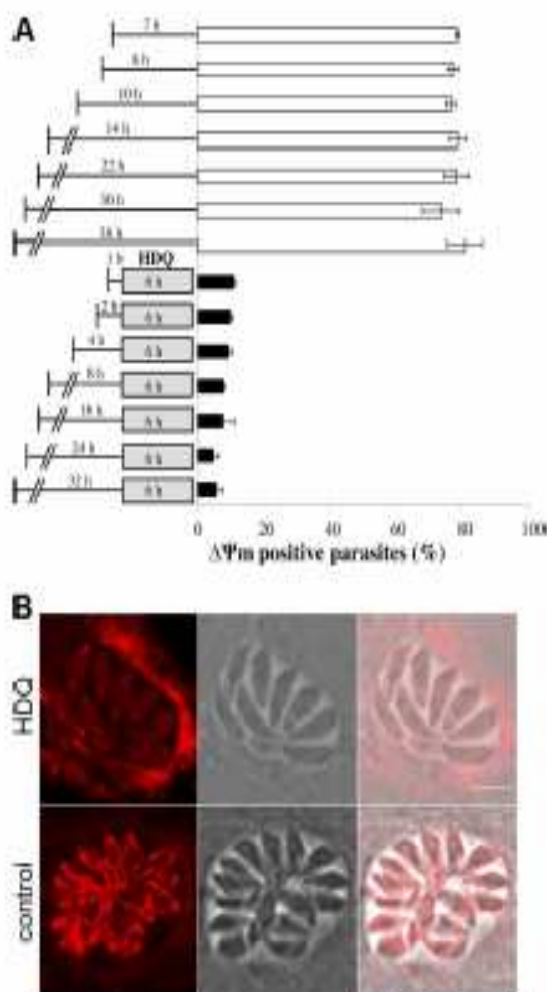
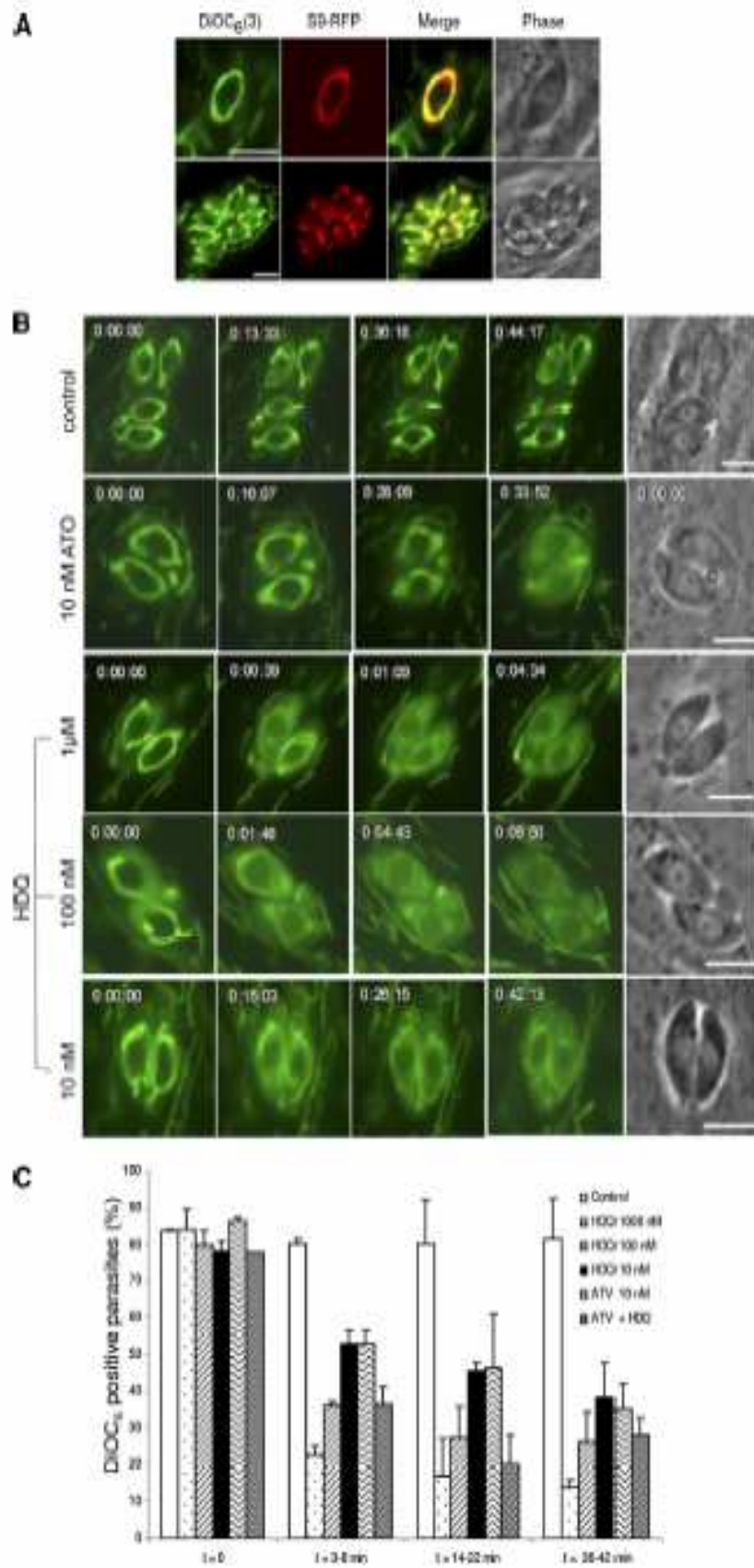


FIG. 1. (A) HDQ treatment decreases the $\Delta\Psi_m$ of intracellular parasites. HFFs were infected with RH strain tachyzoites and treated at the indicated time points with 100 nM HDQ for a period of 6 h, followed by Mitotracker staining and fixation. Drug-untreated controls were stained in parallel at the same time points. The fraction of vacuoles containing $\Delta\Psi_m$ -positive parasites was determined by fluorescence microscopy of at least 100 vacuoles. Results are expressed as means \pm standard deviations (SD) of data from duplicate slides from a representative experiment ($n = 2$). (B) Comparison of the Mitotracker staining patterns from a sample in which the 6-h HDQ treatment period was started 16 h postinfection (top) to those from an untreated control (bottom). Scale bars, 5 μ m.

previously reported observations of the mitochondrial membrane depolarization effect of atovaquone in *T. gondii* (39) and thus demonstrate the suitability of DiOC₆(3) staining for real-time $\Delta\Psi_m$ imaging. The dye could be used for up to 1.5 h in real-time imaging, with a maximum of 10 to 15 exposures taken within this time. Higher numbers of exposures resulted in a significant bleaching effect, and at incubation times longer than 1.5 h, the dye showed a tendency to lose the equal distribution across the mitochondrial membrane and started to accumulate at a single location. We used DiOC₆(3)-based real-time imaging in the following experiments to monitor the kinetics of HDQ-mediated $\Delta\Psi_m$ depolarization.

Kinetics of HDQ-mediated $\Delta\Psi_m$ collapse. DiOC₆(3)-based real-time imaging of the $\Delta\Psi_m$ for parasites treated with 10



nM, 100 nM, and 1 μ M HDQ led to a dose-dependent depolarization of the *T. gondii* mitochondrial membrane (Fig. 2B and C). At 1 μ M HDQ, the mitochondrial membrane from more than 75% of the parasites was completely depolarized within the first 5 min, demonstrating a fast mode of action of the drug (Fig. 2C). The depolarization kinetics of 10 nM HDQ were similar to those of 10 nM atovaquone. A combination of 10 nM HDQ with 10 nM atovaquone resulted in a significantly faster collapse of the $\Delta\Psi_m$ than treatment with 10 nM of the individual drugs, which is in agreement with a synergistic mode of action between HDQ and atovaquone (31).

Substrates for ubiquinone-reducing enzymes lead to $\Delta\Psi_m$ stabilization. Aside from the two type II NADH dehydrogenases, *T. gondii* possesses a further four enzymes that can feed electrons into the ubiquinol pool, namely, succinate dehydrogenase, malate:quinone oxidoreductase, dihydroorotate dehydrogenase (DHODH), and glycerol-3-phosphate dehydrogenase. We investigated whether an excess of substrates for these enzymes could compensate for an HDQ-mediated depolarization of the $\Delta\Psi_m$. Cells were treated for this purpose with 2 μ M digitonin, a concentration which was shown previously to selectively permeabilize the parasite's plasma membrane for metabolites without disturbing the function of the respiratory chain (39). The $\Delta\Psi_m$ of living, intracellular parasites was monitored by DiOC₆(3) staining. In drug-untreated controls, more than 80% of the parasites displayed a strong $\Delta\Psi_m$, confirming that the digitonin treatment itself did not affect the $\Delta\Psi_m$ (Fig. 3). Treatment with TMPD-ascorbate, a combination which is commonly used to feed electrons into complex IV, led to a strongly attenuated $\Delta\Psi_m$ depolarization after HDQ treatment, indicating that HDQ inhibits the ETC upstream of complex IV. The addition of dihydroorotate, glycerol-3-phosphate, malate, or succinate did not prevent an atovaquone-mediated $\Delta\Psi_m$ collapse. This was the expected result, since atovaquone, as a complex III inhibitor, blocks the ETC downstream of ubiquinone reduction. However, each of the four substrates significantly increased the number of $\Delta\Psi_m$ -positive parasites in the presence of HDQ (Fig. 3). The highest number of $\Delta\Psi_m$ -positive parasites in HDQ-treated cultures was achieved when all four substrates were added simultaneously. Oxalacetate was used as a control and did not result in an increased frequency of $\Delta\Psi_m$ -positive parasites. Together, these results suggest that HDQ possesses a different mode of action compared to that of atovaquone and inhibits the ETC upstream of complex III at the level of ubiquinone reduction.

Oligomycin-mediated inhibition of the *T. gondii* F₀F₁-ATPase attenuates HDQ-mediated $\Delta\Psi_m$ depolarization. We next investigated whether the $\Delta\Psi_m$ can be stabilized in HDQ-

treated parasites by an inhibition of the putative *T. gondii* F₀F₁-ATPase. The inner mitochondrial membrane is impermeable to protons, and the only possibility for protons to reenter the mitochondrial matrix is through the F₀ proton channel, which can be inhibited by oligomycin. The *T. gondii* genome contains all genes for the five parts (α , β , γ , δ , and ϵ) that form the F₁ subunit. However, the parasite appears to possess an unusual F₀ subunit, since from the three proteins (F₀-a, F₀-b, and F₀-c) that typically form the F₀ subunit, obvious homologues for F₀-a and F₀-b are lacking (23). This indicates either a high degree of divergence in the lacking parts or an unusual composition of the F₀ subunit. In *Plasmodium*, which is lacking all three F₀-forming proteins, a matrix localization of the F₁ subunit was previously proposed, which implies that the proton gradient cannot be used for ATP synthesis (29). In order to discriminate between a matrix and a membrane association of the F₁ subunit, we examined the localization of the F₁-ATPase in parasites, which expressed an epitope-tagged version of ATPase- β (TgATP- β), which is a part of the F₁-ATPase. Myc-tagged TgATP- β of stably transfected parasites was targeted to the mitochondrion, as shown by the colocalization with the Mitotracker signal (Fig. 4A). After fractionation of the *T. gondii* lysate, ATPase- β was found exclusively in the membrane fraction and was absent in the soluble fraction, suggesting that *T. gondii* possesses a typical, membrane-associated mitochondrial F₁-ATPase (Fig. 4B).

The effect of oligomycin-mediated F₀F₁-ATPase inhibition was further investigated by using 143B/260 cells as host cells for *T. gondii*. This cell line lacks a functional mitochondrial respiratory chain (20), which excludes the possibility that oligomycin has an indirect effect on *T. gondii* via an inhibition of host cell ATP synthesis. The fraction of parasites with positive Mitotracker staining was determined using 143B/260 host cells after HDQ treatment with and without the addition of oligomycin. Oligomycin treatment resulted in a strong increase in levels of $\Delta\Psi_m$ -positive parasites (Fig. 4C), suggesting that the HDQ-mediated $\Delta\Psi_m$ depolarization can be attenuated by preventing protons from reentering the mitochondrial matrix.

HDQ treatment leads to a decreased ATP level. We further examined the influence of HDQ-mediated $\Delta\Psi_m$ collapse on the parasitic ATP level. Infected cultures were incubated with 1 μ M HDQ, and intracellular parasites were mechanically released from host cells by syringe passage at 1, 3, 8, and 24 h after the addition of HDQ. The ATP level of the harvested parasites was determined using a luminescence assay, and the obtained values were normalized for parasite numbers. An oligomycin-treated sample was included in order to quantify ATP levels in parasites in which F₀F₁-ATPase activity was

FIG. 2. Real-time imaging of the *T. gondii* $\Delta\Psi_m$ by DiOC₆(3) staining. (A) Parasites expressing the mitochondrial marker SS-RFP were stained with the cationic fluorophore DiOC₆(3) at different time points postinfection and analyzed by fluorescence live-cell imaging. DiOC₆(3) specifically stained the mitochondria of the parasites and also the host cell mitochondria, which appear to be less intensely stained than the *T. gondii* mitochondria. Scale bars, 5 μ m. (B) Kinetics showing the influence of 10 nM complex III inhibitor atovaquone (ATQ) and 10 nM, 100 nM, and 1 μ M NDH2 inhibitor HDQ on the $\Delta\Psi_m$ of individual parasites. The infected cultures were stained immediately before drug treatment with DiOC₆(3). Scale bars, 5 μ m. (C) Quantification of mitochondrial membrane depolarization kinetics after treatment with 10 nM, 100 nM, and 1 μ M HDQ; 10 nM atovaquone (ATQ); and a combination of 10 nM HDQ and 10 nM atovaquone. The infected cultures were stained immediately before drug treatment with DiOC₆(3), and the fraction of vacuoles containing $\Delta\Psi_m$ -positive parasites was determined by fluorescence microscopy of at least 100 vacuoles at the indicated time periods. The diagram shows the means \pm SD of data from duplicate wells from a representative experiment.

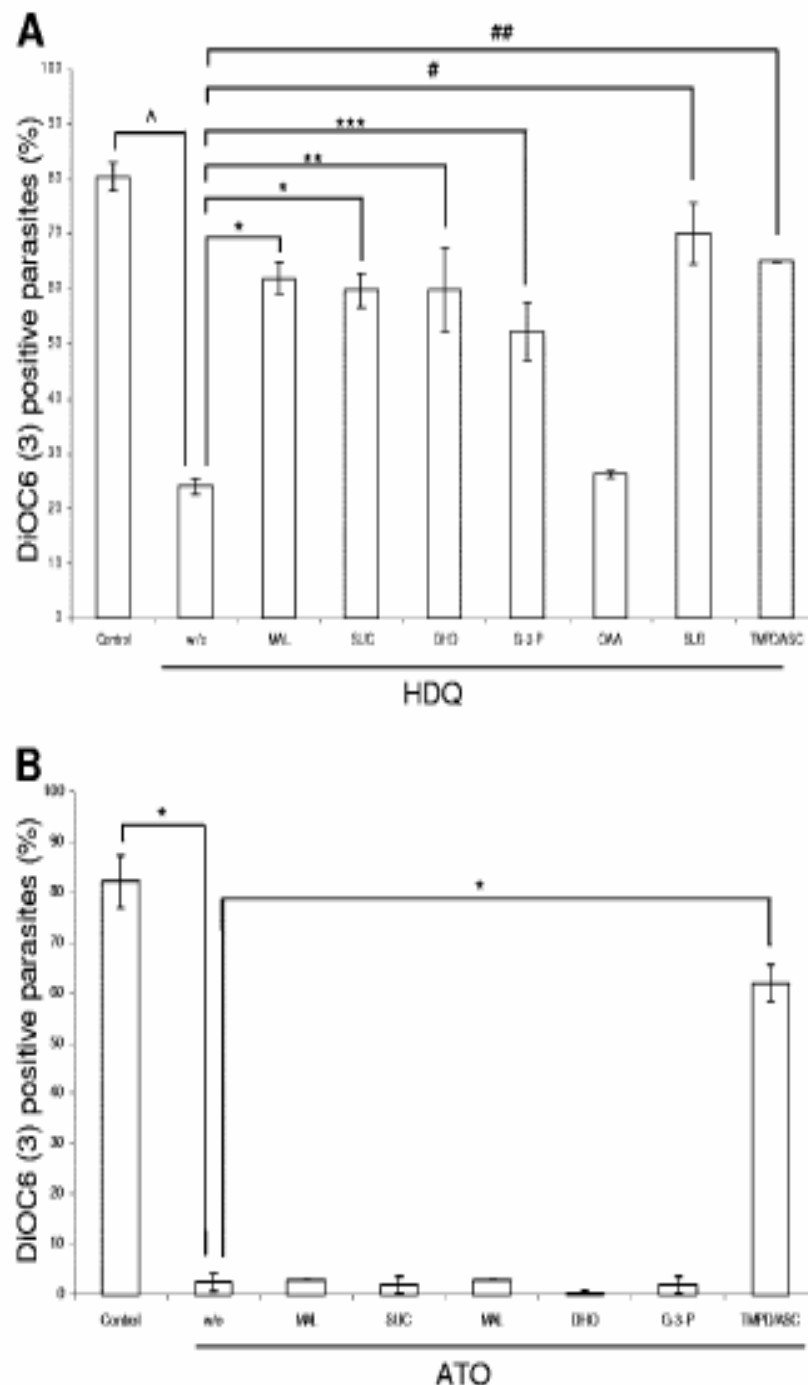


FIG. 3. Substrate supplementation in permeabilized parasites partly decreases HDQ-mediated $\Delta\psi_m$ depolarization. DiOC₆(3)-stained intracellular parasites were digitonin permeabilized and treated with 1 μ M HDQ (A) or 1 μ M atovaquone (ATO) (B) either alone or in combination with 10 mM malate (MAL); 10 mM succinate (SUC); 10 mM dihydroorotate (DHO); 1 mM glycerol-3-phosphate (G-3-P); 10 mM oxaloacetate (OAA); a mixture of malate, succinate, dihydroorotate, and glycerol-3-phosphate (SUB); and 0.2 mM TMPD-4.5 mM ascorbate (TMPD/ASC). The percentage of $\Delta\psi_m$ -positive parasites was determined from pictures taken by fluorescence microscopy after a 15- to 25-min incubation period at 37°C. Results are expressed as means \pm SD of data from duplicate samples from a representative experiment ($n = 2$). *, $P < 0.002$; *, $P < 0.005$; **, $P < 0.03$; ***, $P < 0.02$; #, $P < 0.01$; ##, $P < 0.001$ (determined by a Student's t test) (A). *, $P < 0.003$ (determined by a Student's t test) (B).

inhibited. The kinetics revealed that HDQ leads to a gradual decrease of the parasite's total ATP level, resulting in a $\sim 30\%$ reduction after 1 h and a $\sim 70\%$ reduction after 24 h (Fig. 5). A 70% decrease in the ATP level was also observed after the

complete inhibition of F_0F_1 -ATPase activity using 1 μ M oligomycin.

HDQ growth inhibition is not mediated by pyrimidine starvation. HDQ possesses structural similarities to ubiquinol and

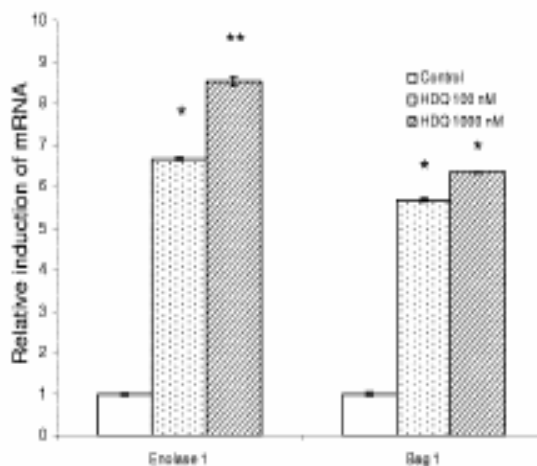


FIG. 7. HDQ treatment upregulates transcript levels of the bradyzoite markers *bag1* and *enolase 1*. HFFs were infected with tachyzoites and cultivated in the presence of 100 nM and 1 μ M HDQ for 72 h. *Enolase 1* and *bag1* mRNA transcripts were determined by real-time PCR. β -Tubulin was used for normalization. The diagram shows *enolase 1* and *bag1* transcript levels of HDQ-treated samples relative to that of a mock-infected control (arbitrarily defined as 1), which was harvested 24 h postinfection. Results are expressed as means \pm SD of data from duplicate samples from a representative experiment. *, $P < 0.0001$; **, $P < 0.0002$ versus mock control (determined by a Student's *t* test).

The frequency of $\Delta\Psi$ m-positive parasites decreases during bradyzoite differentiation. There are several indications that the energy metabolism of bradyzoites is different from that of tachyzoites (12, 41), and it was thus of interest to compare the frequencies of $\Delta\Psi$ m-positive parasites in both stages. Bradyzoite differentiation was induced by an alkaline-pH shift, and the percentage of $\Delta\Psi$ m-positive parasites was determined after DiOC₆(3) staining in living cultures at 24 h, 48 h, and 72 h postinfection. The rate of bradyzoite differentiation was determined using the same samples after fixation and staining with a bradyzoite-specific anti-BAG1 antibody, which detects a cytosolic small heat shock protein, and with a fluorescein isothiocyanate-conjugated *Dolichos biflorus* lectin, which detects a carbohydrate structure on the emerging cyst wall (Fig. 8A). The fraction of $\Delta\Psi$ m-positive parasites gradually decreased from ~85% after 24 h to 20% after 72 h, while the expression of the bradyzoite markers increased to 70 to 80% (Fig. 8B). This suggests that a fraction of parasites lost the $\Delta\Psi$ m during bradyzoite differentiation. A putative concern was that the emerging cyst wall acts as a diffusion barrier and prevents the access of DiOC₆(3) to the bradyzoites. To exclude this possibility, we verified the results using freshly harvested extracellular bradyzoites, which were released from their parasitophorous vacuoles and the emerging cyst wall by extensive syringe passage. Mitotracker staining was applied for the released parasites, followed by fixation, permeabilization, and BAG1 staining. The frequency of Mitotracker-positive parasites in the BAG1-positive population was less than 10%, compared to ~80% Mitotracker-positive parasites in freshly released extracellular tachyzoites (Fig. 8C). These results are in agreement with the data obtained from intracellular parasites and confirm

the strong decrease in levels of $\Delta\Psi$ m-positive parasites during bradyzoite differentiation.

DISCUSSION

We demonstrate in this study that the treatment of intracellular tachyzoites with HDQ, a quinolone-like compound that was previously shown to inhibit TgNDH2-I (22), leads to a fast, dose-dependent collapse of the $\Delta\Psi$ m and subsequently to a decrease in the intracellular ATP level. The mode of action of HDQ in *T. gondii* is thus an inhibition of oxidative phosphorylation. The observed synergism of 10 nM HDQ in combination with 10 nM atovaquone on $\Delta\Psi$ m depolarization is in agreement with the synergism of these drugs to inhibit parasite replication in vitro (31). The addition of succinate, dihydroorotate, glycerol-3-phosphate, or malate to digitonin-permeabilized cells stabilized the $\Delta\Psi$ m in the presence of HDQ, whereas these substrates did not influence atovaquone-mediated depolarization. This observation clearly indicates that HDQ acts as an ETC inhibitor upstream of the atovaquone target, which is complex III, at the level of ubiquinone reduction. The attenuation of HDQ-mediated $\Delta\Psi$ m depolarization in the presence of high substrate concentrations of ubiquinone-reducing enzymes is in agreement with HDQ acting as an NDH2 inhibitor and a replenishment of the ubiquinol pool by an increased level of activity of the corresponding enzymes succinate dehydrogenase, DHODH, glycerol-3-phosphate dehydrogenase, and malate:quinone oxidoreductase. Since physiological substrate concentrations in non-digitonin-treated cells are not sufficient to compensate for the HDQ-mediated $\Delta\Psi$ m depolarization, a major role of NDH2 activity in providing the ETC with reduction equivalents can be assumed under the assumption that HDQ is not affecting any other targets of the ETC. Although we have no indications for potential other targets of HDQ in *T. gondii*, we cannot completely rule out the possibility that HDQ also exerts an inhibitory effect on one or more of the above-mentioned ubiquinone-reducing enzymes. However, we excluded the possibility that pyrimidine starvation is the mode of action by which HDQ inhibits *T. gondii* replication. A recent study reported that HDQ inhibits DHODH of *P. falciparum* (10). This ubiquinone-dependent enzyme catalyzes the dehydrogenation of dihydroorotate to orotate, an essential step for de novo pyrimidine biosynthesis. In contrast to *Plasmodium*, *T. gondii* possesses a pyrimidine salvage pathway, and parasites deficient in de novo pyrimidine synthesis can be rescued with high uracil concentrations (19). Since uracil supplementation did not rescue parasite replication in HDQ-treated cultures, we could exclude that pyrimidine starvation is the major mode of inhibition of HDQ in *T. gondii*.

F_1F_0 -ATPases use the proton motive force across the inner mitochondrial membrane for coupling proton translocation through a membrane-bound, oligomycin-sensitive F_0 subunit with ATP synthesis at the F_1 subunit. The F_0 subunit is typically composed of three proteins (F_0 -a, F_0 -b, and F_0 -c); however, the *T. gondii* genome has no obvious homologues for the F_0 -a and F_0 -b proteins (23). It was thus unclear whether the *T. gondii* F_1 subunit is indeed associated with a putative membrane-bound F_0 subunit or if this enzyme is localized in the mitochondrial matrix, as proposed previously for *Plasmodium*

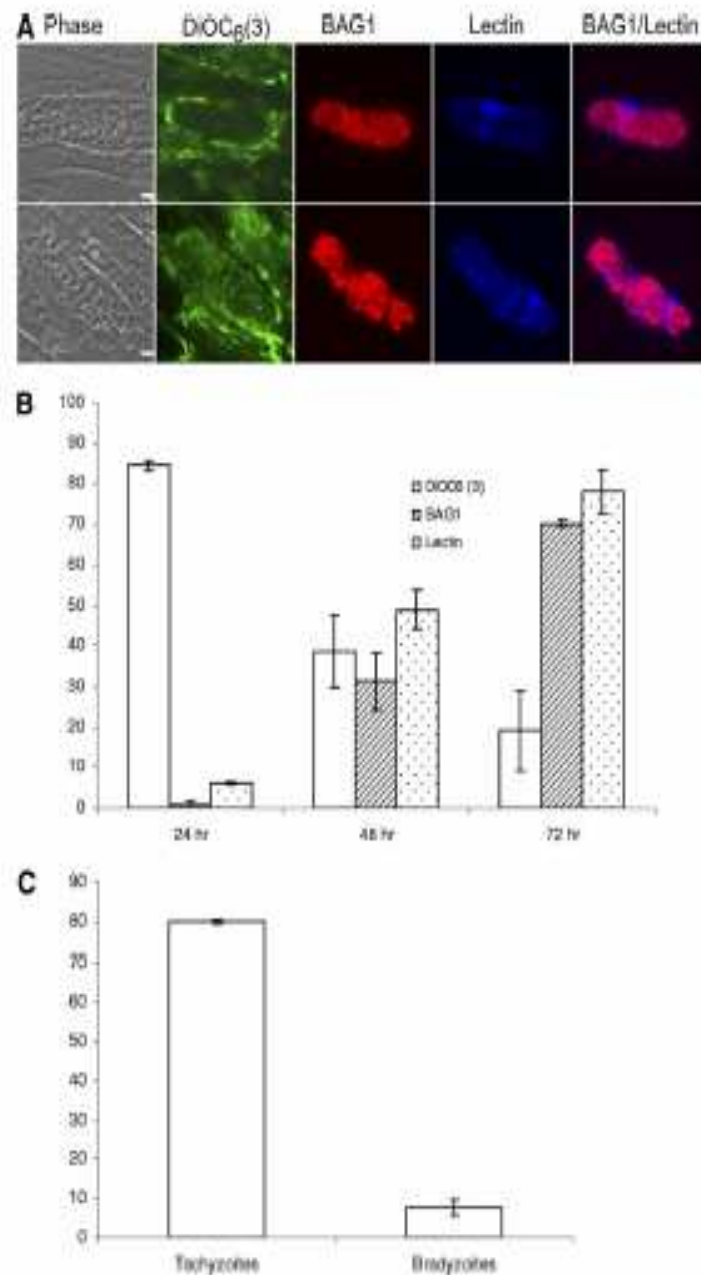


FIG. 8. Loss of $\Delta\psi_m$ during bradyzoite differentiation. Bradyzoite differentiation was induced by an alkaline-pH shift (pH 8.3). At 24 h, 48 h, and 72 h postinfection, living samples were stained with DiOC₂(3) and analyzed by immunofluorescence microscopy, followed by fixation and BAG1 and *Desiokus biflorus* lectin staining. (A) Fluorescence images from a 72-h sample showing a DiOC₂(3)-negative/BAG1-positive/lectin-positive vacuole (top) and a vacuole that is weakly DiOC₂(3) positive (bottom). (B) Kinetics showing the decrease of DiOC₂(3)-positive vacuoles and the increase of BAG1-positive and lectin-positive vacuoles during bradyzoite differentiation. (C) Extracellular parasites were obtained after syringe passage from a 72-h bradyzoite culture and a 24-h tachyzoite culture. The diagram shows the fraction of Mitotracker-positive parasites in the BAG1-positive population (bradyzoites) in comparison to Mitotracker-positive parasites from the tachyzoite culture. More than 100 extracellular parasites were analyzed for each sample. Results are expressed as means \pm standard errors of the means for data from two independent experiments.

(29), which is lacking all three parts of the F_0 subunit. The latter would imply that the proton motive force cannot be used for ATP synthesis. We showed by subcellular fractionation that the F_1 subunit is associated exclusively with the membrane fraction, which suggests an interaction of F_1 with a membrane-

associated F_0 or F_0 -like subunit. A conventional function of the *T. gondii* F_0F_1 -ATPase in coupling the proton gradient with ATP synthesis is consistent with our observation that (i) an HDQ-mediated depolarization of the inner mitochondrial membrane leads to a \sim 30% reduction of the ATP level within

1 h and to a ~70% reduction within 24 h, (ii) treatment with the F_0 subunit inhibitor oligomycin leads to a ~70% reduction of the ATP level, and (iii) oligomycin leads to a stabilization of the $\Delta\Psi_m$ in the presence of HDQ. These results are in agreement with data from previous biochemical analyses in which the level of O_2 consumption of digitonin-treated extracellular *T. gondii* was shown to be increased in the presence of ADP and decreased in the presence of the F_0 subunit inhibitor oligomycin (39).

The relative contribution of oxidative phosphorylation to total ATP synthesis is still a matter of debate for *T. gondii*, as it is for other apicomplexan parasites (24, 33). Our studies suggest that oxidative phosphorylation is indispensable for sufficient ATP generation in the growing-tachyzoite stage and that other ATP-generating pathways such as glycolysis cannot fully compensate for its loss. The HDQ-mediated depolarization of the $\Delta\Psi_m$ occurs within minutes, while the onset of the ATP decrease started with a delay of ~30 min. It is conceivable that a reserve energy system of limited capacity contributes to a stable ATP amount within the first minutes after the inhibition of oxidative phosphorylation. A likely candidate for such an energy buffer system is the adenylate kinase reaction, which converts two ADP molecules into ATP and AMP in a reversible reaction. A common response to the inhibition of oxidative phosphorylation, which might also occur in *T. gondii*, is an increased metabolic flux through other energy-generating pathways, like glycolysis. High substrate concentrations at the beginning of the inhibition process, for example, of glucose-6-phosphate, might also contribute to a timely, limited stabilization of the ATP level until these resources are reduced in concentration.

The fraction of parasites with a detectable $\Delta\Psi_m$ is not constant throughout the life cycle but is strongly decreased during tachyzoite-to-bradyzoite conversion. This is in agreement with the concept that *T. gondii* adapts its metabolism during the transition from tachyzoites to long-term persistent bradyzoites, which are believed to possess a reduced metabolism (4, 12, 41). The close link between energy metabolism and stage conversion is furthermore supported by our observation that long-term treatment with HDQ for 3 days leads to an upregulation of mRNA transcripts for bradyzoite markers. This is in agreement with previously reported observations that inhibitors of the respiratory chain and of oxidative phosphorylation lead to an induction of bradyzoite differentiation (4, 37). The parasite appears to respond in a situation of energy starvation with a differentiation into the dormant stage.

ACKNOWLEDGMENTS

HDQ was kindly provided by W. Oetmeier (University of Bochum). This study has been supported by a grant from the Deutsche Forschungsgemeinschaft to W.B. (BO 1557/3-1). S.S.L. is supported by a Croucher overseas scholarship award.

REFERENCES

- Buggiah, A. L., and B. R. Hill. 2002. Antiparasitic agent atovaquone. *Antimicrob. Agents Chemother.* 46:1163-1173.
- Biagini, G. A., P. O. Viriyavejakul, P. M. O'Neill, P. G. Bray, and S. A. Ward. 2006. Functional characterization and target validation of alternative complex I of *Plasmodium falciparum* mitochondria. *Antimicrob. Agents Chemother.* 50:1841-1851.
- Bohme, W., J. Hoesmann, and U. Gross. 1993. Induction of bradyzoite-specific *Toxoplasma gondii* antigens in gamma interferon-treated mouse macrophages. *Infect. Immun.* 61:1141-1145.
- Bohme, W., J. Hoesmann, and U. Gross. 1994. Reduced replication of *Toxoplasma gondii* is necessary for induction of bradyzoite-specific antigens: a possible role for nitric oxide in triggering stage conversion. *Infect. Immun.* 62:1761-1767.
- Bohme, W., U. Gross, D. J. Ferguson, and J. Hoesmann. 1995. Cloning and characterization of a bradyzoite-specifically expressed gene (hsp30/bag1) of *Toxoplasma gondii*, related to genes encoding small heat-shock proteins of plants. *Mol. Microbiol.* 16:1221-1230.
- Brandt, U. 2006. Energy converting NADH:quinone oxidoreductase. *Annu. Rev. Biochem.* 75:69-90.
- Crawford, M. J., N. Thomsen-Zieger, M. Ray, J. Schachter, D. S. Ross, and F. Seiber. 2006. *Toxoplasma gondii* scavenges host-derived lipic acid despite its de novo synthesis in the apicoplast. *EMBO J.* 25:3214-3222.
- DeBocker, A., C. B. Hagan, J. E. Froelich, J. E. Feagin, and M. Parsons. 2000. Analysis of targeting sequences demonstrates that trafficking to the *Toxoplasma gondii* plastid branches off the secretory system. *J. Cell Sci.* 113:3069-3077.
- Donald, R. G., and D. G. Ross. 1993. Stable molecular transformation of *Toxoplasma gondii*: a selectable dihydrofolate reductase-thymidylate synthase marker based on drug-resistance mutations in malaria. *Proc. Natl. Acad. Sci. USA* 90:11703-11707.
- Dong, C. K., V. Patel, J. C. Yang, J. D. Dyerin, M. T. Duraisingh, J. Clardy, and D. F. Wirth. 2009. Type II NADH dehydrogenase of the respiratory chain of *Plasmodium falciparum* and its inhibition. *Bioorg. Med. Chem. Lett.* 19:972-975.
- Dziensinski, F., O. Popescu, C. Touraud, C. Slomiany, R. Yakhizoi, and S. Tamayo. 1999. The protozoan parasite *Toxoplasma gondii* expresses two functional plant-like glycolytic enzymes. Implications for evolutionary origin of apicomplexans. *J. Biol. Chem.* 274:24888-24895.
- Dziensinski, F., and L. J. Knell. 2007. Biology of bradyzoites, p. 303-320. In L. M. Weiss and K. Kim (ed.), *Toxoplasma gondii*—the model apicomplexan: perspectives and methods. Academic Press, London, United Kingdom.
- Echenmans, A., A. Galka, W. Oetmeier, U. Brandt, and S. Karscher. 2005. HDQ (1-hydroxy-2-dodecyl-4(1H)quinolone), a high affinity inhibitor for mitochondrial alternative NADH dehydrogenase. *J. Biol. Chem.* 280:3138-3142.
- Flaig, T., K. Fischer, D. J. P. Ferguson, U. Gross, and W. Bohme. 2007. Carbohydrate metabolism in the *Toxoplasma gondii* apicoplast: localization of three glycolytic isoenzymes, the single pyruvate dehydrogenase complex, and a plastid phosphate translocator. *Eukaryot. Cell* 6:984-996.
- Flaig, T., N. Pfaff, U. Groß, and W. Bohme. 2008. Localization of gluconeogenesis and TCA-cycle enzymes and first functional analysis of the TCA-cycle in *Toxoplasma gondii*. *Int. J. Parasitol.* 38:1121-1132.
- Fisher, N., P. G. Bray, S. A. Ward, and G. A. Biagini. 2007. The malaria parasite type II NADH:quinone oxidoreductase: an alternative enzyme for an alternative lifestyle. *Trends Parasitol.* 23:305-310.
- Fisher, N., P. G. Bray, S. A. Ward, and G. A. Biagini. 2008. Malaria-parasite mitochondrial dehydrogenases as drug targets: too early to write the obituary. *Trends Parasitol.* 24:9-10.
- Foth, B. J., L. M. Stumler, E. Handman, B. S. Crabb, A. N. Hodler, and G. I. McFadden. 2005. The malaria parasite *Plasmodium falciparum* has only one pyruvate dehydrogenase complex, which is located in the apicoplast. *Mol. Microbiol.* 55:39-53.
- Fox, B. A., and D. J. Beik. 2002. De novo pyrimidine biosynthesis is requisite for virulence of *Toxoplasma gondii*. *Nature* 415:926-929.
- Jacobson, M. D., J. F. Burke, M. P. King, T. Miyashita, J. C. Reed, and M. C. Raff. 1993. Bcl-2 blocks apoptosis in cells lacking mitochondrial DNA. *Nature* 361:365-369.
- Karscher, S., V. Zickmann, and U. Brandt. 2008. The three families of respiratory NADH dehydrogenases. *Res. Protoc. Cell Differ.* 4:8185-222.
- Liu, S. S., S. Karscher, A. Sakthi, U. Brandt, U. Gross, and W. Bohme. 2008. The *Toxoplasma gondii* type-II NADH dehydrogenase TgNDH2-I is inhibited by 1-hydroxy-2-alkyl-4(1H)quinolones. *Biochim. Biophys. Acta Bioenerg.* 1777:1455-1462.
- Mather, M. W., K. W. Henry, and A. B. Vaidya. 2007. Mitochondrial drug targets in apicomplexan parasites. *Curr. Drug Targets* 8:49-60.
- Mather, M. W., and A. B. Vaidya. 2008. Mitochondria in malaria and related parasites: ancient, diverse and streamlined. *J. Bioenerg. Biomembr.* 40:425-433.
- Meisner, M., S. Brecht, H. Bujard, and D. Soldati. 2001. Modulation of myosin A expression by a newly established tetracycline represson-based inducible system in *Toxoplasma gondii*. *Nucleic Acid Res.* 29:E115.
- Meisner, M., D. Schlater, and D. Soldati. 2002. Role of *Toxoplasma gondii* myosin A in powering parasite gliding and host cell invasion. *Science* 298:837-840.
- Melo, A. M., T. M. Bandeira, and M. Teixeira. 2004. New insights into type II NAD(P)H:quinone oxidoreductase. *Microbiol. Mol. Biol. Rev.* 68:603-616.
- Melo, E. J., M. Attias, and W. De Souza. 2000. The single mitochondrion of tachyzoites of *Toxoplasma gondii*. *J. Struct. Biol.* 130:27-33.
- Painter, H. J., J. M. Mearns, M. W. Mather, and A. B. Vaidya. 2007.

- Specific role of mitochondrial electron transport in blood-stage *Plasmodium falciparum*. *Nature* 446:88–91.
30. Ross, D. S., R. G. Donald, N. S. Merrisotte, and A. L. Moulton. 1994. Molecular tool for genetic dissection of the protozoan parasite *Toxoplasma gondii*. *Methods Cell Biol.* 45:27–63.
 31. Saleh, A., J. Fricson, S. Baumister, U. Gross, and W. Bokre. 2007. Growth inhibition of *Toxoplasma gondii* and *Plasmodium falciparum* by nanomolar concentrations of 1-hydroxy-2-dodecyl-4(1H)quinolone, a high-affinity inhibitor of alternative (type II) NADH dehydrogenase. *Antimicrob. Agents Chemother.* 51:1217–1222.
 32. Seiber, F., D. J. P. Ferguson, and U. Gross. 1998. *Toxoplasma gondii*: a paraformaldehyde-insensitive diaphotase activity acts as a specific histochemical marker for the single mitochondrion. *Exp. Parasitol.* 91:137–139.
 33. Seiber, F., J. Linenitakis, and B. Soldati-Favre. 2008. Apicomplexan mitochondrial metabolism: a story of gains, losses and retentions. *Trends Parasitol.* 24:468–478.
 34. Sests, M., D. Camus, and J. F. Dubrenetz. 1994. Experimental induction of bradyzoite-specific antigen expression and cyst formation by the RH strain of *Toxoplasma gondii* in vitro. *Exp. Parasitol.* 78:361–370.
 35. Soldati, B., and J. C. Boothroyd. 1993. Transient transfection and expression in the obligate intracellular parasite *Toxoplasma gondii*. *Science* 260:349–352.
 36. Striepen, B., M. J. Crawford, M. K. Shaw, L. G. Tilney, F. Seiber, and D. S. Ross. 2000. The plastid of *Toxoplasma gondii* is divided by association with the centrosomes. *J. Cell Biol.* 151:1423–1434.
 37. Tamura, S., and J. C. Boothroyd. 1995. Interconnection between organellar functions, development and drug resistance in the protozoan parasite, *Toxoplasma gondii*. *Int. J. Parasitol.* 25:1293–1299.
 38. Vaidya, A. B., H. J. Painter, J. M. Morrissey, and M. W. Mather. 2008. The validity of mitochondrial dehydrogenases as antimalarial drug targets. *Trends Parasitol.* 28:8–9.
 39. Vercesi, A. E., C. O. Rodrigues, S. A. Uyemura, L. Zhang, and S. N. Morona. 1998. Respiration and oxidative phosphorylation in the apicomplexan parasite *Toxoplasma gondii*. *J. Biol. Chem.* 273:31040–31047.
 40. Weinstein, E. A., T. Yano, L. S. Li, D. Avarkock, A. Avarkock, D. Helm, A. A. McCalm, K. Duncan, J. T. Loudale, and H. Rubin. 2005. Inhibitors of type II NADH:menaquinone oxidoreductase represent a class of antitubercular drugs. *Proc. Natl. Acad. Sci. USA* 102:4548–4553.
 41. Weiss, L. M., and K. Kim. 2007. Bradyzoite development, p. 341–366. In L. M. Weiss and K. Kim (ed.), *Toxoplasma gondii—the model apicomplexan: perspectives and methods*. Academic Press, London, United Kingdom.

Publications

Original Papers

Lin SS, Gross U, Bohne W. (2009). Type II NADH dehydrogenase inhibitor 1-hydroxy-2-dodecyl-4(1H)quinolone leads to collapse of mitochondrial inner-membrane potential and ATP depletion in *Toxoplasma gondii*. *Eukaryot Cell*. **8**: 877-887.

Lin SS, Kerscher S, Saleh A, Brandt U, Gross U, Bohne W. (2008). The *Toxoplasma gondii* type-II NADH dehydrogenase TgNDH2-I is inhibited by 1-hydroxy-2-alkyl-4(1H)quinolones. *Biochim Biophys Acta Bioenerg*. **1777**: 1455-1462.

Brooks CF, Johnsen H, van Dooren GG, Muthalagi M, Lin SS, Bohne W, Fischer KB, Striepen B. (2009). The phosphate translocator is the source of carbon and energy for the *Toxoplasma* apicoplast and essential for parasite survival (under review).

Abstracts for Conferences

Lin SS, Gross U, Bohne W. (2009). Functional analysis of *Toxoplasma gondii* type II NADH dehydrogenases. 20th Annual Molecular Parasitology Meeting 2009. Woods Hole, MA, USA.

(oral presentation)

Lin SS, Kerscher S, Bohne W. (2009). Biochemical characterization of *Toxoplasma gondii* mitochondrial type II NADH dehydrogenase isoform I as a potential drug target. Experimental Biology 2009 Annual Meeting. New Orleans, LA, USA.

(poster presentation)

Lin SS, Bohne W. (2008). Biochemical characterization of *Toxoplasma gondii* type II NADH dehydrogenase isoform I as a putative drug target. COST Action 857 4th PhD Students Retreat. Geneva, Switzerland.

(oral presentation)

Lin SS, Kerscher S, Gross U, Bohne W. (2008). Enzymatic characterization of *T. gondii* type II NADH dehydrogenase isoform I as a putative drug target. 16th Japanese-German Cooperative Symposium on Protozoan Diseases. Goettingen, Germany.

(oral presentation)

Bohne W, Lin SS, Kerscher S, Naujok B, Gross U. (2008). The type II NADH dehydrogenase TgNDH2-I of *Toxoplasma gondii* is inhibited by the quinolone-like compound HDQ. 23rd Meeting of the German Society for Parasitology. Hamburg, Germany.

(oral presentation)

Lin SS, Kerscher S, Gross U, Bohne W. (2008). Characterization of Alternative NADH dehydrogenase in the respiratory chain of *Toxoplasma gondii* as putative Drug Targets. 3rd Short Course for young Parasitologists. Hamburg, Germany.

(oral presentation)

Curriculum Vitae

San San Lin

Institute of Medical Microbiology,
University of Goettingen,
Kreuzbergring 57, 37075, Goettingen, Germany
Tel No.: +49 551 3914344
Email Address: sansan.lin@yahoo.com

Education

- | | |
|---------------------|--------------------------------------------------------------------------------------------------------------------------------------|
| Nov 2006 - present | <u>The University of Goettingen</u> (Germany)
Candidate for the Degree of Doctor of Philosophy |
| Sep 2002 - Aug 2004 | <u>The University of Hong Kong</u> (Hong Kong)
Degree of Master of Philosophy |
| Sep 1999 - Aug 2002 | <u>The Hong Kong University of Science & Technology</u> (Hong Kong)
First Class honor for the Degree of Bachelor of Chemistry |

Academic Achievements

- | | |
|-------------------|-------------------------------------------------------------------------------------------------------|
| Nov 2006- present | Croucher Scholarship |
| April 2009 | American Society of Pharmacology and Experimental Therapeutics (ASPET) Graduate Travel Award |
| 29-31Oct 2008 | Grant funded by the European Union for COST Action 857 4 th PhD Students Retreat in Geneva |
| Aug - Oct 2006 | DAAD Language Scholarship |
| Oct 2004 | Competed Young Investigator Awards (Hong Kong Cancer Congress 2004, one of eight finalists) |
| Sep 2002 - 2004 | Postgraduate Research Studentship |
| Sep 2002 | Dean's List |
| Mar 2002 | Elizabeth Gardner Scholarship |
| Sep 2001 | Dean's List |
| Mar 2001 | Dow of Hong Kong Scholarship |
| Feb 2000 | Dean's List |

Publications

- PhD Thesis Biochemical Characterization of *Toxoplasma gondii* type II NADH dehydrogenases – physiological Impact on mitochondrial functions and energy metabolism
- MPhil Thesis Mechanism of Epstein-Barr virus Latent Membrane Protein 1-regulated Cytokine Expression
- Original papers
- Lin SS, Lee DC, Law AH, Chua ST and Lau AS (2009). Protein Kinase PKR regulates latent membrane protein 1-induced IL-6 and IL-10 expression (under review).
- Brooks CF, Johnsen H, van Dooren GG, Muthalagi M, Lin SS, Bohne W, Fischer KB and Striepen B (2009). The phosphate translocator is the source of carbon and energy for the *Toxoplasma* apicoplast and essential for parasite survival (under review).
- Lin SS, Gross U and Bohne W (2009). Type II NADH dehydrogenase inhibitor 1-hydroxy-2-dodecyl-4(1H)quinolone leads to collapse of mitochondrial inner-membrane potential and ATP depletion in *Toxoplasma gondii*. *Eukaryot Cell*. **8**: 877-887.
- Cheng SM, Li JC, Lin SS, Lee DC, Liu L and Lau AS (2009). Induction of Suppressor of cytokine signaling 2 by HIV-1 Tat contributes to IFN inhibition in Human Blood Monocyte. *Blood*. **113**: 5192-5201.
- Lin SS, Kerscher S, Saleh A, Brandt U, Gross U and Bohne W (2008). The *Toxoplasma gondii* type-II NADH dehydrogenase TgNDH2-I is inhibited by 1-hydroxy-2-alkyl-4(1H)quinolones. *Biochim Biophys Acta Bioenerg*. **1777**: 1455-1462.
- Xie G, Uttamchandani M, Chen GY, Bu Z, Lin SS, Wong KM, Yan W, Yao SQ and Guo Z (2002). Substrate spectrum of tyrocidine thioesterase probed with randomized peptide N-acetyl-cysteamine thioesters. *Bioorg Med Chem Lett*. **12**: 989-992.
- Lin SS (2001). Project Manual: ‘Colorimetric Quantification of Cyanobacterial Off-flavors’ for *Science Division of Government Water Supplies Department, Hong Kong*.

